ERDC/EL TR-01-32

Environmental Laboratory

US Army Corps of Engineers®
Engineer Research and Development Center

In-House Laboratory Independent Research Program

Computed-Tomography Imaging SpectroPolarimeter (CTISP) – A Passive Optical Sensor

Volume 1, Main Text and Appendix A

Hollis H. (Jay) Bennett, Jr., Ricky A. Goodson, and John O. Curtis

September 2001

Approved for public release; distribution is unlimited.

The contents of this report are not to be used for advertising, publication, or promotional purposes. Citation of trade names does not constitute an official endorsement or approval of the use of such commercial products.

The findings of this report are not to be construed as an official Department of the Army position, unless so designated by other authorized documents.

PRINTED ON RECYCLED PAPER

In-House Laboratory Independent Research Program

ERDC/EL TR-01-32
September 2001

Computed-Tomography Imaging SpectroPolarimeter (CTISP) – A Passive Optical Sensor

Volume 1, Main Text and Appendix A

By Hollis H. (Jay) Bennett, Jr., Ricky A. Goodson, John O. Curtis

Environmental Laboratory
U.S. Army Engineer Research and Development Center
3909 Halls Ferry Road
Vicksburg, MS 39180-6199

Final report

Approved for public release; distribution is unlimited

Prepared for Assistant Secretary of the Army
Washington, DC 20315

Contents

List of Figures

List of Tables

Preface

The prototype imaging spectropolarimeter documented in this report is the product of a research effort begun in 1996 by Dr. Brian Miles, a former employee of the U.S. Army Engineer Research and Development Center (ERDC), Vicksburg, MS, and continued through the efforts of the authors. Original funding for this effort was provided through ERDC's In-House Laboratory Independent Research (ILIR) program. The title of the ILIR project was: "UXO and Mine Detection via a Nonscanning Imaging Polarimeter/Spectrometer," Additional funding was provided by the Army's Environmental Quality RDT&E Restoration Program through project 62720A/AF25, entitled: "Optical Technologies for Improved UXO Discrimination."

The research was conducted and the report was compiled by Messrs. Hollis H. (Jay) Bennett, Jr., and Ricky A. Goodson, and Dr. John O. Curtis. The research effort and report were coordinated by Dr. Curtis. The data processing was performed by Mr. Goodson. The hardware modifications were implemented by Mr. Bennett.

This study was conducted under the direct supervision of Dr. Ernesto Cespedes, Team Leader, UXO Characterization Team. Mr. Harold W. West was Chief of the Environmental Systems Branch. Dr. Dave Tazik was Chief, Ecosystem Evaluation and Engineering Division, and Dr. Edwin A. Theriot was Acting Director, Environmental Laboratory.

At the time of publication of this report, Dr. James Houston was Director of ERDC, and COL John W. Morris III, EN, was Commander and Executive Director.

The contents of this report are not to be used for advertising, publication, or promotional purposes. Citation of trade names does not constitute an official endorsement or approval of the use of such commercial products.

1 Introduction

This report documents the development of a novel optical sensor system, the Computed-Tomography Imaging SpectroPolarimeter (CTISP), designed to collect both wavelength-dependent and polarization-dependent reflected energy from man-made and natural surfaces. Originally funded as a technology that could be applied to the problem of distinguishing surface unexploded ordnance (UXO) from natural backgrounds, this unique sensor system has other applications as well, including land cover classification, land-use studies, and numerous agricultural issues.

The prototype sensor described herein was first envisioned in 1996 by Dr. Brian Miles, a former U.S. Army Engineer Research and Development Center (ERDC), formerly the Waterways Experiment Station, Vicksburg, MS, employee, as part of his doctoral studies under Prof. Eustace Dereniak at the University of Arizona (Miles 1999). Dr. Miles left ERDC in 1999, and the responsibility for the continuation of the development of the system was assumed by the authors. Two of the initial hurdles the authors had to address follow. First, new optical hardware had to be acquired to replace the hardware that was loaned to Dr. Miles during his initial development of the CTISP system. Second, to aid in making the CTISP measurement system more portable, computer hardware was purchased to allow for the operation of CTISP by a laptop computer. After addressing these hurdles, the authors supplemented Dr. Miles' laboratory measurements on specialized targets with data collected on numerous coated surfaces and some natural surfaces to evaluate CTISP's spectroscopic capabilities as well as to establish its sensitivity to surface polarization effects.

Chapter 1 provides background information on terminology, the physics of reflected light, and the physics of diffracted light, all of which will be discussed in this chapter. Chapter 2 describes, in detail, the design and operation of the sensor, while Chapter 3 focuses on a set of measurements made with the prototype hardware which will include data collected on reflectance standards, several coated metal plates, two natural background materials, and a representative UXO item. The report will conclude with a discussion of future research and development issues (Chapter 4) that have naturally evolved from the efforts described in these pages.

Terminology

Irradiance and exitance

In many textbooks, the term "light intensity" refer to the flow of light energy per unit area per unit time through which it passes or is intercepted. Where intensity is a measure of the concentration of power of radiant energy it is also referred to as radiant flux density. In this report, radiant flux density that is incident on a surface will be called the irradiance, while the radiant flux density that is reflected from the surface will be called the exitance.

Polarized light

Light has a dual nature, i.e., it can be described as either a propagating wave of energy or a moving packet of energy (a photon). The most convenient way to describe its behavior when passed through polarizing filters is to consider light as propagating waves of electromagnetic energy. These waves consist of both electric field vectors and magnetic field vectors whose magnitudes and directions may be constantly changing, but which both lie in a plane normal to the direction of propagation. The polarization character of a light wave is associated with its electric field vector.

Most light sources radiate energy from innumerable atomic and molecular sources that have no preferred electric field orientation or frequency of oscillation. If, however, one imagines light propagating toward them as light from a single source and of a single wavelength, or color, then its electric field vector may be thought of as an arrow whose tip is oscillating back and forth at a fixed frequency. If the tip of the vector traces a straight line as seen by the observer, then that light source is said to be linearly polarized. If the electric field vector rotates as it propagates toward the observer, then the envelope of the electric field vector is, in general, an ellipse, and the light is said to be elliptically polarized. In fact, linear polarization and circular polarization are just special cases of the more general elliptical polarization. All such states can be mathematically defined by the superposition of two orthogonal sinusoidal waves with a specified relative phase and specified amplitudes.

By convention, vertically polarized light is light whose electric field vectors can oscillate only in the plane perpendicular to the earth's surface; horizontally polarized light oscillates parallel to the earth's surface. Right-hand circular light is light whose electric field vectors rotate clockwise as seen by the observer.

Polarization by reflection

One of the more common uses of polarizing filters that almost all of us have some experience with is that of sunglasses with polarizing lenses. We use them

to reduce the glare from sunlight reflecting off smooth surfaces such as glass windshields, the hoods of our automobiles, and calm water bodies. The lenses in our "polaroid" sunglasses are linear polarizing filters that pass only light whose electric field vectors are oriented perpendicular to the bridge of the glasses, and the reflected light tends to be linearly polarized. When randomly polarized natural light reflects from relatively smooth surfaces, it becomes partially polarized. An electron oscillator model (Hecht 1987) can be used to explain why there is a tendency for the reflected light to be polarized parallel to the smooth surface.

The following simple experiment that demonstrates polarization by reflection can be conducted by anyone on a bright, clear day. First of all, position yourself near an automobile whose color is dark enough and whose surface finish is smooth enough to reflect an image of the blue sky and white clouds. The light coming from the clouds and sky is randomly polarized. However, the light that is reflected from the painted surface is polarized in a direction parallel to the surface. To prove this, look at the surface and the reflected image through a Polaroid sheet or through Polaroid sunglasses. As long as the polarizing direction of the sheet or lens is parallel to the surface, the reflected image is unaffected. However, if one turns the filter or lens so that its polarizing direction is perpendicular to the surface, the reflected image is eliminated. This polarization effect is one of the parameters that CTISP measures for a surface of interest. CTISP may be able to take advantage of polarization by reflection to distinguish man-made surfaces from natural surfaces.

Stokes parameters

Optical polarization filters are devices designed to allow light having only certain polarization states to pass through and are an integral part of the apparatus described in this report. In 1852, the British physicist, Sir George Stokes, suggested a means of describing the polarization state of any light that makes use of a set of polarization filters. He first measured the total irradiance of a light source, and called it I_0. Then he measured the source after it had passed through a filter that allowed only light with a horizontal polarization to pass and labeled that intensity, I_1. Another measurement, I_2, was made after passing light through a linear filter whose transmission axis was rotated 45 deg clockwise from the vertical. A final measurement was made after light was passed through a filter that transmitted only right-circularly polarized light, and it was labeled, I_3. Implicit in the arguments that follow is that each of the four filters passes the same relative amount of light energy. Four parameters can be defined that completely describe the polarization state of the light source (Chipman 1993):

$$
\begin{aligned}
S_0 &= I_0 \\
S_1 &= 2I_1 - I_0 \\
S_2 &= 2I_2 - I_0 \\
S_3 &= 2I_3 - I_0
\end{aligned}
\tag{1}
$$

S_0 then represents the total irradiance of the light source. S_1 is an indication of its tendency to be horizontally polarized (>0) or vertically polarized (<0). S_2 recognizes light that is linearly polarized at +45 deg from the vertical (>0) or at –45 deg (<0). Finally, S_3 reveals a tendency toward right-hand circularly (RHC) polarized light (>0) or left-hand circularly (LHC) polarized light (<0). If these four Stokes parameters are normalized to S_0, then S_1 is bound by +1 for pure horizontal polarization and –1 for pure vertical polarization, S_2 is bound by +1 for a pure +45-deg state and –1 for a pure –45-deg state, and finally, S_3 is bound by +1 for a pure RHC state and –1 for a pure LHC state.

If a beam of light is simply a superposition of randomly oriented electric field vectors, then S_1 , S_2 , and S_3 are all zero, and the light is said to be unpolarized. If, on the other hand, the light is totally polarized, i.e., some combination of horizontal, vertical, +45, -45, RHC, and LHC, then it can be shown by considering Stokes parameters in terms of time-averaged energy densities that

$$(S_0)^2 = (S_1)^2 + (S_2)^2 + (S_3)^2 \tag{2}$$

It follows that a convenient parameter that can be used to describe partially polarized light is the <u>degree of polarization</u> (DOP):

$$\mathrm{DOP} = [(S_1)^2 + (S_2)^2 + (S_3)^2]^{1/2} / S_0 \tag{3}$$

Diffraction Gratings

When light passes through an opaque object that has numerous thin parallel slits, constructive and destructive interference patterns can be set up on some focal plane that consist of parallel light and dark strips. (This process of diffraction can be physically described using Huygen's Principle.) The light patterns produced by such a device, also referred to as a transmission amplitude diffraction grating, are called orders, with higher-numbered orders being farther from the optical axis. If a single square aperture replaces the slits, then a two-dimensional (2-D) interference pattern is set up on the screen where the light spots are most visible along a pair of perpendicular lines centered on the optical axis (the line along which the line source is shining). A family of square apertures that are regularly ordered, produces a two-dimensional pattern in which the off-axis orders are more visible. Each of these diffraction orders contains all of the light source wavelengths. Another form of grating, the transmission phase diffraction grating, is fabricated by etching a family of parallel surface notches in a transparent glass plate. Each notch serves as a source of scattered light, and interference patterns are generated because of differences in phase of each light source.

A key element of the optical sensor system described in this report is a 2-D transmission phase diffraction grating made for this laboratory by personnel at the Jet Propulsion Laboratory, Pasadena, CA. It is conceptually similar to the ordered pattern square aperture grating referred to above. They refer to their product as a computer-generated hologram (CGH) disperser (Descour et al. 1997). It was designed to provide a five-by-five array of nearly equal irradiance orders. The effective grating line spacing of the CGH is 20 microns. If the entire CGH (17.5-mm width) is being illuminated, then its effective wavelength resolving power is less than a nanometer for all five orders and at any wavelength (Hecht 1987).

CTISP – The Acronym Revisited

Armed with some of the requisite terminology, one can better appreciate the direction taken to develop this unique piece of optical sensor hardware. Working backwards in the acronym, one starts with "polarimeter." CTISP possesses a filter wheel with linear and circular polarizing filters. Data collected by passing light through these filters are used to calculate Stokes parameters, and, as was pointed out above, the Stokes parameters completely described the polarization state of what is in the sensor's field of view.

The "spectro" part of the acronym refers to the fact that wavelength (or color) information is available in the CTISP imagery. The diffraction grating element generates a diffraction pattern that contains all of the wavelength information in the light passing through the CTISP optical path. The advantage of CTISP over many spectrometers is that the wavelength information in the sensor field of view is collected instantaneously through the diffraction procedure. There is no need to pass light through a wavelength filter wheel to obtain spectral data.

"Imaging" has greater significance for CTISP than for conventional optical systems, because CTISP does not generate just a simple "visual" image of what is being viewed. Software developed for this sensor system is utilized to generate an image of each Stokes parameter at a number of fixed wavelengths.

Finally, the "computed tomography" part of the acronym refers to the data inversion process that is used to generate all of the images. Each pixel in each diffraction order that is digitally imaged by CTISP has wavelength information and spatial information about what is in the optics field of view. Tomography is the process of reassembling all of those data into meaningful images.

Potential Applications of CTISP Technology

Clearly, if one has an imaging device that can provide both spectral (color) information and information on the polarization state of whatever is in the sensor's field of view, then one has a powerful tool for analyzing targets. CTISP collects spectral data through the clever processing of diffraction imagery and

utilizes four polarization filters to generate Stokes parameters, whose value as discrimination tools is still being explored.

On a small scale, one of the obvious applications of this technology would be to distinguish “shiny”, “colored” objects, such as land mines, from natural backgrounds in a battlefield environment. Similarly, the same technology mounted on either a remotely piloted (or autonomously piloted) vehicle could be useful in surface cleanup of UXO from firing ranges that are being turned back to the private sector.

On a larger scale (from higher flying aircraft or satellites), there are many remote sensing applications for this technology. One can think immediately of land-use issues; i.e., mapping man-made structures vs. natural terrain. Spectral content of images taken from airborne Multispectral Scanners or LANDSAT and SPOT satellites is already being used to conduct terrain classification studies. Certainly, having additional information about the state of polarization may improve the reliability of terrain classification algorithms (Curran 1982). Other potential applications of a CTISP-like device could include soil moisture assessments (for both agricultural and military applications) and crop or vegetation surveys.

2 CTISP Operational Concepts

Hardware

The precise specifications for the design of CTISP and the acquisition of optical elements, etc., are discussed in detail in other publications (Miles 1999, Miles et al. 1999a, b), and several of the following figures are from those documents. What follows is a general description of CTISP hardware and a few simple diffraction images that will provide the reader who has a minimal background in optics with a good understanding of the operating principles of this unique sensing tool.

Figure 1 is a photograph of the CTISP sensor package as it was configured to collect the data on painted surfaces reported in the next chapter. The optical elements of the system are housed in the black cylinder mounted on the tripod. They are connected to the imaging control box (the black box on the rolling table) and to a desktop computer, which serves as the system controller, via the cables shown in the photograph.

Figure 1. CTISP configuration for a recent laboratory measurement program

On the right end of the tripod-mounted black cylinder in Figure 1 is the only moving part of the CTISP sensor package, an analyzer wheel, which is shown in close-up in Figure 2. Located on this wheel are five apertures through which reflected light enters into the CTISP optical path. One of the apertures is just a hole in the wheel. The other four contain four different polarization filters: a horizontal linear filter, a +45 deg linear filter, a vertical linear filter, and a right-circular filter. During the collection of data on a particular target area, in-house-developed software triggers a motor housed in the CTISP box that rotates the analyzer wheel to the appropriate filter as it is needed.

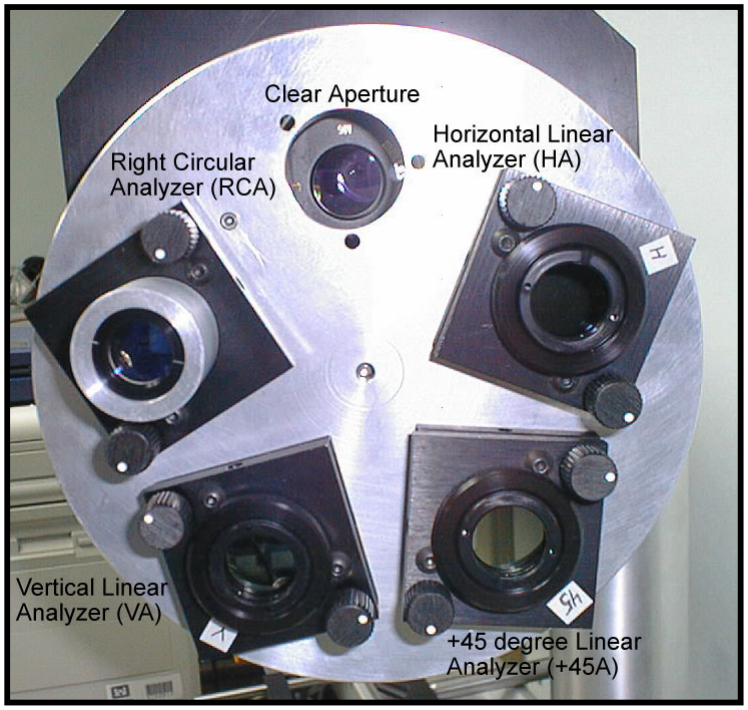

Figure 2. Analyzer wheel with polarizers

Figure 3 is a labeled photograph of the CTISP optics box with its cover removed which shows each of the elements along the optical path. Light enters from the right in this photograph through either the clear aperture or one of the four polarization filters. Only wavelengths within a 440- to 740-nm band are allowed into the optical path. This is accomplished by the IR filter behind the analyzer wheel and the UV filter on the front of the objective lens.

The 28-mm objective lens focuses an image at the field stop, which is 1.75 mm square. The focal length of the objective lens and the size of the field stop result in a 3.5-deg field of view.

Before the incoming light can be passed through the computer-generated hologram (CGH) diffraction grating, it must be collimated. This is achieved by inserting an inverted 80-mm lens into the optical path, which expands the field stop image into a parallel bundle of light rays through a 19.6-mm-diam pupil.

Then the collimated light is diffracted through the CGH into the 105-mm reimaging lens which focuses the five-by-five diffraction orders onto a focal plane array (FPA) in the charged couple device (CCD) camera at the end of the CTISP optical path. The FPA is a 16-bit, 1,024- by 1,024-element array of light-sensitive diodes covering an area of about 25 mm square.

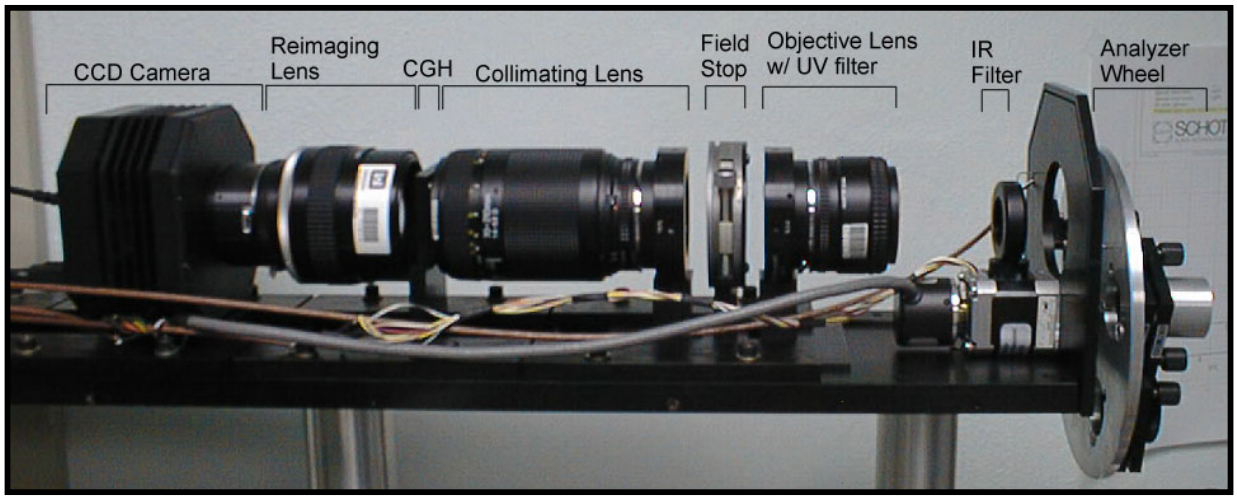

Figure 3. CTISP optical hardware without its cover

Referring to Figure 3, the focusing of the CTISP optical hardware is reviewed. All lenses are set to 4.6 f-stop. If the lens does not have a 4.6 f-stop, then the f-stop is set to the next greater diameter f-stop (Miles 1999, Miles et al. 1999a, b). The CCD Camera with the Reimaging Lens attached is mounted to the black CTISP base. The lens is focused to infinity and images are taken of items greater than 15 m (50 ft) away to evaluate the focus of the lens on the FPA. If the images are not in focus, then the setscrews on the mounting collar can be loosened so that the lens can be moved to produce a focused image. (Note: No adjustments were needed for the Reimaging Lens.) Next, the CGH is mounted on the CTISP base followed by the Collimating Lens. The Collimating Lens is adjusted to 80 mm, and the lens is focused to infinity. The Field Stop is placed on the CTISP base, but the mounting bolts are not tightened. Images of the Field Stop are taken. The Field Stop distance from the Collimating Lens must be adjusted until the images taken of the Field Stop shows a crisp clean edge for the Field Stop. Once this position is located, then the mounting bolts are tightened. Finally, the Objective Lens is placed on the CTISP base, but the mounting bolts are not tightened. The Objective Lens is focused to infinity and images are taken of items greater than 15 m (50 ft) away. The Objective Lens position is adjusted until the images are in focus. Once this position is determined, the mounting bolts are tightened.

Example Diffraction Images

Several FPA images of simple targets will help the reader better understand the complexity inherent in the FPA data for real targets. First of all, Figure 4 contains a diffraction image of a fiber optic source of 632.8-nm wavelength light. The 200-nm diam optical fiber was placed in front of the analyzer wheel and its five-by-five diffraction pattern is shown in Figure 4. Ideally, one would prefer that a point source of light could be made available that would illuminate only one pixel on the FPA. However, that is not an achievable goal. The result of imaging a finite-sized optical fiber is that each of the illuminated "spots" on the FPA contains several pixels. For this particular image, the zeroth-order diffraction at the center of the image covers about a two-by-two array of pixels. The outer orders of the image are ellipsoidal blotches of light that may have a long dimension of seven or eight pixels.

Figure 5 is a single-wavelength (632.8-nm) diffraction image of the f-stop, which was acquired by illuminating a white surface with a He-Ne laser. Note that at a single wavelength, the square geometry of the f-stop is preserved. Shorter wavelength light would have produced a tighter pattern of squares, while the gaps between orders would have been much larger for higher wavelength light. The zeroth-order image at the center of the figure contains the true image of what is being viewed through the field of view. The area illuminated by the zeroth-order image is about 96 pixels by 96 pixels on the FPA. Given a full-angle field of view of about 3.5 deg, the resulting angular resolution of CTISP as it is currently configured is about 0.036 deg or about 0.6 milliradians.

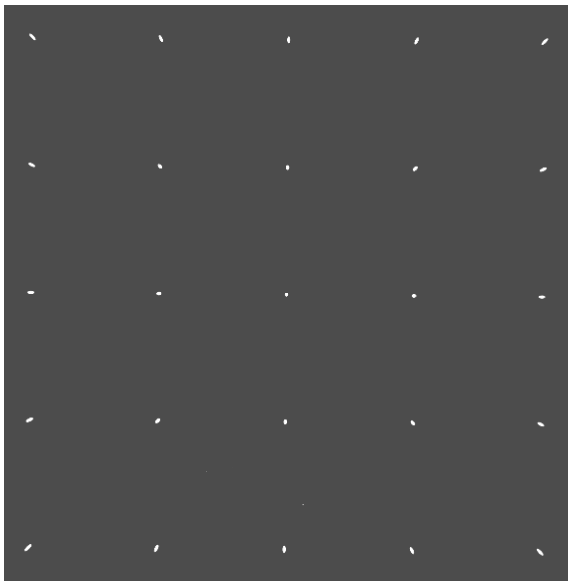

Figure 4. Diffraction image of a fiber optic light source (632.8 nm)

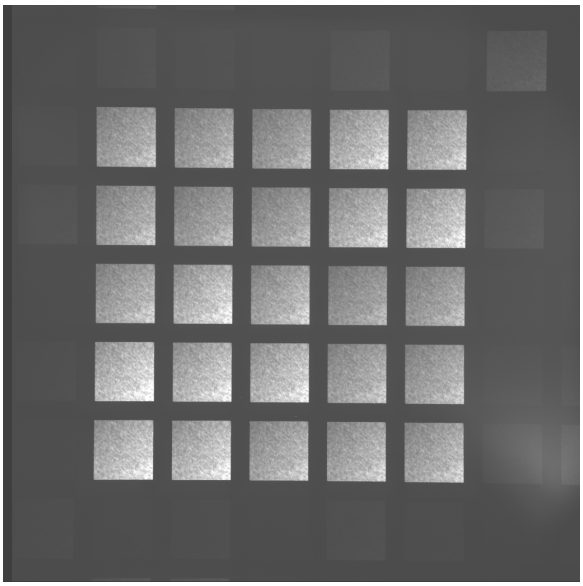

Figure 5. Diffraction image of the f-stop illuminated by single wavelength light (632.8 nm)

The next diffraction image (Figure 6) is of a target having 2-D features; namely, the letters W, E, and S as white characters on a black background. He-Ne light was once again used to illuminate the target. Note that at a single wavelength, each diffraction order retains the geometry of the target; i.e., the letters are clearly visible in all orders. Note also that there was some reflection of light from the "black" paper, which results in a halo effect about the characters in each order.

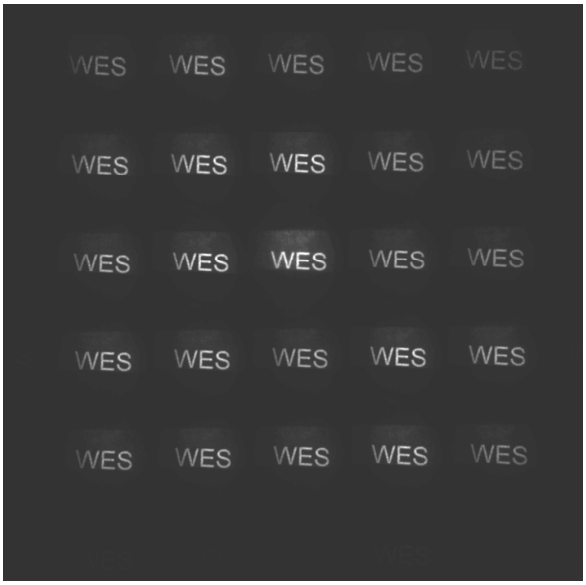

Figure 6. Diffraction image of alphabetic letters illuminated by single wavelength light (632.8 nm)

Finally, Figure 7 contains the diffraction image of the same "WES" target illuminated with a flashlight. In other words, it was illuminated with unpolarized light covering the entire visible spectrum. Here one sees the extent of distortion of a simple target in the diffraction orders produced by the CGH disperser. The zeroth-order diffraction at the center of the FPA image is undistorted as expected. Therefore, the FPA data for any target will always contain a "visible" image of the target, as well as diffraction orders that contain both field of view geometric information and reflected light wavelength information. Software was written at ERDC to invert the distorted diffraction order imagery to produce spectroscopic data and polarization state data on any target seen within the field of view.

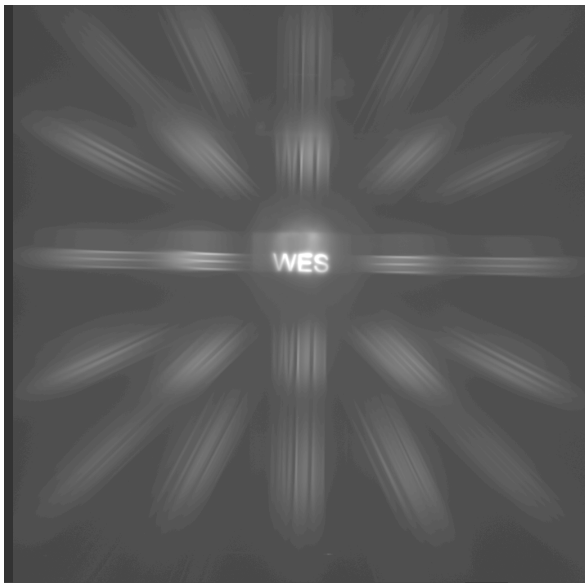

Figure 7. Diffraction image of alphabetic letters illuminated by white light

The Mathematics of CTISP Operations

The operation of CTISP is perhaps best described in the language of linear algebra. Coupled with a novel three-dimensional (3-D) graphical visualization of what CTISP "sees" when it is pointed toward a target, the linear algebra can also be used to describethe system calibration procedure, which is discussed in the next section.

The "voxel" viewpoint

To begin with, imagine that you are at the f-stop of the CTISP optical hardware path looking out through the objective lens. What you "see" is the reflected light energy, or existence, from all of the physical elements within the lens' field of view. The IR and UV filters have restricted the wavelengths of this energy to the 440- to 740-nm band. One can then think of these exitance values as having three dimensions, two orthogonal spatial dimensions that describe where the exitance is coming from within the field of view, and a spectral, or wavelength, dimension.

The spatial resolution of CTISP is controlled by the number of pixels on the FPA that collects diffraction image intensity values. As it is currently configured, the nondiffracted, or white light, or zeroth-order image illuminates a square set of pixels on the FPA, approximately 96-by-96 elements in size. However, to reduce data storage requirements and to minimize data processing time, the 96-by-96 is "binned" by averaging the intensities of three-by-three subarrays, so that the effective spatial dimensions of what is "seen" by CTISP are defined by an area of 32 horizontal elements by 32 vertical elements. Furthermore, the wavelength band has been arbitrarily subdivided into 16 different subbands, each having a width of 20 nm.

The end result of real world limitations placed on CTISP by hardware and software is that CTISP "sees" a 3-D cube of exitance values as depicted in Figure 8. Each element of this **object cube**, which can be thought of as a pixel with volume, or **voxel**, contains the exitance for some position in the field of view (on a 32-by-32 orthogonal grid) at one of 16 wavelength bands.

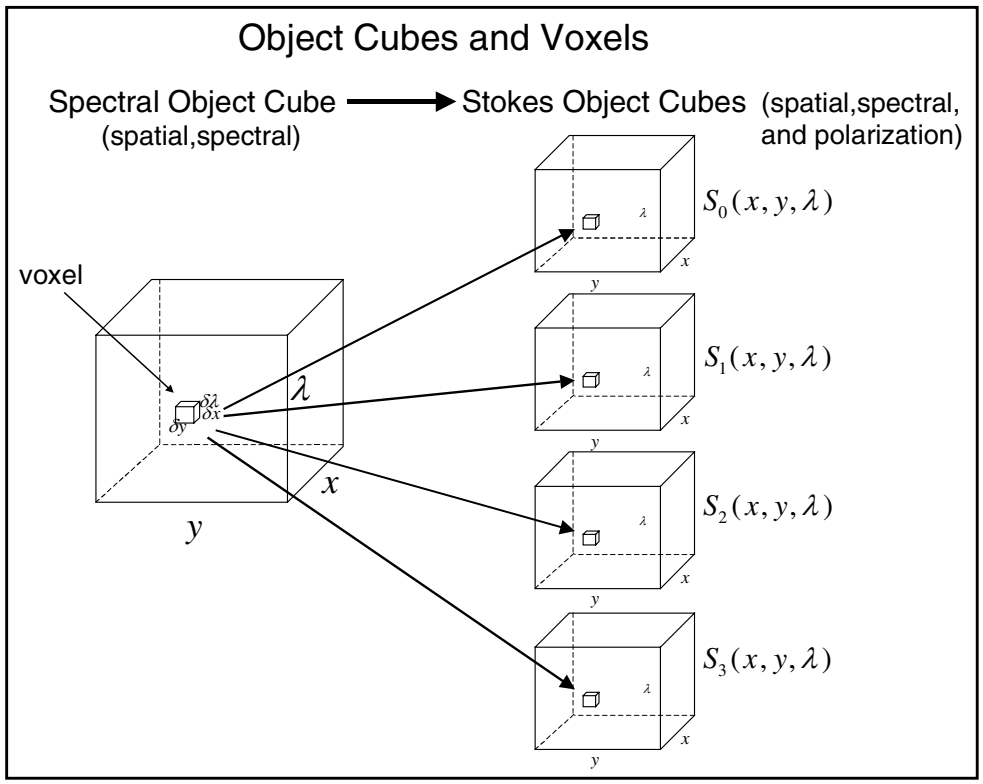

Figure 8. Object cube visualizations of CTISP data

However, through the use of four different optical filters on the hardware analyzer wheel, a clever calibration scheme, and software development effort, CTISP produces polarization information for each voxel; namely, the four Stokes parameters described in an earlier section. Thus, the spectral object cube is transformed into a set of four Stokes object cubes as illustrated in Figure 8.

Actually, the process is not quite that simple. As CTISP collects data from what it sees in its field of view, the light passes through four different optical filters, one passes only vertically polarized light, one passes only horizontally polarized light, one is set for linearly polarized light at 45 deg from the vertical, and one passes only right circularly polarized light. Therefore, for each voxel, CTISP views a four-element vector:

$$\vec{f}_n = \begin{bmatrix} f_{VA,n} \\ f_{HA,n} \\ f_{+45A,n} \\ f_{RCA,n} \end{bmatrix} \tag{4}$$

where $f_{\alpha,n}$ is the exitance of the nth voxel as viewed through the α filter on the analyzer wheel.

Since the purpose of CTISP is to derive polarization information from field of view exitances, what is now needed is a way to transform voxel exitances into voxel Stokes vectors:

$$\vec{S}_n = \begin{bmatrix} S_{0,n} \\ S_{1,n} \\ S_{2,n} \\ S_{3,n} \end{bmatrix} \tag{5}$$

This is accomplished through the development of a voxel calibration matrix, W_n, which is defined by the matrix equation:

$$\vec{f}_n = W_n \vec{S}_n \tag{6}$$

Once the voxel calibration matrix has been derived by the calibration procedure described in the next paragraph, the Stokes vector, and hence the polarization state of the nth voxel can be calculated from:

$$\vec{S}_n = W_n^{-1} \vec{f}_n \tag{7}$$

Voxel calibration

Continuing with the language of linear algebra , W_n is a four-by-four matrix that relates the exitance, $\vec{f}_n$, "seen" by CTISP to a vector, $\vec{S}_n$, that describes the polarization state of a particular voxel. One technique for determining the elements of this voxel calibration matrix is to manipulate the polarization state of each voxel in a controlled way and to record the resulting exitance. If as many independent polarization conditions can be chosen as there are unknown

elements in the calibration matrix, then those elements can be uniquely determined. For example, consider the first of the four equations represented by the Matrix Equation 6.

$$f_{VA,n} \quad = \quad W_{1,1,n}S_{0,n} + W_{1,2,n}S_{1,n} + W_{1,3,n}S_{3,n} + W_{1,4,n}S_{4,n} \tag{8}$$

If a calibration apparatus could be developed that produced four independent polarization states for the nth voxel as viewed through the vertical filter on the analyzer wheel, then one would have four equations and four unknowns (the *W* coefficients). This is exactly what the CTISP calibration apparatus achieves.

Pictured in Figure 9, the calibration hardware generates a monochromatic spot of light at a chosen (x,y) location within the CTISP's field of view (FOV). Software has been developed (Appendix A) that controls stepper motors and solenoids that, in turn, position various filters and retarders with the optical path of the apparatus to produce known voxel polarization states, or basis states (Miles 1999). The four basis states chosen for calibration represent the same four polarizations used on the CTISP analyzer wheel; namely, vertical, horizontal, +45-deg, and right circular polarizations. Normalized to the total irradiance of the optical fiber, the Stokes vector representations of these four states are:

$$(\vec{S}_n)_{VL} = \begin{bmatrix} 1 \\ -1 \\ 0 \\ 0 \end{bmatrix}, (\vec{S}_n)_{HL} = \begin{bmatrix} 1 \\ 1 \\ 0 \\ 0 \end{bmatrix}, (\vec{S}_n)_{+45L} = \begin{bmatrix} 1 \\ 0 \\ 1 \\ 0 \end{bmatrix}, (\vec{S}_n)_{RCL} = \begin{bmatrix} 1 \\ 0 \\ 0 \\ 1 \end{bmatrix} \tag{9}$$

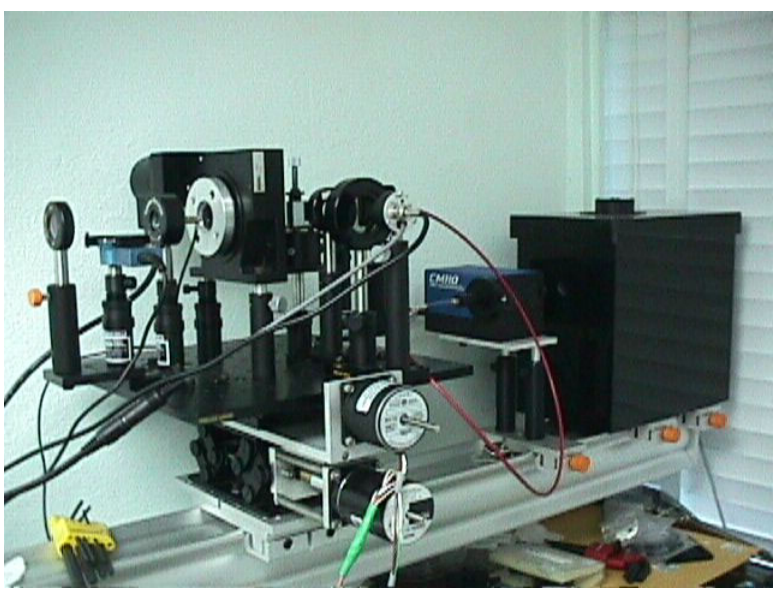

Figure 9. The CTISP calibration apparatus

Each of these four independent polarization basis states results in a different CTISP exitance measurement, which, when plugged into Equation 8, results in a set of four independent equations in the four unknown elements from the first row of the calibration matrix. The voxel calibration scheme can now be summarized in the following way:

a. Set the analyzer wheel on CTISP to one of the four filters.

b. Generate the four voxel polarization basis states using the CTISP calibration hardware and record the four voxel exitances.

c. Solve the equations simultaneously for the four unknown elements of the chosen row of the calibration matrix.

d. Repeat the process for the elements of the other three rows.

The end result is that voxel calibration requires a total of 16 measurements: 4 analyzer wheel settings and 4 polarization basis states for each analyzer position.

A new software visualization program was developed during the project to aid in evaluating the calibration of the system. Figures 10 and 11 show the graphical output of the program. The 16 measurements for each of the frequencies are graphed in the output. The nomenclature for the labeling of each data set is as follows: C represents circular polarization, H represents horizontal polarization, V represents vertical polarization, and 45 represents 45-deg polarization. The first letter is the state of the analyzer wheel and the second letter is the state of the calibration hardware (i.e., H/V indicates that the analyzer wheel is set to the horizontal filter and the calibration hardware is set to vertical polarization.

An example for the use of the calibration visualization program can be described using Figure 10. Figure 10 shows that the calibration data collected through the horizontal polarization filter (the data sets with the H as the first character) of the analyzer wheel are stronger than those of the vertical polarization filter (the data sets with the V as the first character) and the 45-deg polarization filter (the data sets with the 45 as the first character) of the analyzer wheel. This can be an indication of a number of nonideal conditions. One condition is that the optical densities of the polarization filters in the analyzer wheel are different. Another condition is that the calibration source is biased toward horizontal polarization. One more condition is that the 45-deg polarization filter and the vertical polarization filter in the analyzer wheel are not orientated 45 deg and 90 deg, respectively, from the horizontal polarization filter in the analyzer. Figure 11 shows an improved calibration data collection.

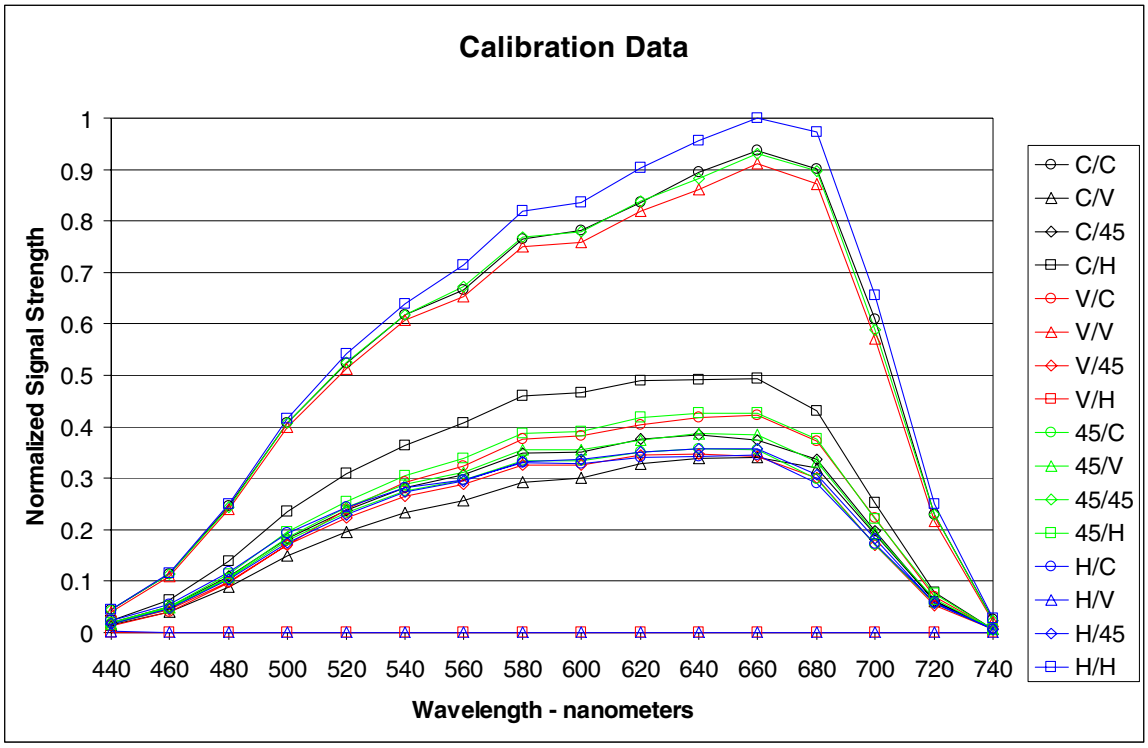

Figure 10. CTISP calibration curves

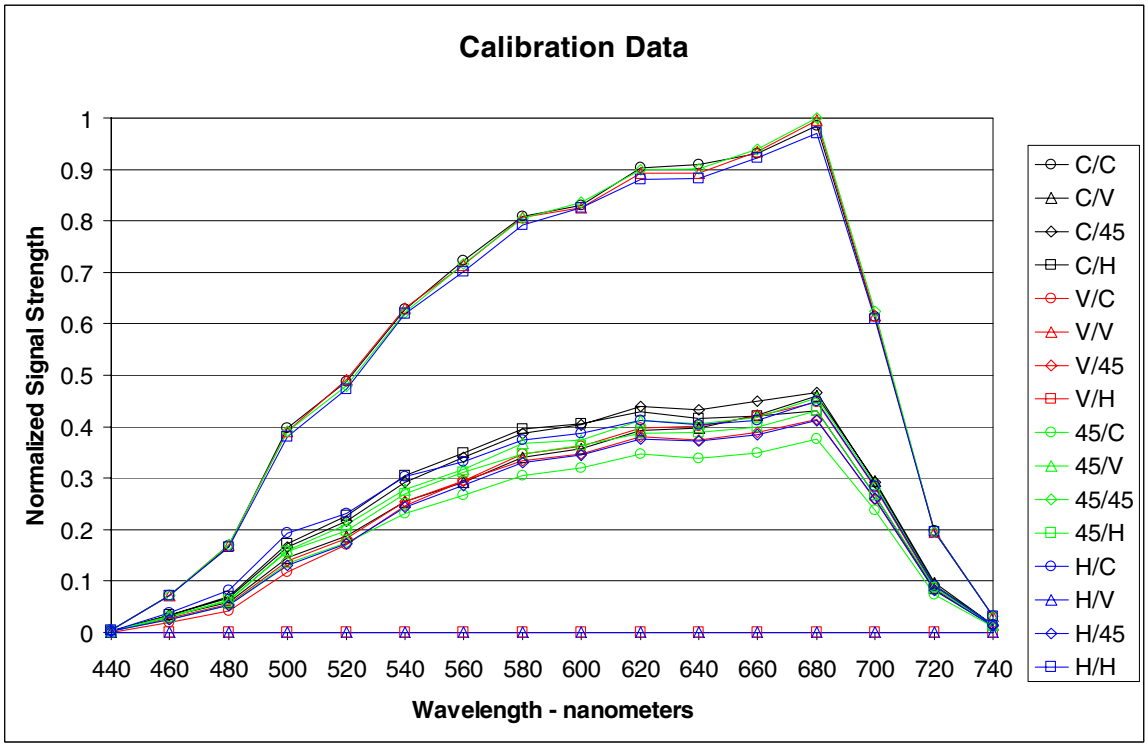

Figure 11. Improved CTISP calibration curves

With respect to relative positioning of the polarization filters on the analyzer wheel and within the calibration hardware, a new procedure was developed to quickly evaluate the relative positions of the linear polarizations filter. After mapping the 360-deg response of the linear polarization filters used on the analyzer wheel and the calibration hardware, it was found that the angular sensitivity of two filters was minimal at 90 deg. However, the angular sensitivity at 45 deg was the greatest. Therefore, balancing of the 45-deg responses can be used to determine the 90-deg location of a given filter with respect to another filter. This method should only be used after the 360-deg mapping of two filters has been performed to verify the high angular sensitivity at the 45-deg angles and the symmetry of the polarization response of the two filters.

One final note, during the repeatability testing of the system, it was found that the optical switch used to reposition the linear polarization filter in the calibration hardware was inducting up to a 3-deg error in the positioning of the linear polarization filter. Therefore, the optical switch repositioning algorithm was disabled in the calibration software and a visual cue was placed on the linear polarization filter for the operator to quickly verify if the linear polarization filter was at the 0-deg position.

The polarization filter in the calibration hardware is instructed to move to 0-, 4-, and 90-deg angles during the calibration procedure. It is moved to the 0-deg angle position at the end of the calibration. Only if there was an equipment failure during calibration did the polarization filter in the calibration hardware have to be repositioned with respect to the filters in the analyzer wheel.

Instrument calibration

Equation 6 does not represent the complete mathematical description of CTISP operations. $\vec{f}_n$ is not a summary of what CTISP measures. It is a vector that represents the perceived exitance from a particular spatial location with the FOV of the instrument at a particular wavelength. Therefore, it represents the light intensity entering the CTISP optical path.

The FPA is the data recording element within the CTISP hardware. It records, on a 1,024- by 1,024-element array of light-sensitive diodes, the intensities of light that have entered CTISP through the objective lens, have been focused on the f-stop, collimated by another lens, diffracted by the CGH disperser, and finally refocused on the FPA pixel array. For each analyzer wheel filter, α , another matrix equation can be written to summarize this process:

$$\vec{g}_\alpha = H_\alpha \vec{f}_\alpha \tag{10}$$

$\vec{g}_\alpha$ is a column vector that contains FPA irradiance values that have passed through the CTISP optical path, including analyzer wheel filter, α. The same binning process that produced a 32-by-32 element FOV is used in the current CTISP configuration to reduce the number of elements in $\vec{g}_\alpha$ to about 116,000.

$\vec{f}_\alpha$ is also a column vector and, consistent with previous notation, contains the voxel irradiances as seen by CTISP through analyzer wheel filter, α . It is, in fact, the object cube discussed previously whose voxel intensities have been arranged into a column vector. The number of elements in $\vec{f}_\alpha$ is the number of voxels, which, in the current CTISP configuration, is 32 × 32 × 16, or 16,384. Note that the four elements in the $\vec{f}_n$ vector described in the previous section are just the nth elements in the four $\vec{f}_\alpha$ vectors in Equation 10.

H_α is called the instrument calibration matrix. It defines how the exitances from a target scene are mapped onto the FPA of CTISP for each filter on the analyzer wheel. The elements of the instrument calibration matrix come from the same set of measurements used to determine the voxel calibration matrix as discussed previously (Miles 1999). Monochromatic light from the calibration apparatus is filtered to match the analyzer wheel filter on CTISP. At this point, all of the elements of $\vec{f}_\alpha$ are zero except one, which we can call the nth element. The diffraction pattern on the FPA yields $\vec{g}_\alpha$, which is, in effect, the nth column of H_α. The measurement is repeated for another wavelength at the same spatial location within the FOV, which yields another column in the instrument calibration matrix. Observed invariance of diffraction patterns resulting from spatial location of the calibration light source is used to justify duplication of appropriate columns.

Data acquisition procedure

Once the instrument calibration matrix has been determined, CTISP can be used to generate an object cube representation of all that it sees at any instant within its FOV. Voxel exitance values can be "reconstructed" from the FPA data by inverting Equation 10:

$$\vec{f}_\alpha = H_\alpha^{-1} \vec{g}_\alpha \tag{11}$$

In other words, for any target scene being viewed by CTISP, FPA intensities can be used to reconstruct an object cube containing spatial and spectral information. Because of its size, the inversion of H_α is accomplished by an iterative scheme, referred to as the Expectation-Maximization algorithm (Miles 1999). Given the object cube representation of the target scene for each analyzer wheel filter, all of the polarization information for each voxel within the object cube can be determined using Equations 4 and 7. Code listings for system calibration and data processing are located and discussed in Appendix A.

The final product of any CTISP data collection and analysis effort is a set of four object cubes, one for each of the four Stokes parameters. Current software produces 16-layer object cubes, each layer of voxels representing a different average wavelength. One way of displaying the four Stokes cubes is to unstack the 16 wavelength layers and to arrange them in columns as shown in Figure 12.

These data were collected in a very early experiment in which a mortar and a bomblet on a black background were illuminated by sunlight and imaged through CTISP.

The image mosaic in Figure 12 was not enhanced to produce the most viewable snapshots of Stokes parameters or to support any particular hypothesis. Rather, these images are shown simply as a demonstration of how CTISP data can be displayed. However, even with its poor spatial resolution and lack of contrast, the mosaic does reveal a sensible spectral behavior. For example, the reddish orange body of the bomblet at the upper left of each image is brighter at higher wavelengths. Similarly, the green body of the mortar is brightest at the midrange wavelengths.

The white painted tail of the bomblet and the unpainted aluminum tail of the mortar are bright at all visible wavelengths. Note, also, that the images at 440 and 740 nm are relatively poor. This is explained by the use of the UV and IR filters within the optical path of CTISP to block short wavelength and long wavelength light from entering the instrument.

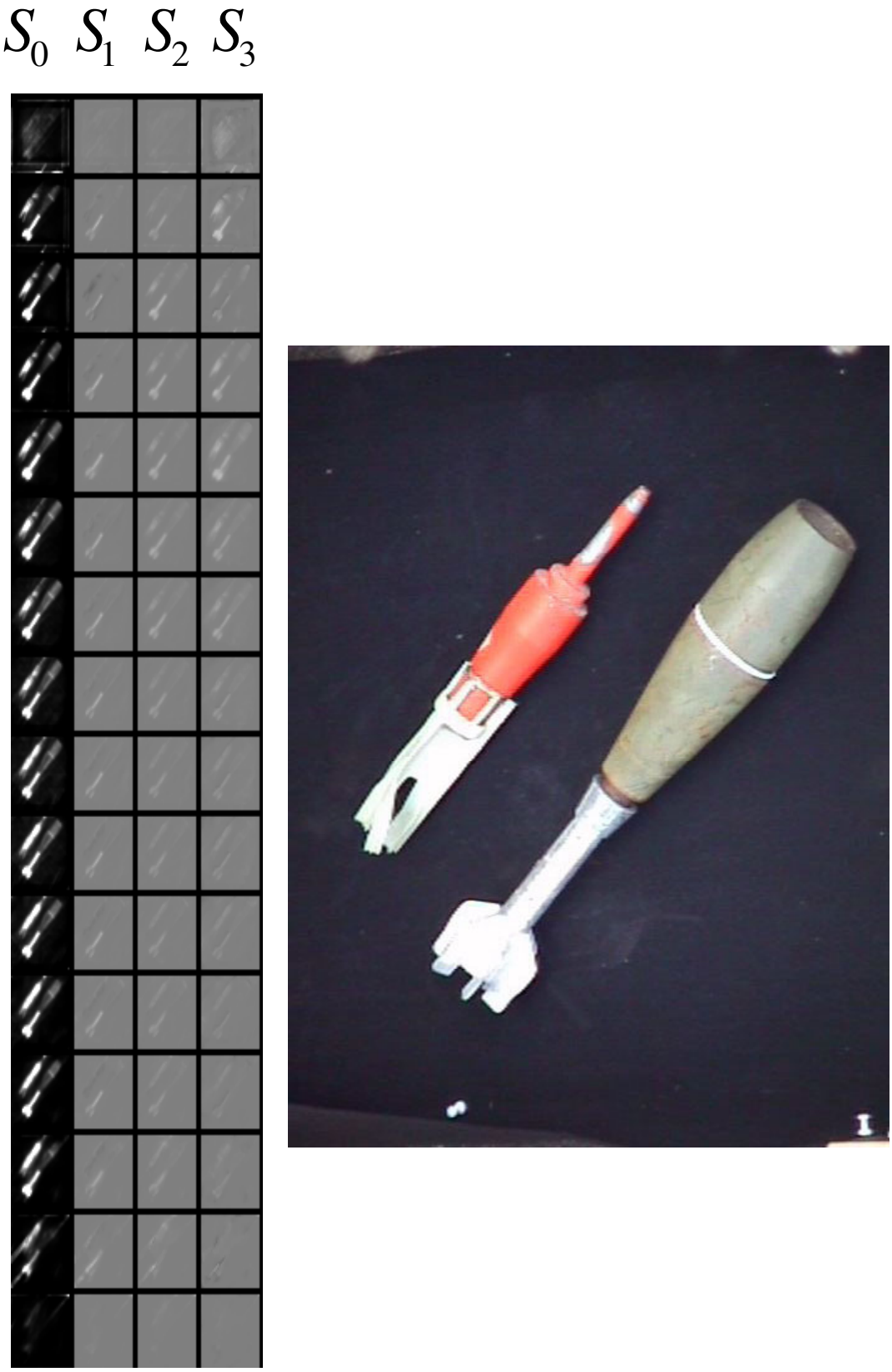

Figure 12. Unstacked Stokes parameter object cubes for a bomblet and a mortar

3 Data Collection

A Portable Measurement Apparatus

Following its initial development, CTISP was limited to use in a very controlled laboratory environment (Miles 1999). During development, the optical hardware remained bolted to an optical bench and was driven by a nearby PC. The data used to generate the Stokes parameter mosaic in Figure 12 were obtained by pointing CTISP through a window toward a large mirror that reflected the images of the bomblet and mortar from where they lay on a parking lot surface into the CTISP optical path.

For the measurements discussed in this report, CTISP has been made somewhat more portable by placing the optical hardware on a heavy-duty tripod as shown on the right side of Figure 13. Illumination for indoor measurements can come from any source like the floodlamp shown on the left side of the figure. The source used for the following measurements was a 500-W blue-coated tungsten bulb.

As currently configured, CTISP measurements are controlled by a laptop computer with a docking station (located on the table at the center of the figure). The docking station is needed to provide a Peripheral Component Interconnect (PCI) slot for the card that controls the operation of the charge-coupled device (CCD) camera. The motor that controls the analyzer wheel is triggered out of the serial port on the laptop. Image storage is facilitated by a 10 Gbyte hard disk. More details on the hardware configuration used to collect CTISP data are given in Appendix B.

The apparatus configuration shown in Figure 13 is what will be referred to as an “in-plane” measurement later in this chapter. The light source, the target(s), and the axis of the CTISP hardware all lie in a plane that is perpendicular to the earth’s surface. The targets in Figure 13 are two flat surfaces on a black background. One surface is a standard reflectance plate, and the other is a green paper folder. Another set of measurements that will be discussed will be those called “90 deg out-of-plane”. In this case, the illumination source was rolled to a position in the foreground of Figure 13 so that the angle between the axis of the bulb reflector and the axis of the CTISP hardware was about 90 deg. Both the

bulb and the tripod-mounted CTISP hardware are pointed downward at an angle of approximately 45 deg.

Figure 13. Portable CTISP hardware configuration

Reflectance Standards

Figures 14-21 contain Stokes parameter data for four different diffuse reflectance standard surfaces. Manufactured by Labsphere, Inc., North Sutton, NH, these four Spectralon Reflectance Targets have design reflectance ratios of 2, 25, 50, and 75 percent. It is important to note that these plates were not designed as polarization reflectance standards, only as spectral reflectance standards. Being diffuse reflectors, it is extremely difficult to say what effect surface composition and roughness will have on the polarization properties of the reflected flux. Nevertheless, for completeness, all of the measured Stokes parameters are displayed in this section.

Consider, first, the in-plane S_0 data shown in Figure 14. One can immediately draw two conclusions about the response of CTISP in its current configuration. First of all, the spectral response of the FPA is not flat as one might desire. That is a function of the sensitivity of the FPA elements; apparently

they are more sensitive at longer wavelengths. The second observation is that the UV and IR filters in the CTISP optical path have quite a spillover effect on decreasing the intensities of light at the short and long wavelength ends of the visible spectrum, respectively. These data were used to justify displaying only data from 480 to 700 nm in later charts.

Figures 15-17 contain the other in-plane Stokes parameter values for the four reflectance plates. Note that each reflectance standard exhibits linear and circular polarization responses. As stated above, one does not know the polarization effects of the diffuse reflectance standards; therefore, there is no way to know whether or not the displayed results have any particular meaning. However, one observation is worth noting. It appears that the signal-to-noise ratio for the 2-percent standard may be low enough that such a standard would probably be useless as a normalizing factor for measurements of other targets.

Out-of-plane measurements for the four reflectance standards are shown in Figures 18- 21. These data behave similarly to the in-plane data in all respects. Superimposed on Figure 18 is the spectral response of the 25-percent reflectance standard as measured by a Jobin Yvon THR640 Spectrometer. The spectrometer does not have the long-wavelength sensitivity problem that the CTISP FPA possesses; therefore, its reflectance measurements provide a good spectral characterization of the light source used for all of the measurements reported here.

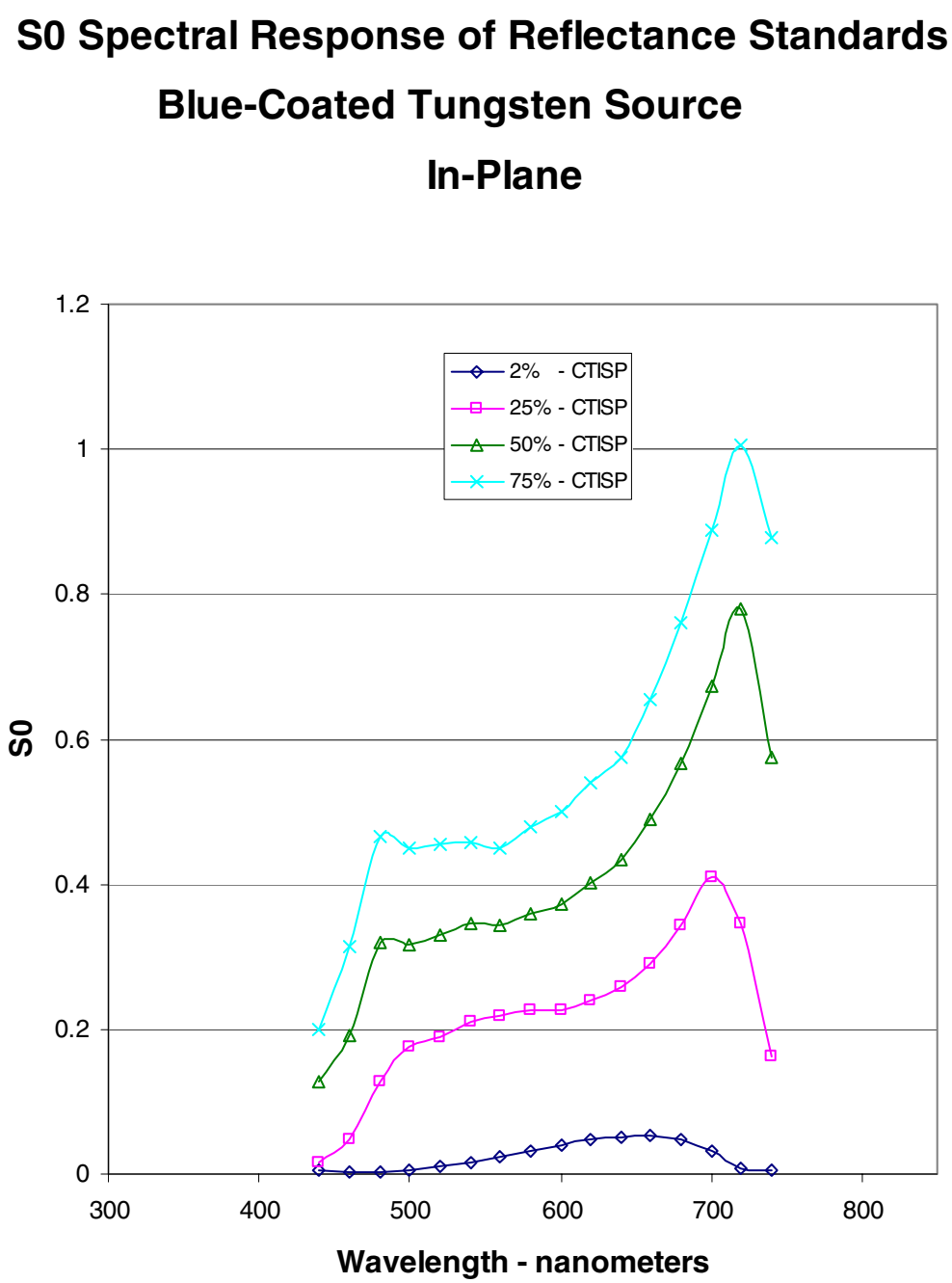

Figure 14. In-plane S0 spectral response of reflectance standards

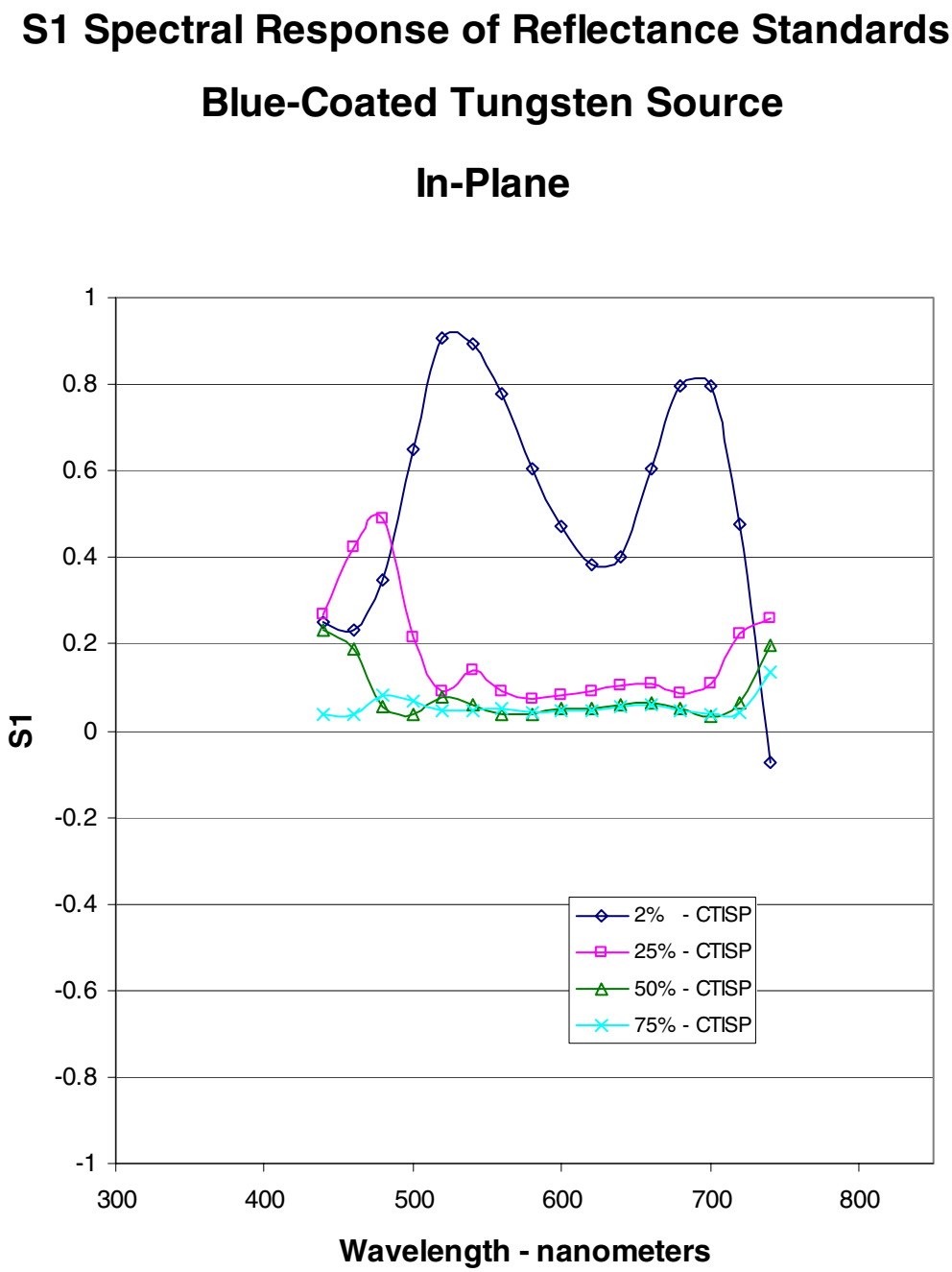

Figure 15. In-plane S1 spectral response of reflectance standards

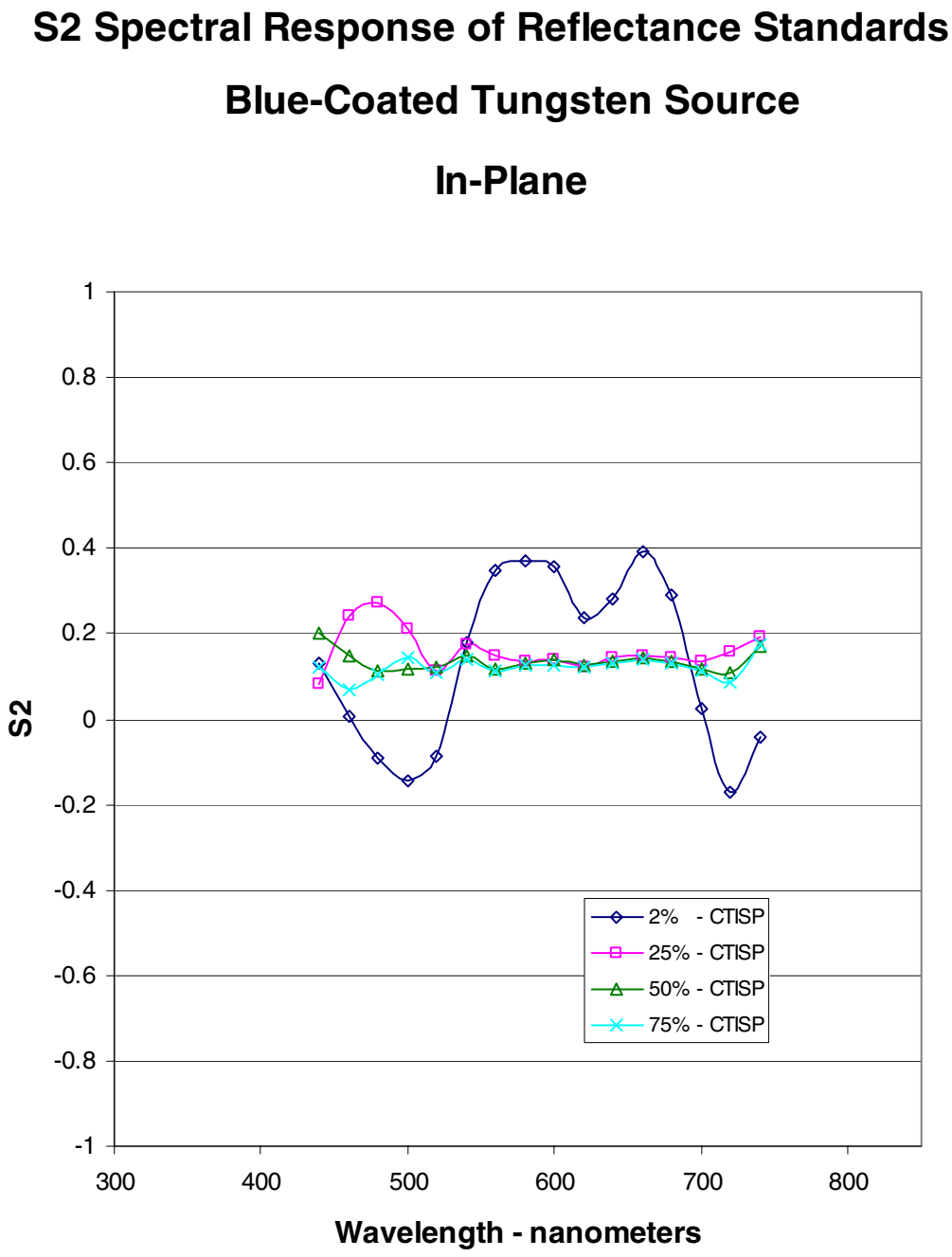

Figure 16. In-plane S2 spectral response of reflectance standards

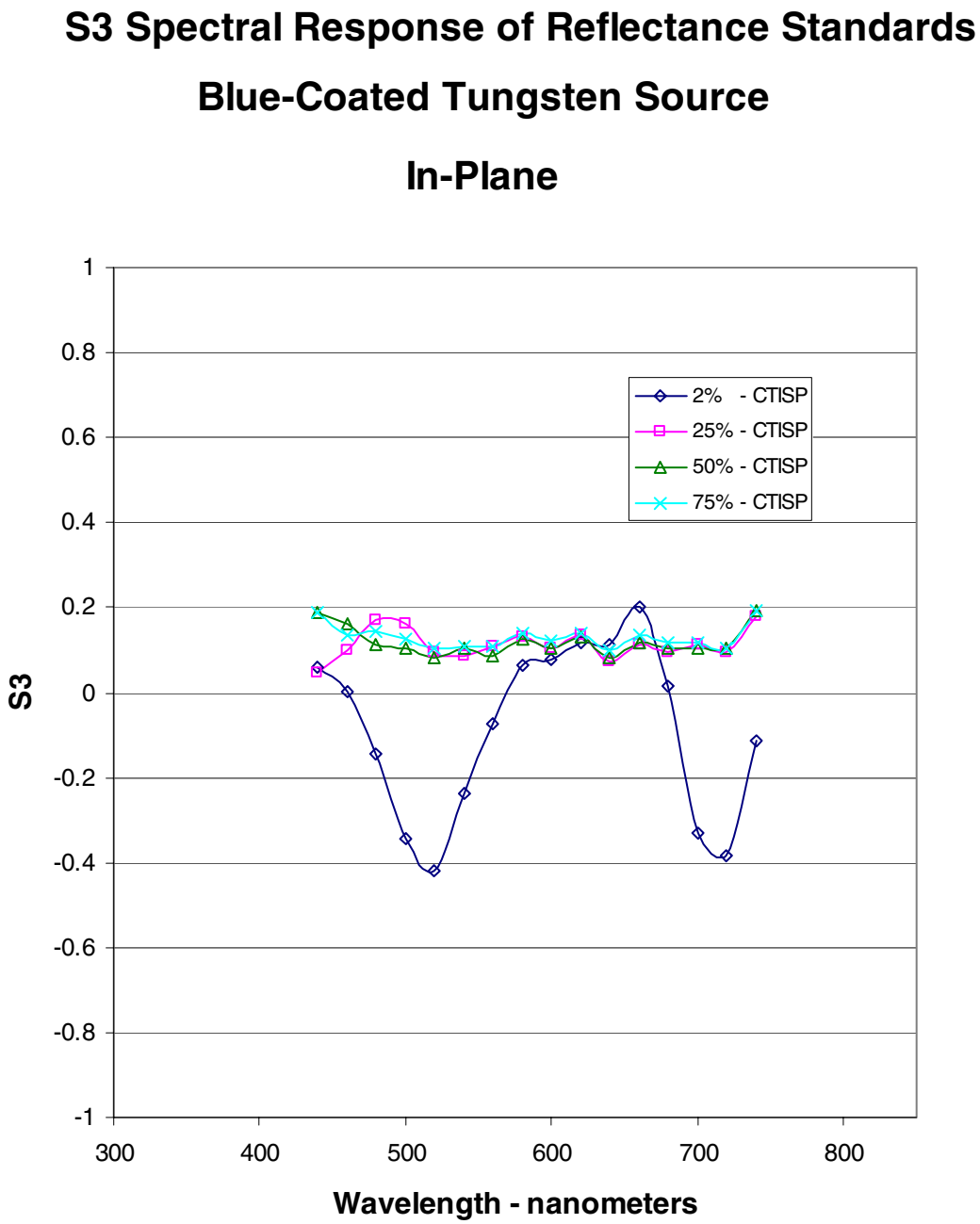

Figure 17. In-plane S3 spectral response of reflectance standards

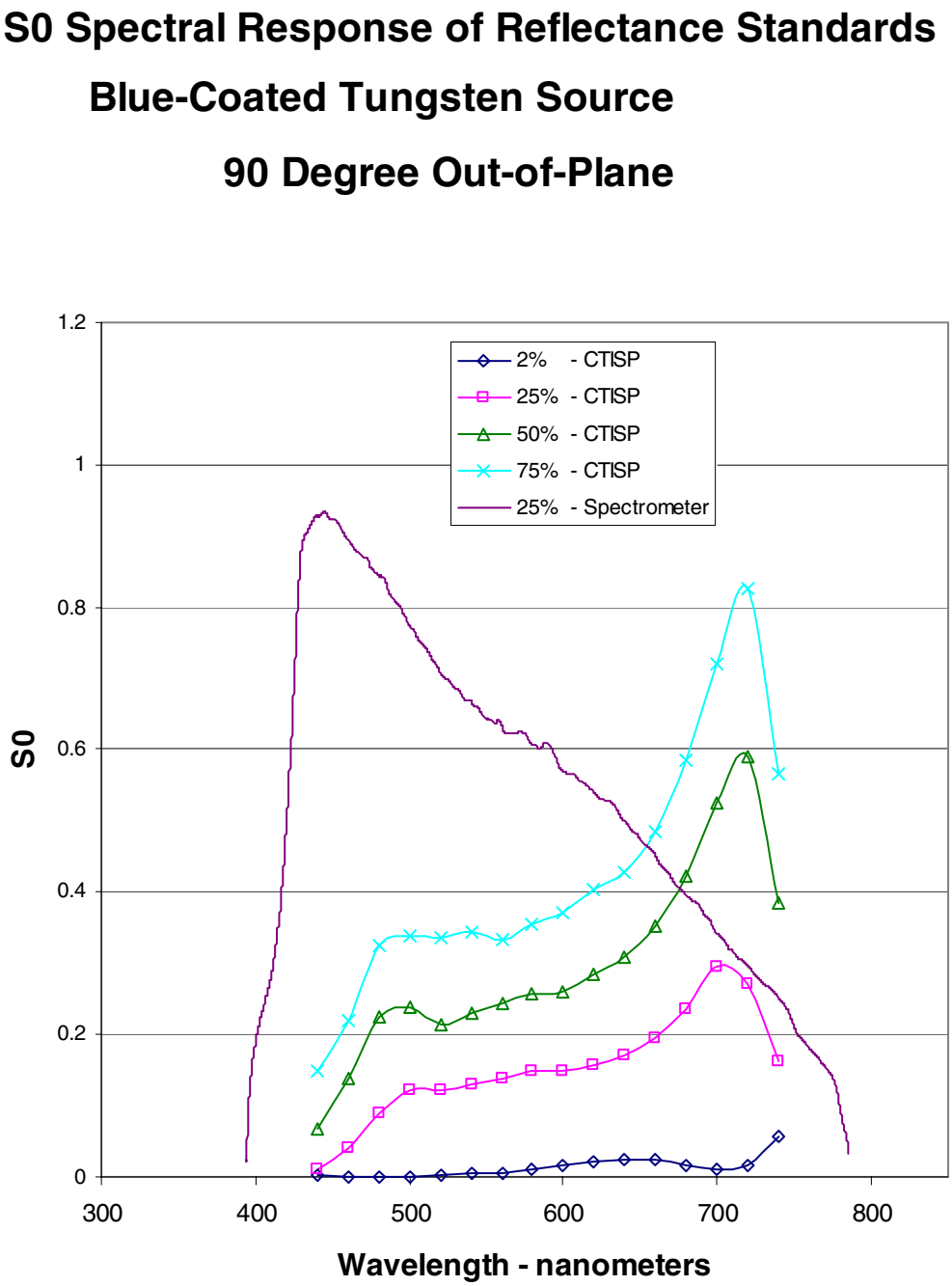

Figure 18. Out-of-plane S0 spectral response of reflectance standards

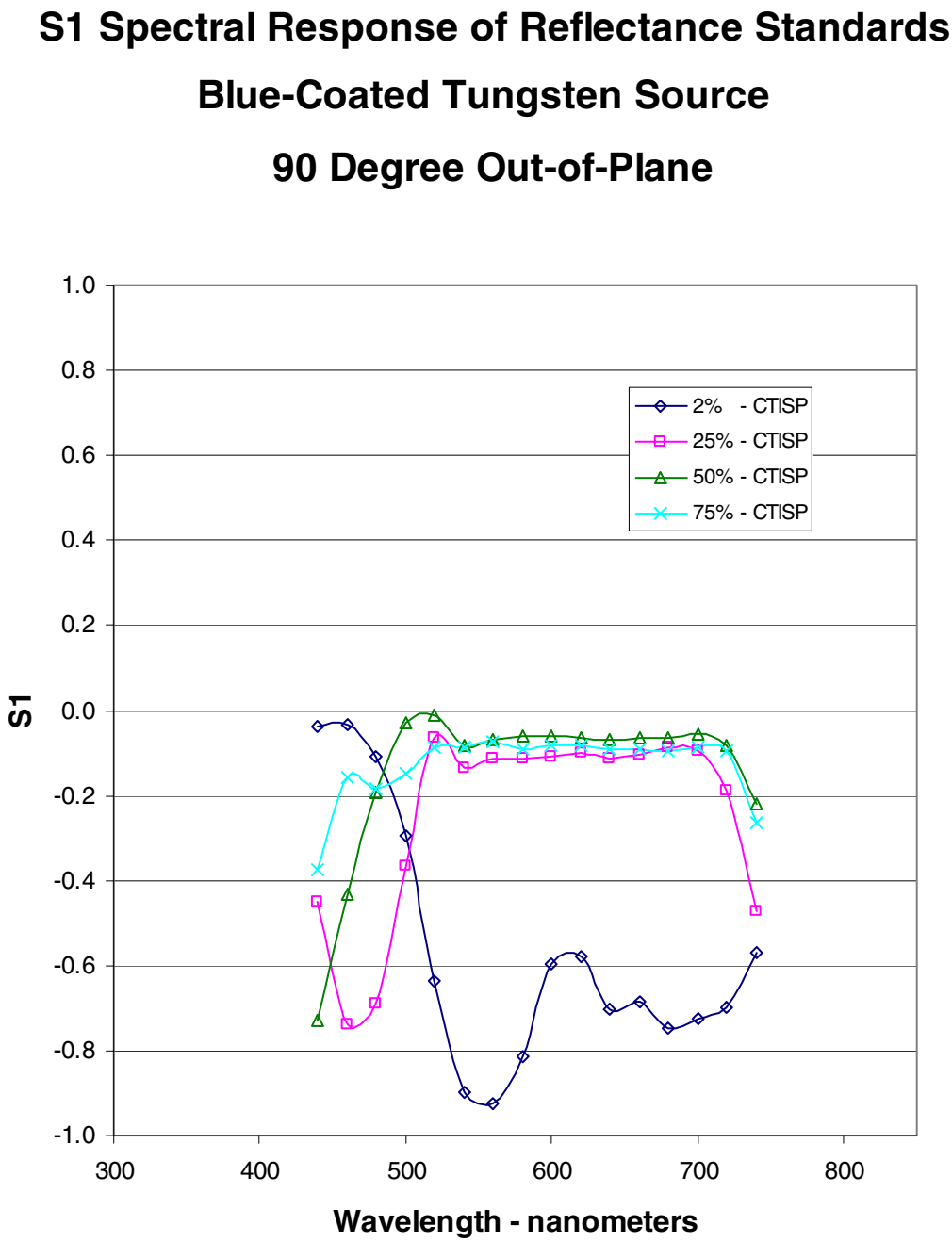

Figure 19. Out-of-plane S1 spectral response of reflectance standards

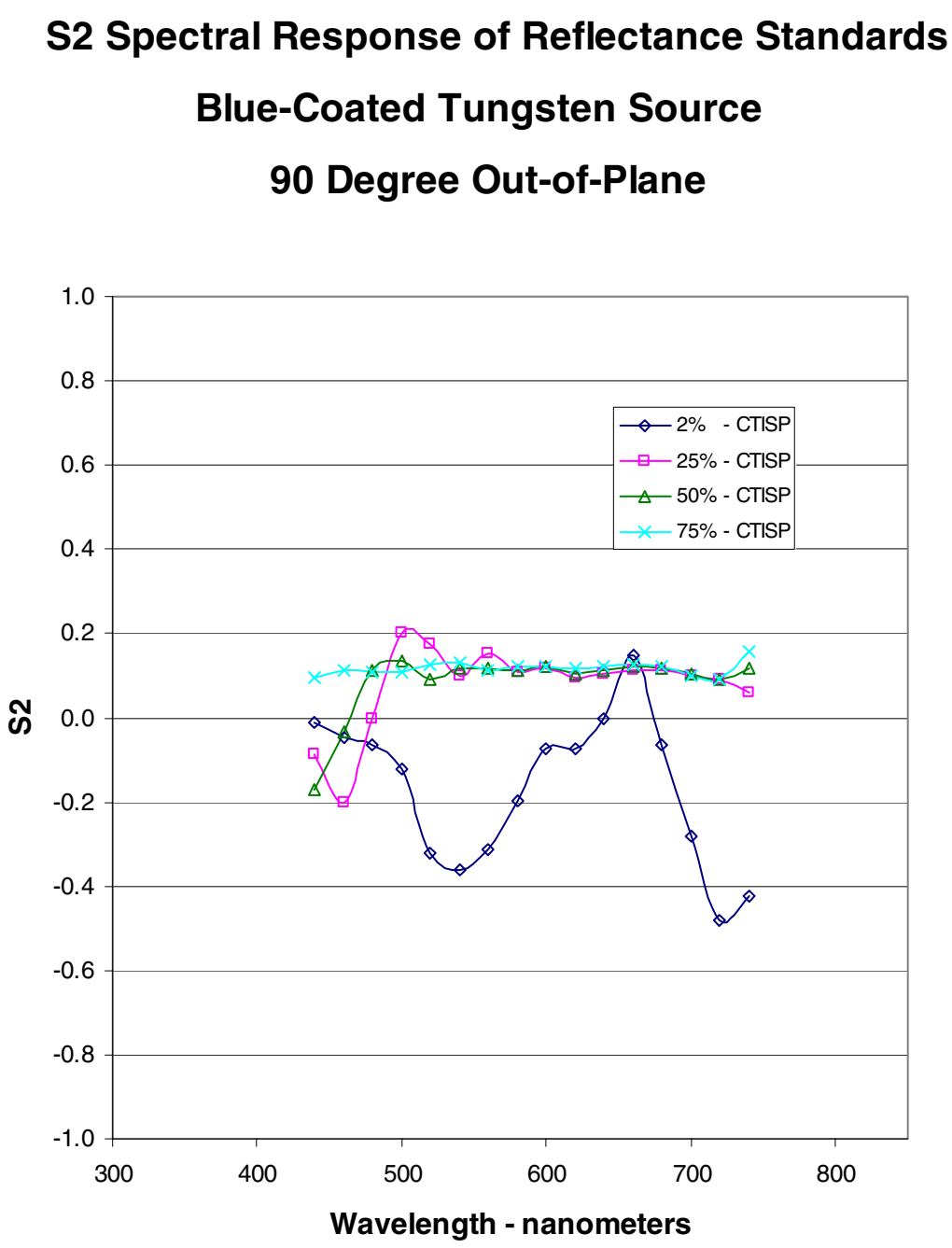

Figure 20. Out-of-plane S2 spectral response of reflectance standards

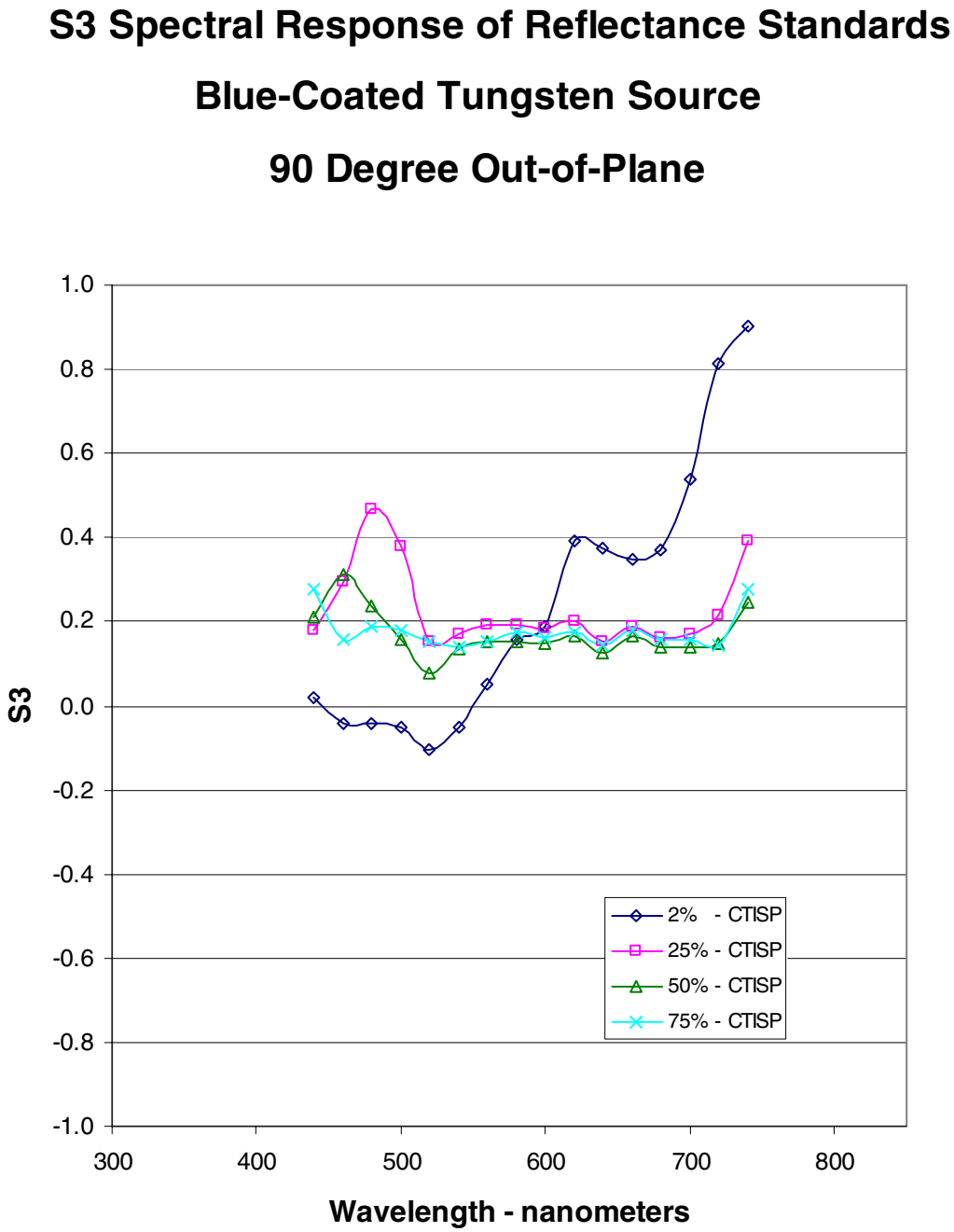

Figure 21. Out-of-plane S3 spectral response of reflectance standards

CTISP-Spectrometer Comparisons

One test of CTISP performance that can be easily performed is to measure the spectral exitance of surfaces that have also been viewed by a reliable laboratory spectrometer. In Stokes parameter terminology, these will be S_0 measurements. Four surfaces were chosen for comparing CTISP measurements to spectrometer measurements. These included a bright green paper, referred to as the "Green Folder" in the following charts, and three metal plates coated with special paints that were used in another sensor development program. The three plates will be referred to as "Plate 1," which was supposed to be a light tan color but appears to be more of a very light olive color, "Plate 9," which was painted a reddish-brown color, and "Plate 12," whose color was a deep forest green. Plates 1 and 9 were very smooth to the touch, while the surface of Plate 12 was much rougher. No quantitative surface roughness measurements were obtained.

Figure 22 contains the results of out-of-plane measurements of these four surfaces by the CTISP hardware (symbols and dashed lines) and the Jobin Yvon THR640 spectrometer (solid lines). From this point on, only 12 CTISP wavelength band measurements will be displayed (480 to 700 nm) because of the filter-induced drop-off problem discussed in the previous section. CTISP and spectrometer data were adjusted to have matching intensities at 580 nm to more readily compare the shapes of these spectral responses.

Generally speaking, CTISP and spectrometer data compared quite well over this range of wavelengths. If these data had been normalized at a higher wavelength, the CTISP response would have been consistently lower than that of the spectrometer. How much of that behavior can be attributed to the short wavelength lack of sensitivity for the CTISP FPA is open to conjecture.

One sees that the spectral response of the coated plates is relatively flat, and, with hindsight, one could argue that better surfaces could have been chosen for this test. Brightly colored paper would probably have provided more distinctive spectral responses.

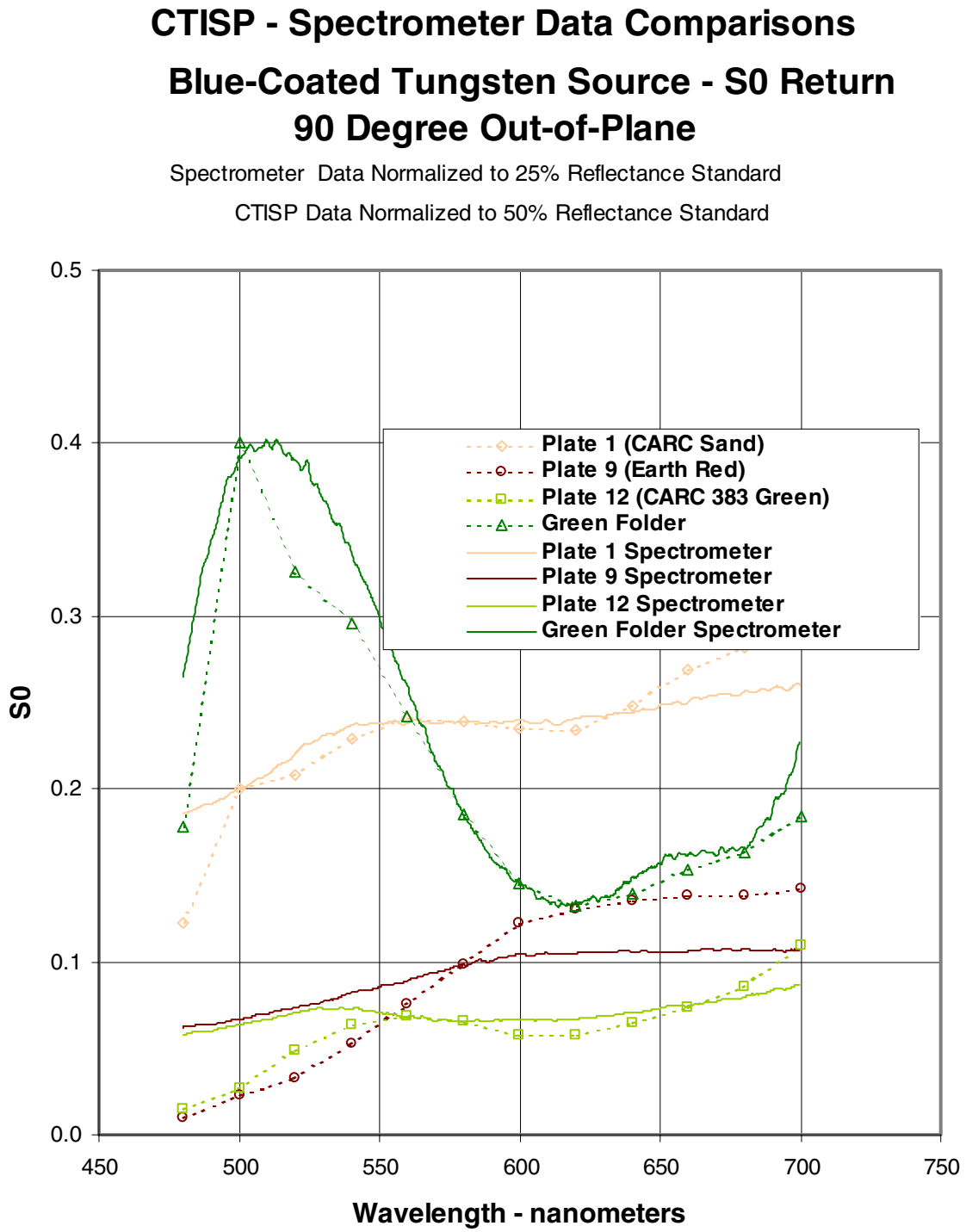

Figure 22. CTISP-spectrometer comparisons of colored surfaces

CTISP Polarization Data for Colored Surfaces

This and the following section contain all of the Stokes parameter measurement data that have been collected with CTISP on light reflected from colored surfaces and from nonstandard surfaces, respectively. Table 1 lists the figure numbers for the colored surface measurements. These surfaces are the three coated aluminum plates and the green paper folder whose total reflectances were compared to spectrometer results in the previous section.

Table 1
Stokes Parameter Spectra Charts for Colored Surface Measurements

Light Source Polarization	In-Plane Measurements	Out-of-Plane Measurements
Random	Figure 23 - Figure 26	Figure 27 - Figure 30
Horizontal	Figure 31 - Figure 34	Figure 35 - Figure 38
Vertical	Figure 39 - Figure 42	Figure 43 - Figure 46

The “Light Source Polarization” column requires further explanation. Random polarized light is simply the light that came from the blue-coated tungsten bulb and was focused on the targets by the scoop shown in Figure 13. Horizontally and vertically polarized light was produced by placing a sheet of Polaroid between the light scoop and the illuminated target.

Drawing on the powerful lessons of hindsight, it has become quite clear that these measurements, while demonstrating some predictable behavior, have serious shortcomings that must be addressed in the next phase of CTISP development. Specific concerns are:

a. The polarization properties of the light source used for indoor measurements are not known. It is possible that the scoop, in combination with the filament design of the bulb, generates preferred polarization directions (particularly through the phenomenon of polarization by reflection). One way to answer this concern would be to point CTISP directly into the light scoop to measure its Stokes parameters.

b. The Polaroid sheet was not precisely positioned for producing horizontally and vertically polarized light. There is some uncertainty as to the quality of the sheet and as to the exact orientation of its axis. Axis orientation could be precisely set by measuring the Stokes parameters of optically flat surfaces, both in-plane and out-of-plane.

c. Coupled to item 'b' is the concern that the CTISP hardware mounted on the tripod is properly oriented, which includes the orientation of the filters on the analyzer wheel. Given that the polarization properties of the light source were well understood, or possibly by using the sun as the light source, one should be able to make in-plane and out-of-plane Stokes parameter measurements of an optically flat surface to ensure that the geometry of the CTISP system is correct.

The bottom line of all of these concerns is that analysis of the measurements reported in this and the next section suffer from the lack of polarization standards.

In spite of these shortcomings, some qualitative observations of the Stokes parameter measurements of colored surfaces can be made. For example, even though the polarization properties of the colored surfaces are not known, one should expect that in-plane S_1 data for horizontally polarized light should be positive (Figure 30), while out-of-plane data should be negative (Figure 34); when viewed out-of-plane, horizontally polarized light should appear vertically polarized. Similarly, in-plane S_1 data for vertically polarized light should be negative (Figure 38) while out-of-plane S_2 data should be positive (Figure 43). The reason for the latter observation is tied to the measurement geometry. Recall from Figure 11 and the word description of the measurement setup that a vertically polarized source being viewed out-of-plane will appear to have a large component at 45 deg.

Another observation that can be made for these relatively smooth surfaces is the evidence for the phenomenon of polarization-by-reflection, referred to in the introductory chapter. S_1 data for randomly polarized light should be positive for both in-plane measurements (Figure 22) and for out-of-plane measurements (Figure 26). However, the data (Figure 26) show that the out-of-plane measurements see vertically polarized reflections. If the light source is truly randomly polarized, and the surface is relatively smooth, there should be a strong horizontally polarized component of reflected energy from all view angles. These data indicate that the source may have a strong horizontal component. The wavelength dependency of these observations is not yet understood but may be a complicated function of system geometry, surface roughness, and surface chemistry.

While there are genuine concerns about the behavior of these CTISP measurements, they represent the only data that have been collected since the apparatus was separated from the optical bench on which it was developed. They must be reported, and further developments of the system and in processing of the data are required for complete analysis.

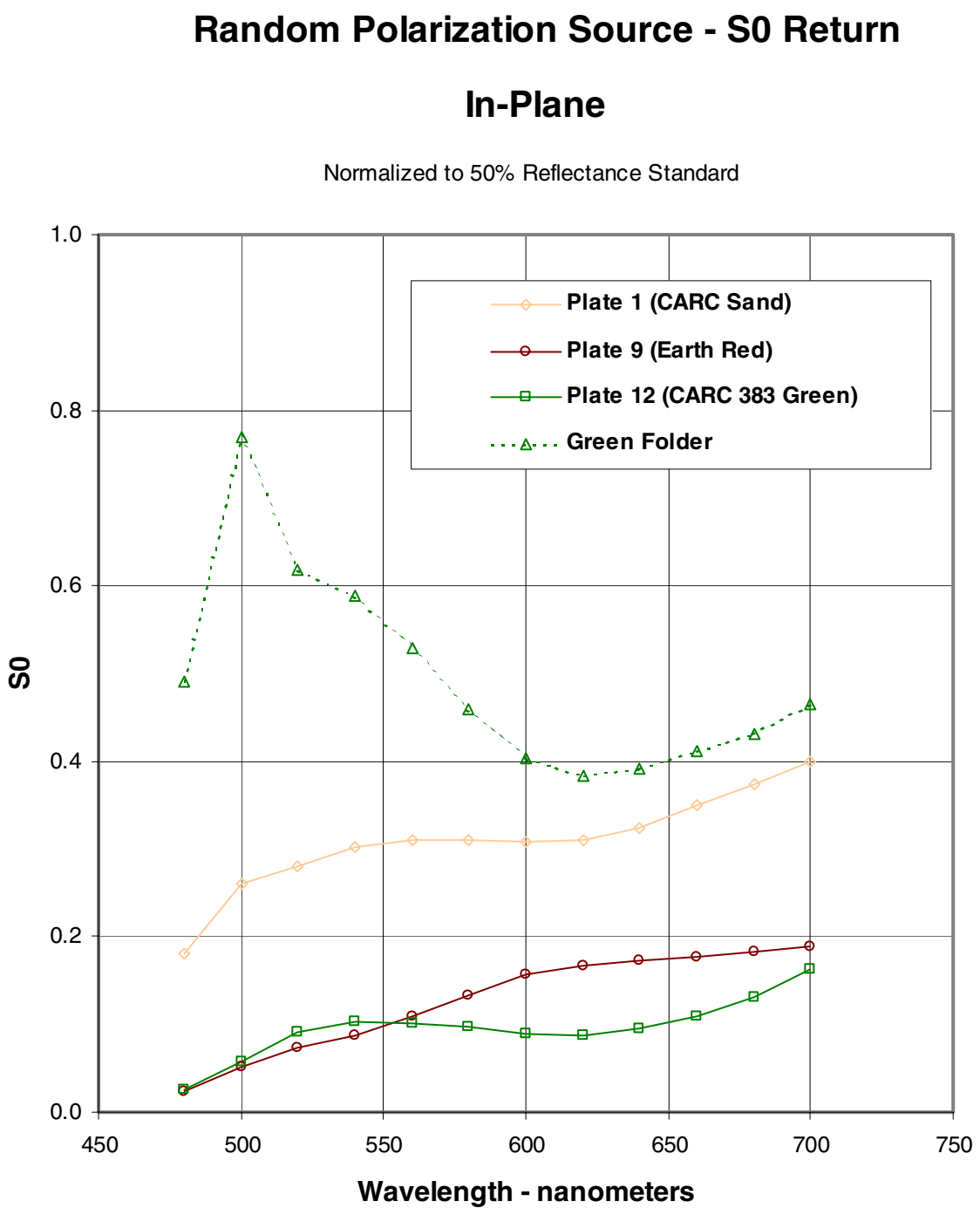

Figure 23. In-plane S0 spectral response of colored surfaces - random source

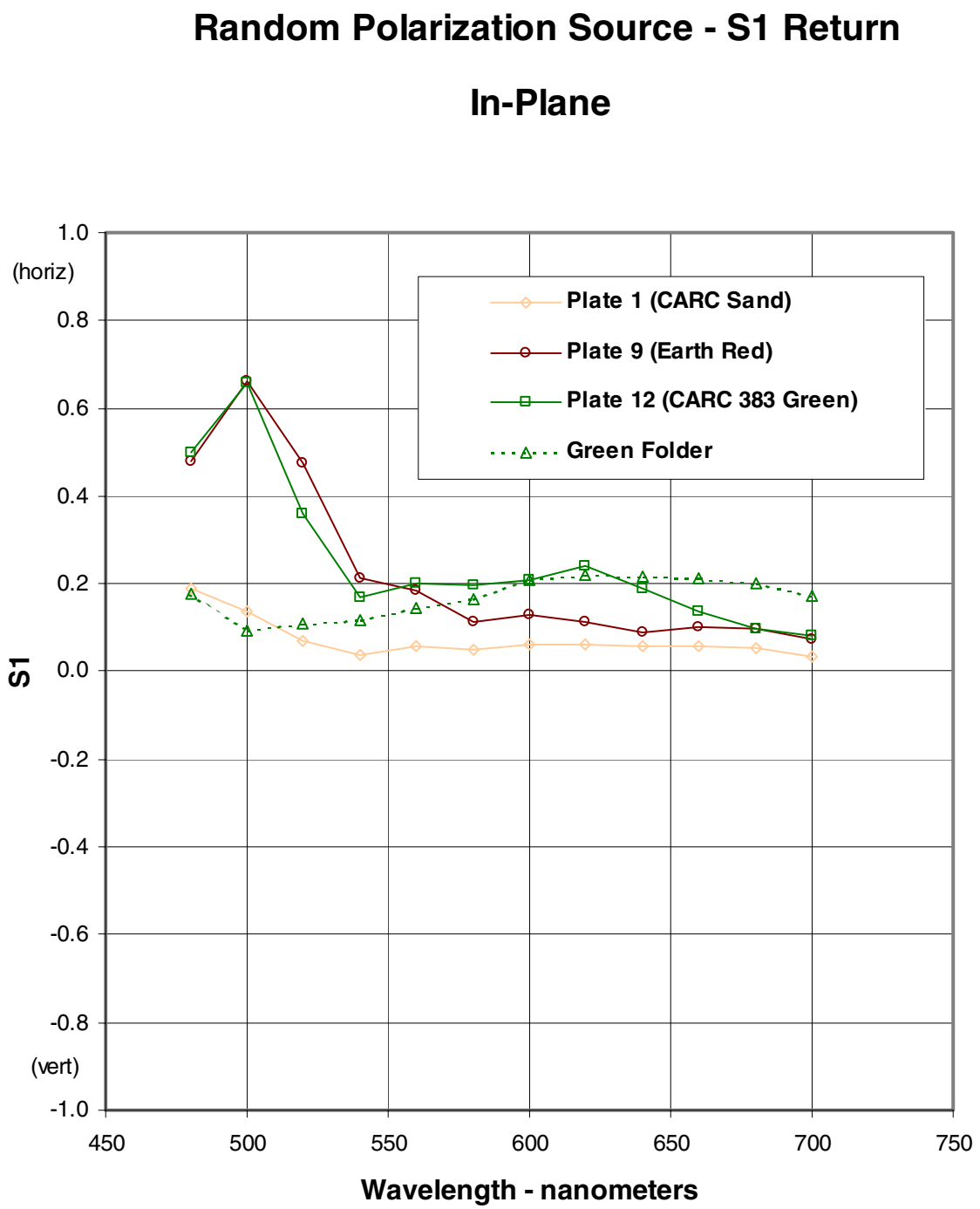

Figure 24. In-plane S1 spectral response of colored surfaces - random source

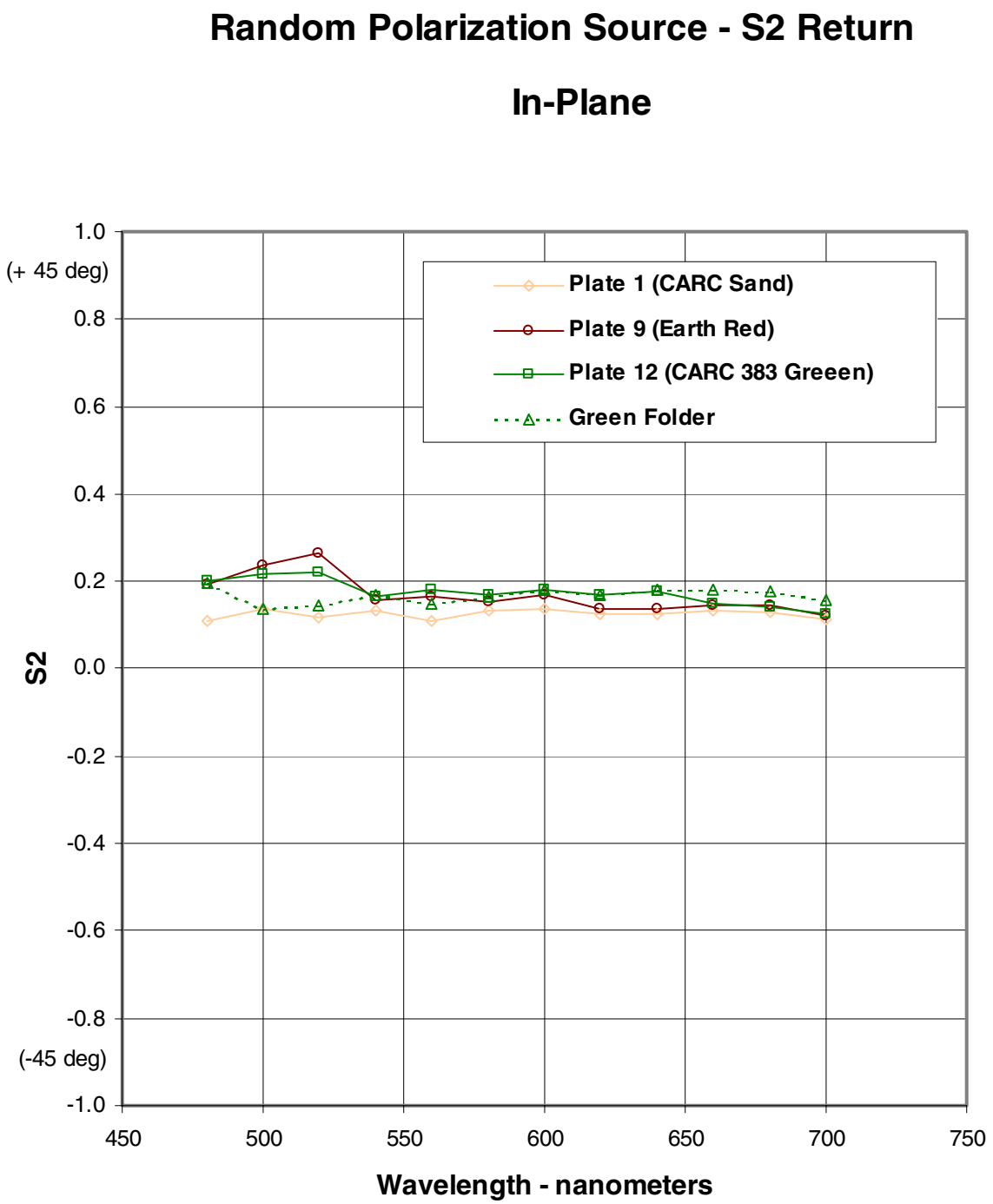

Figure 25. In-plane S2 spectral response of colored surfaces - random source

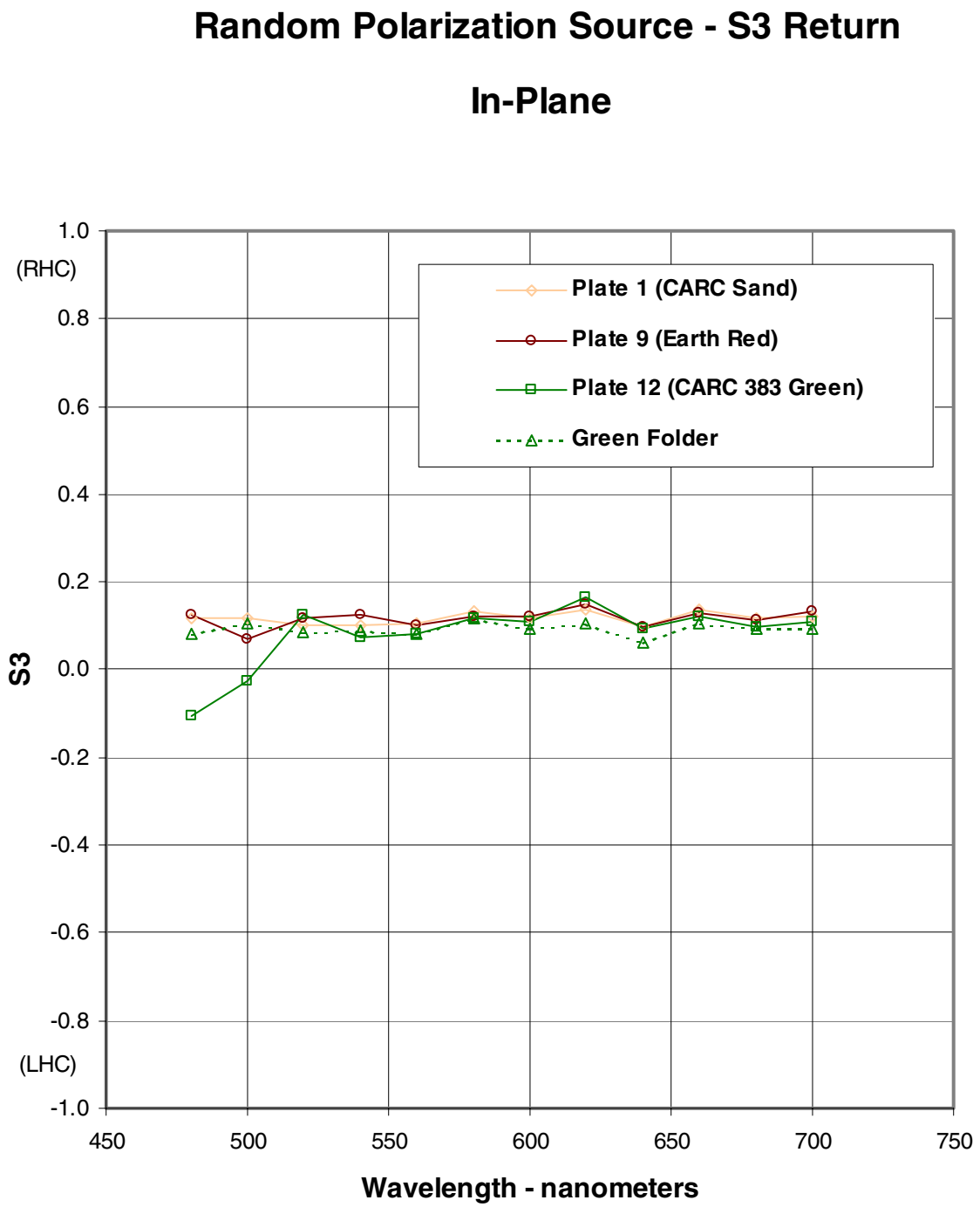

Figure 26. In-plane S3 spectral response of colored surfaces - random source

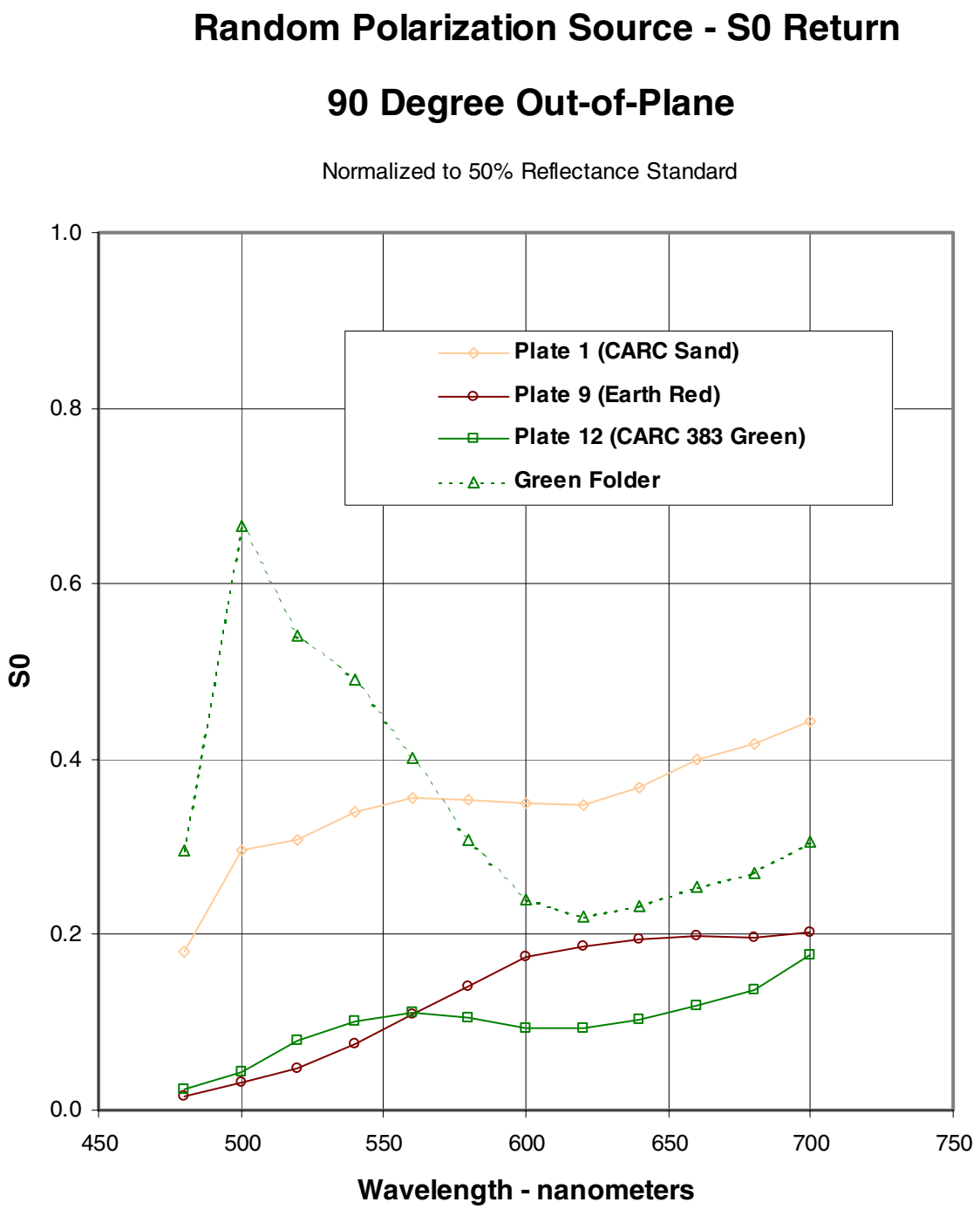

Figure 27. Out-of-plane S0 spectral response of colored surfaces - random source

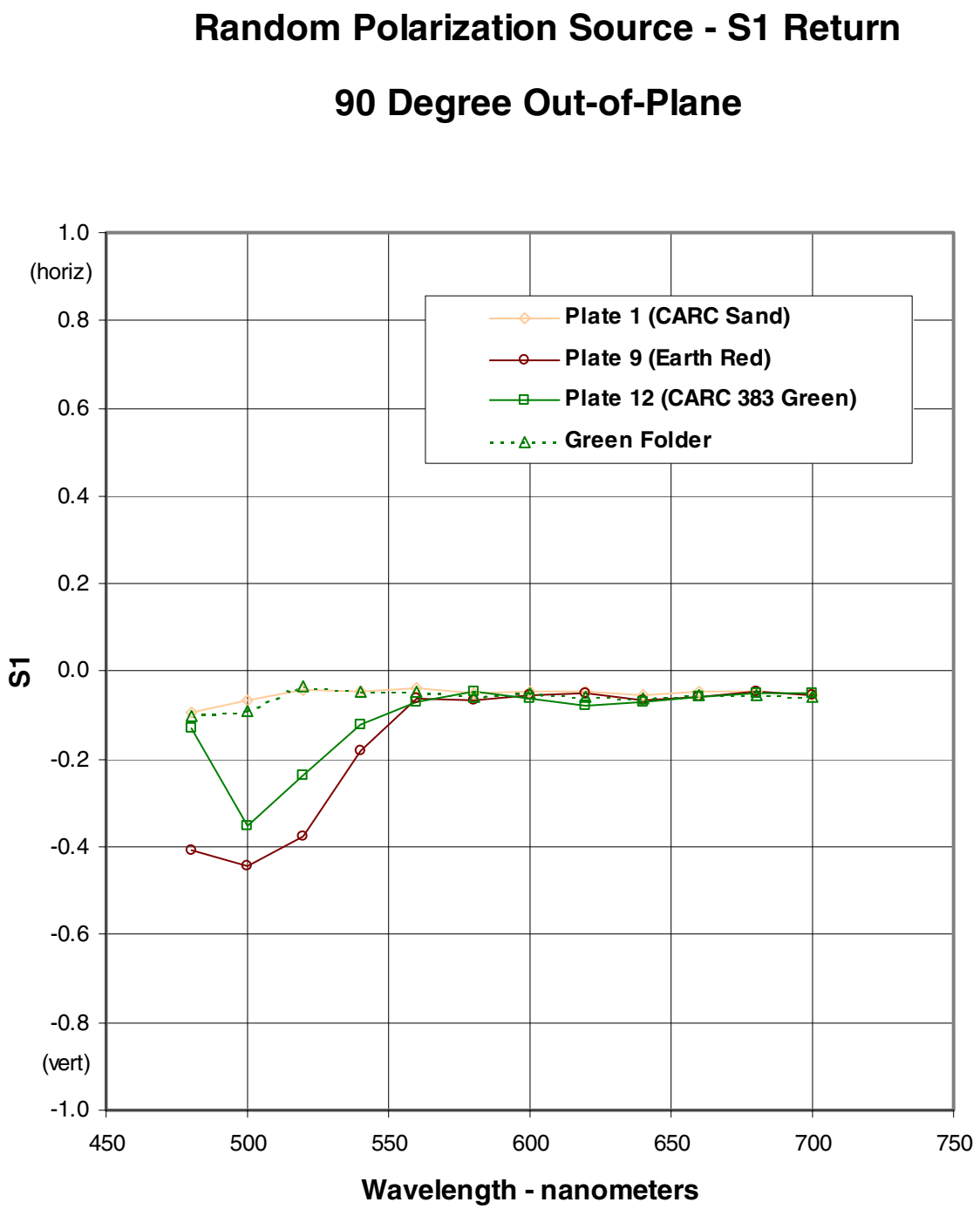

Figure 28. Out-of-plane S1 spectral response of colored surfaces - random source

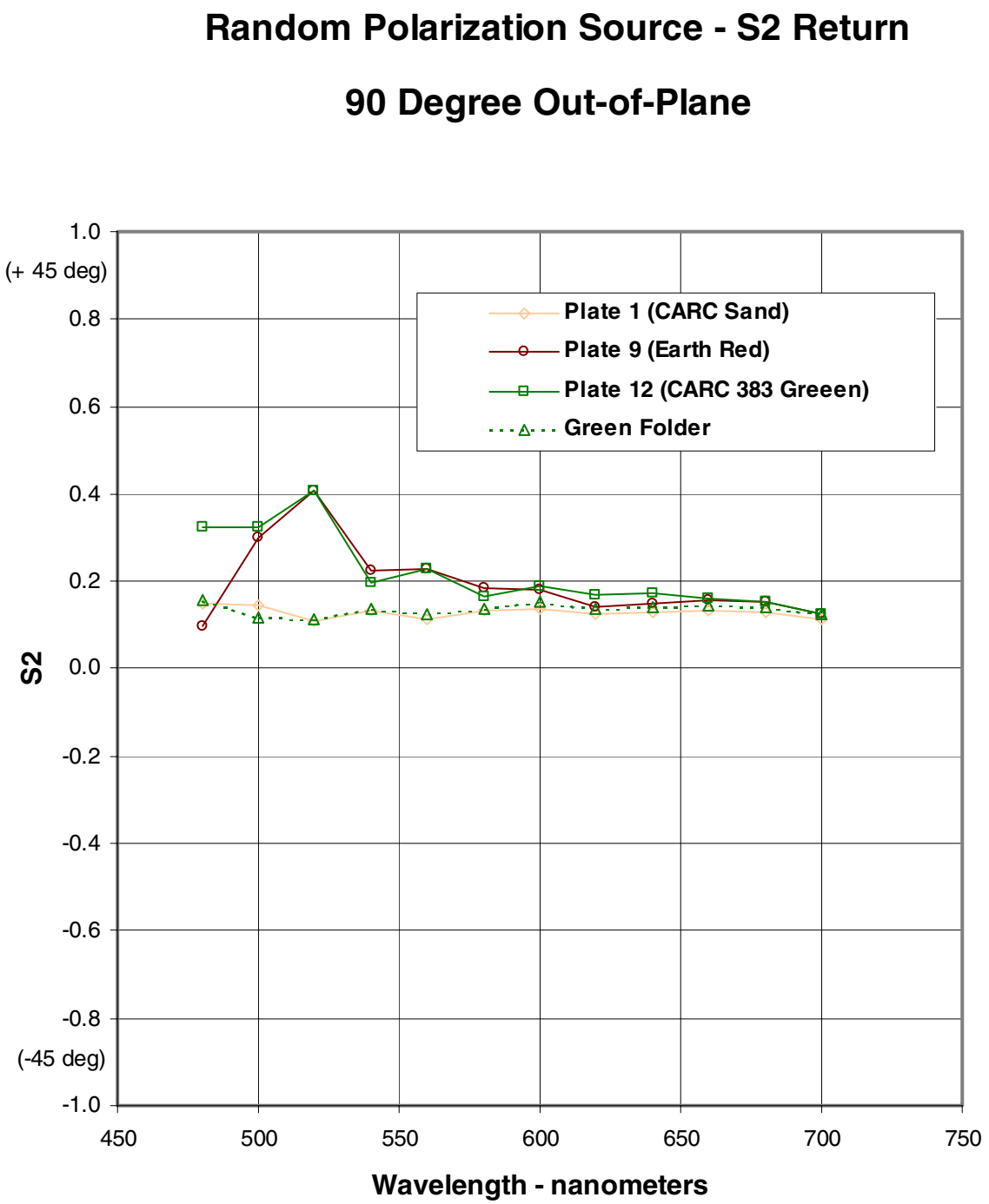

Figure 29. Out-of-plane S2 spectral response of colored surfaces - random source

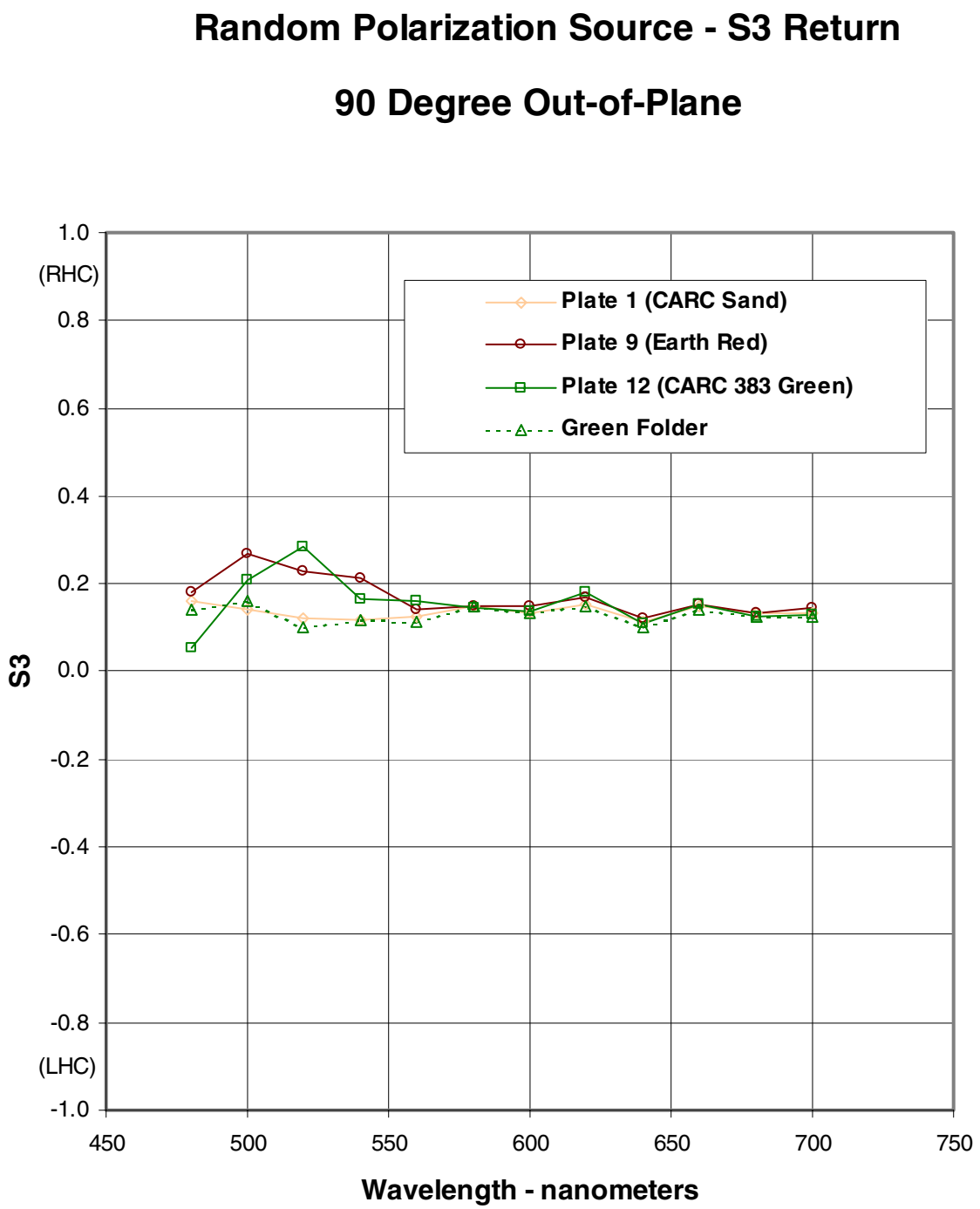

Figure 30. Out-of-plane S3 spectral response of colored surfaces - random source

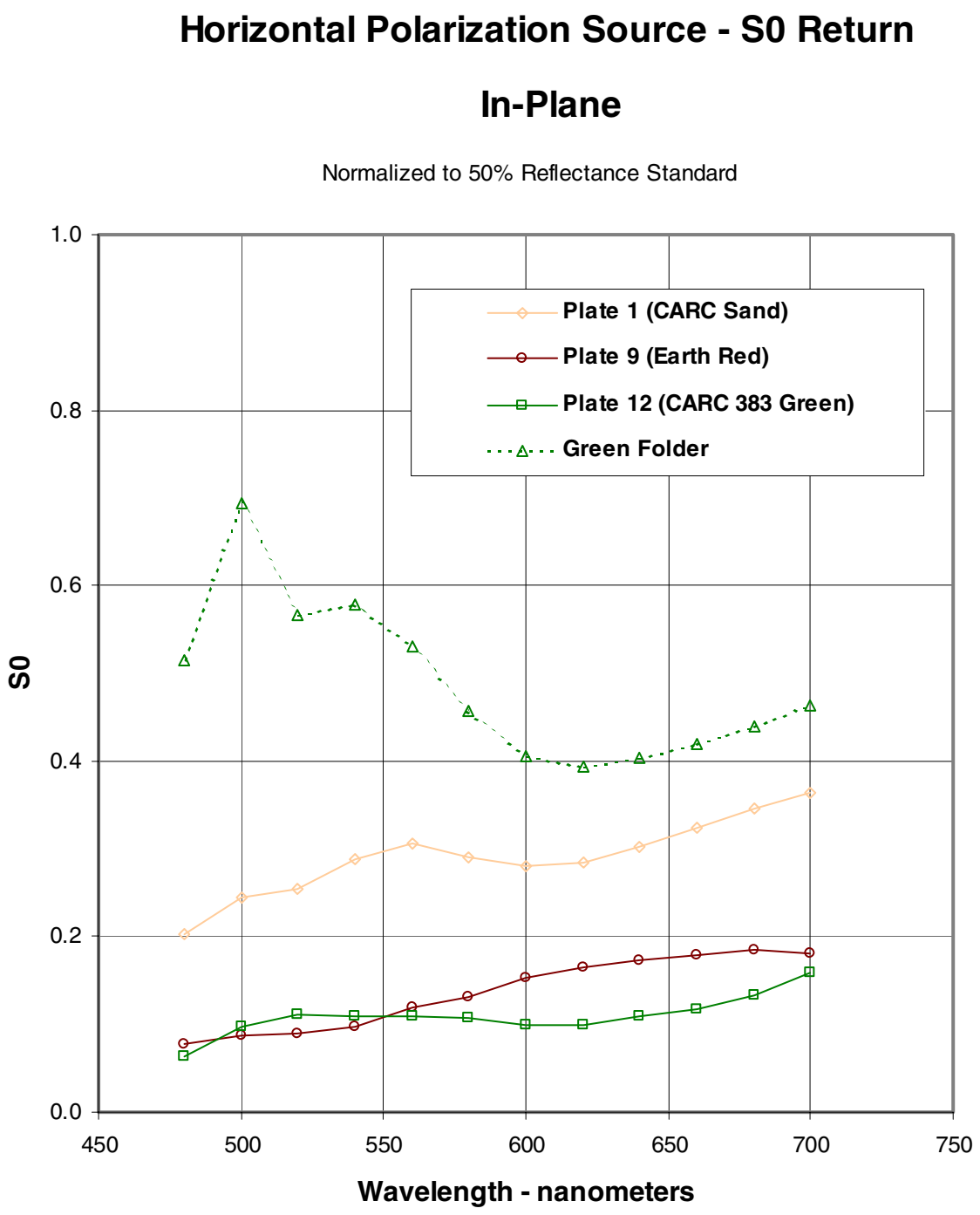

Figure 31. In-plane S0 spectral response of colored surfaces - horizontal source

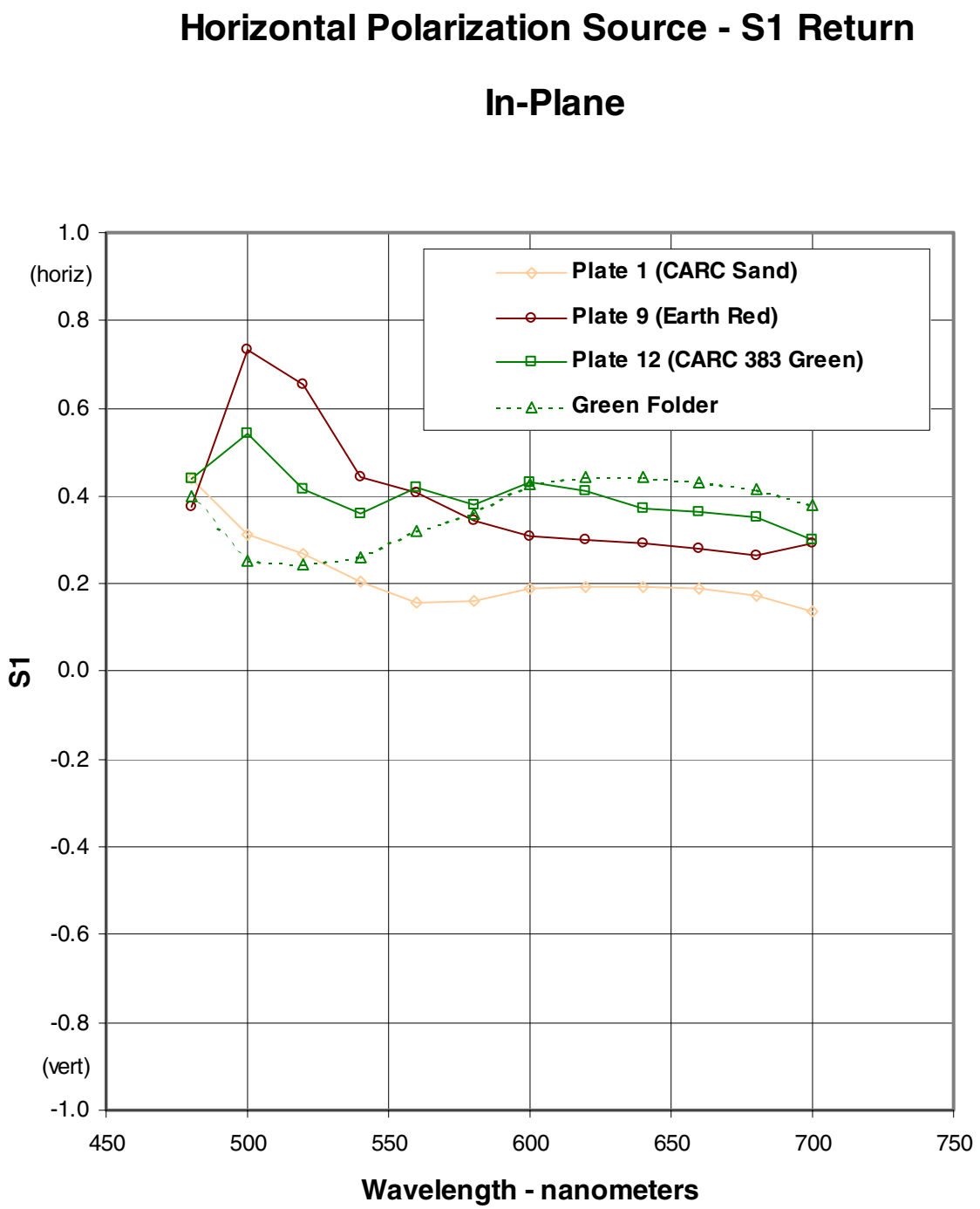

Figure 32. In-plane S1 spectral response of colored surfaces – horizontal source

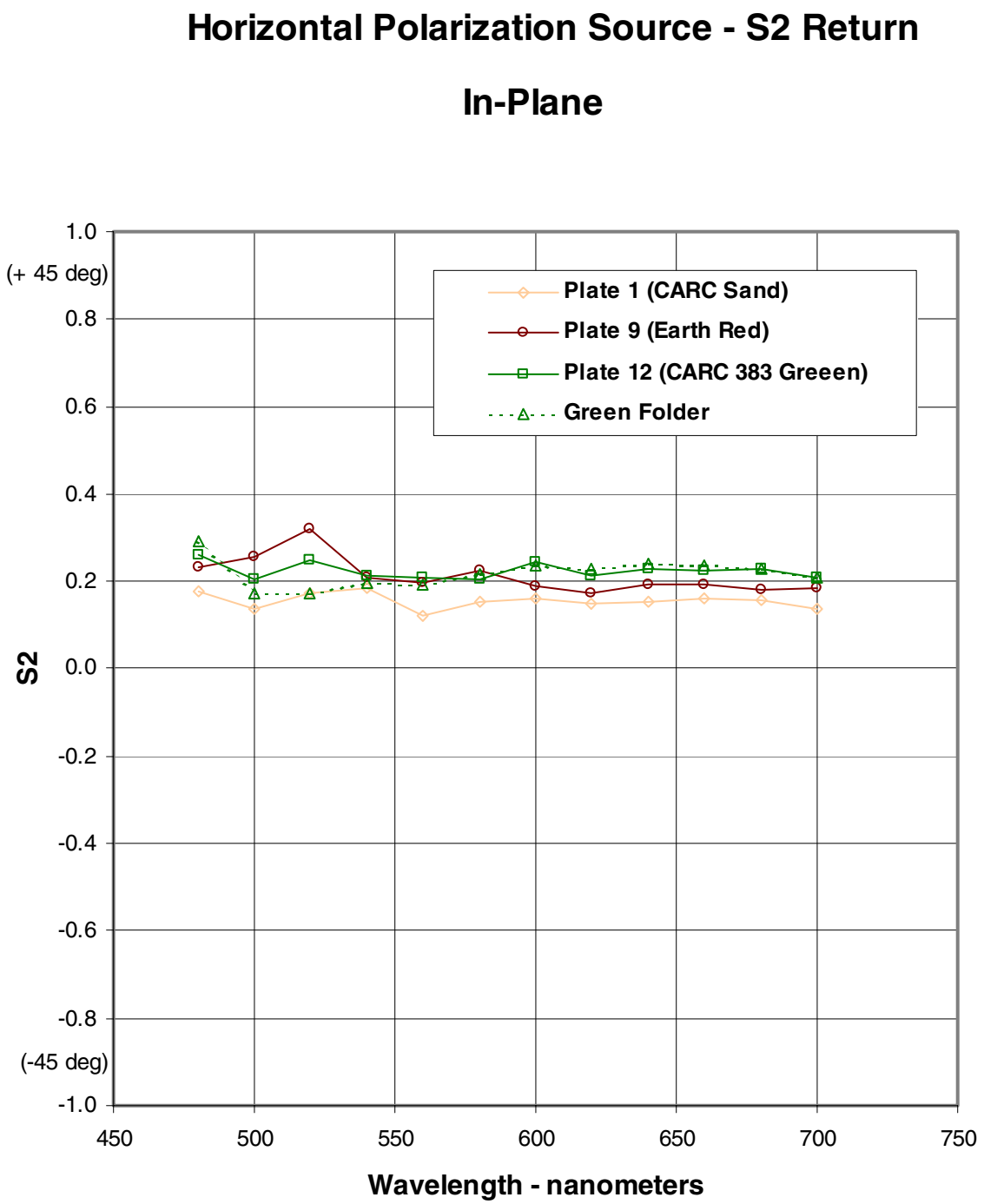

Figure 33. In-plane S2 spectral response of colored surfaces - horizontal source

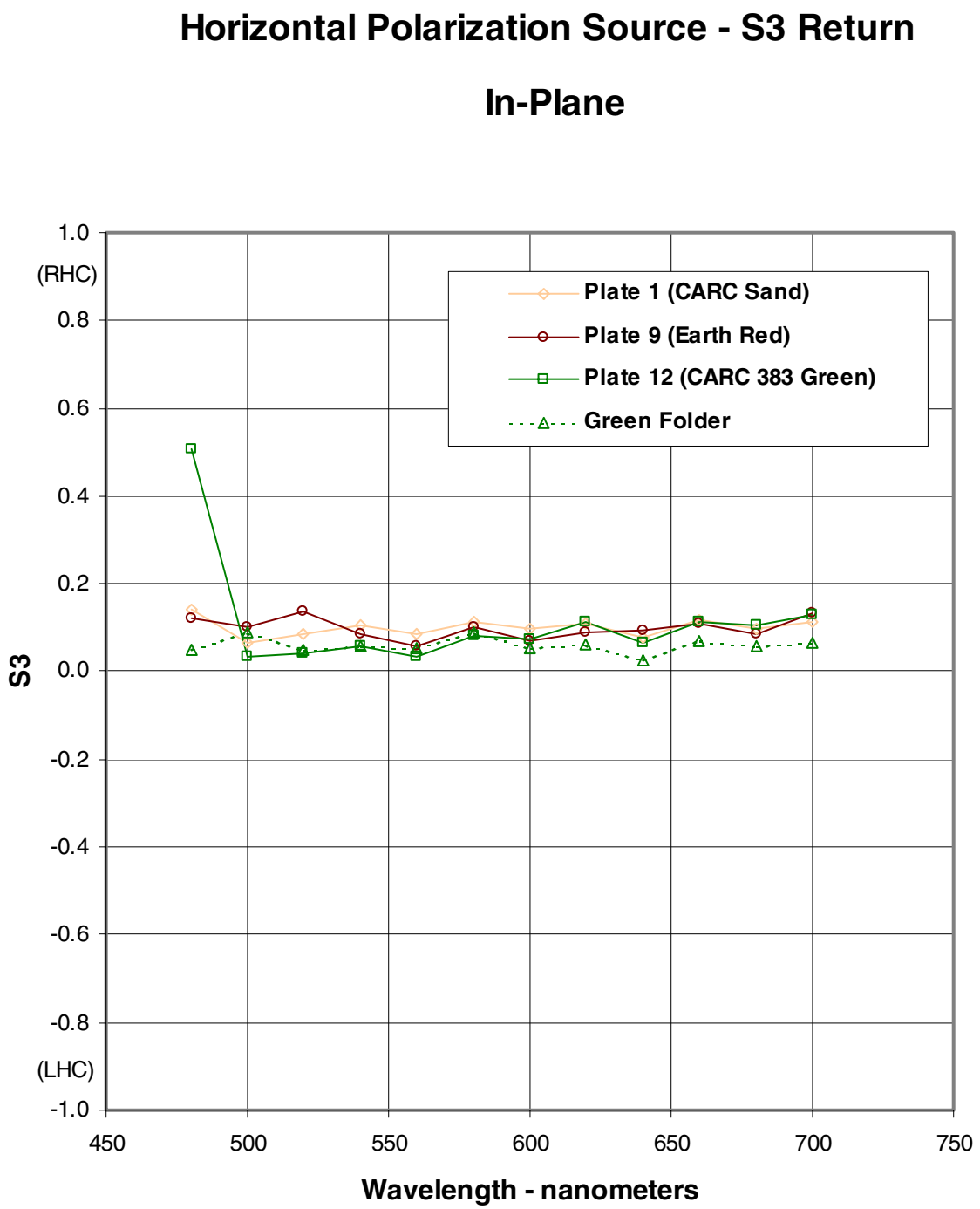

Figure 34. In-plane S3 spectral response of colored surfaces - horizontal source

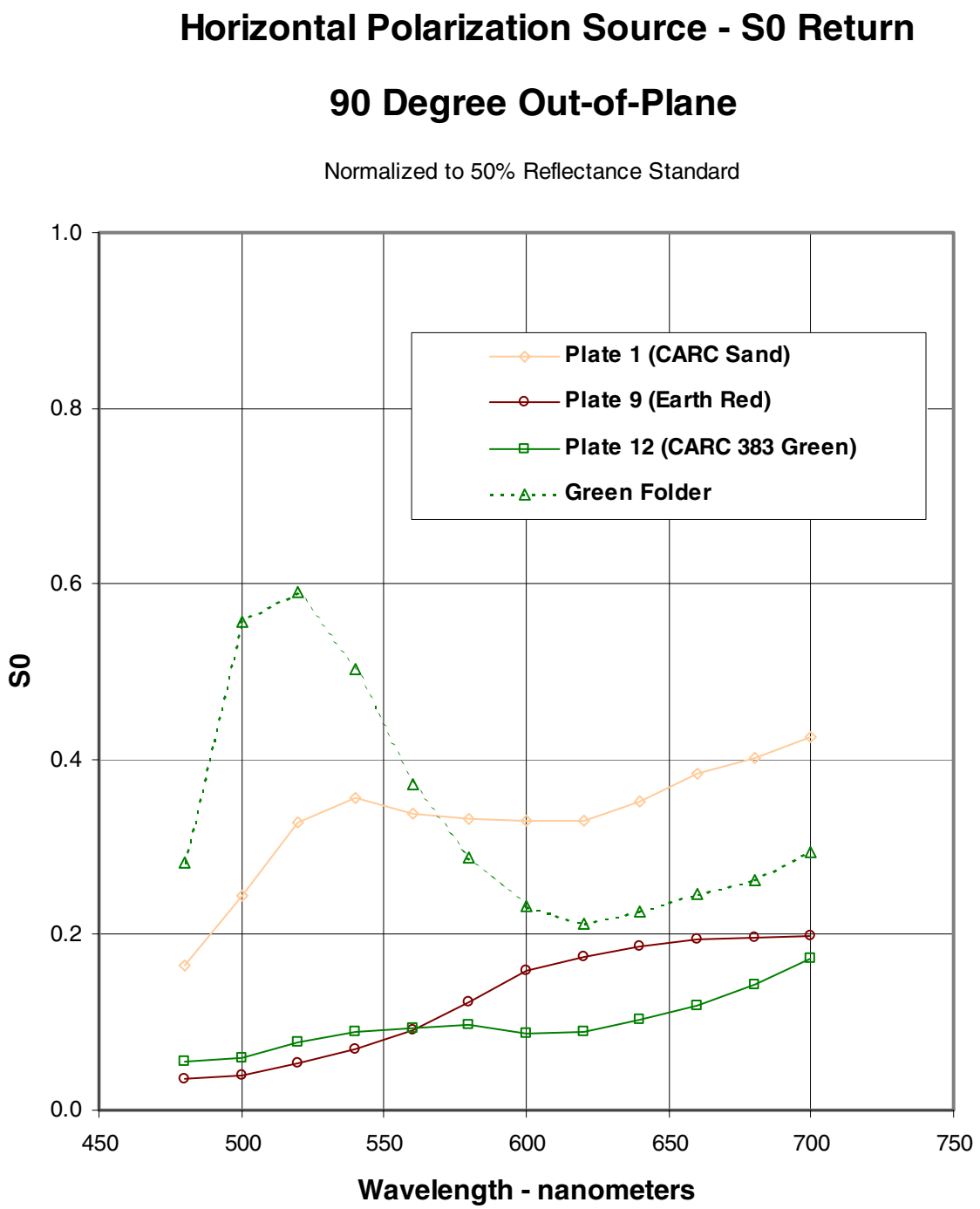

Figure 35. Out-of-plane S0 spectral response of colored surfaces - horizontal source

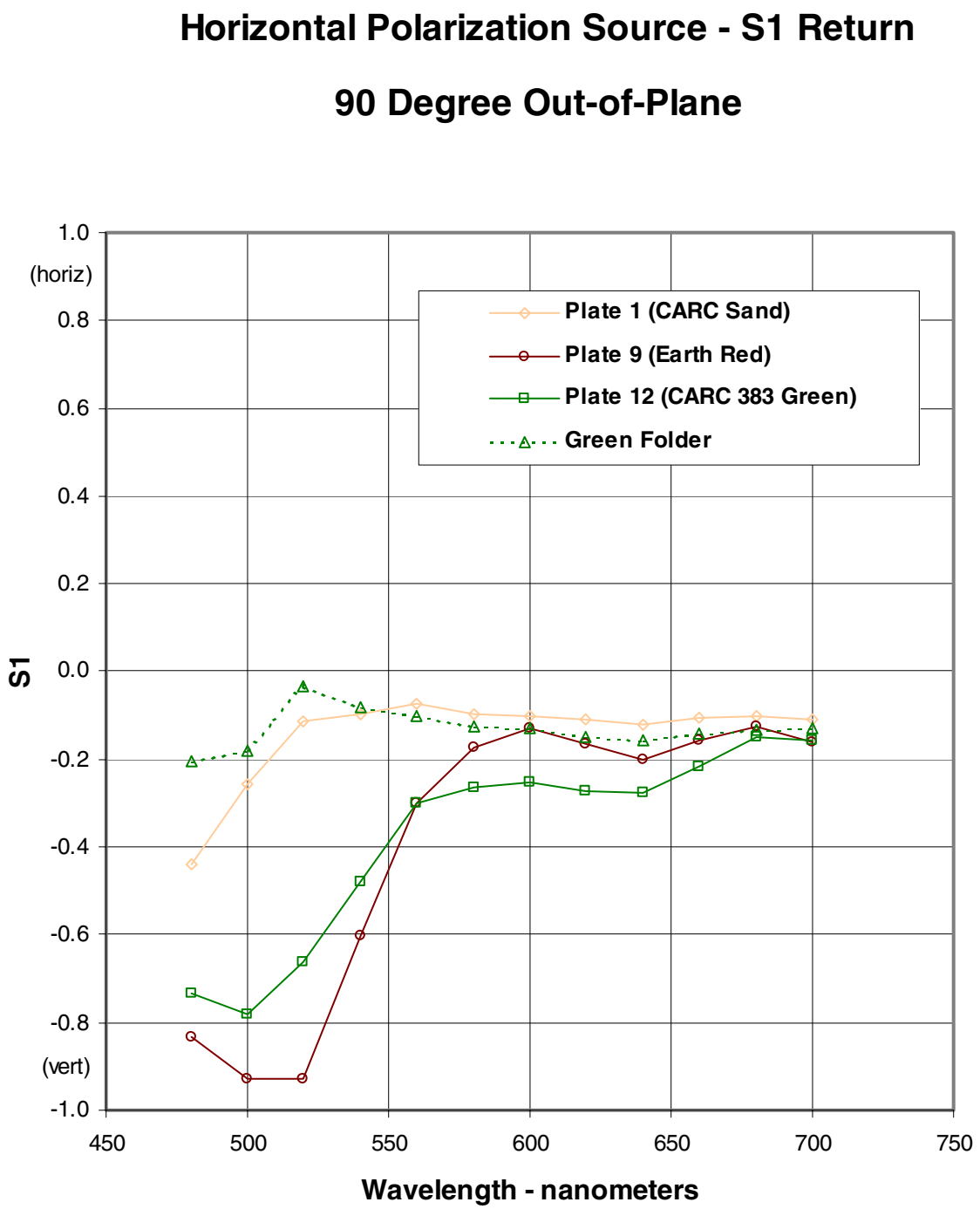

Figure 36. Out-of-plane S1 spectral response of colored surfaces - horizontal source

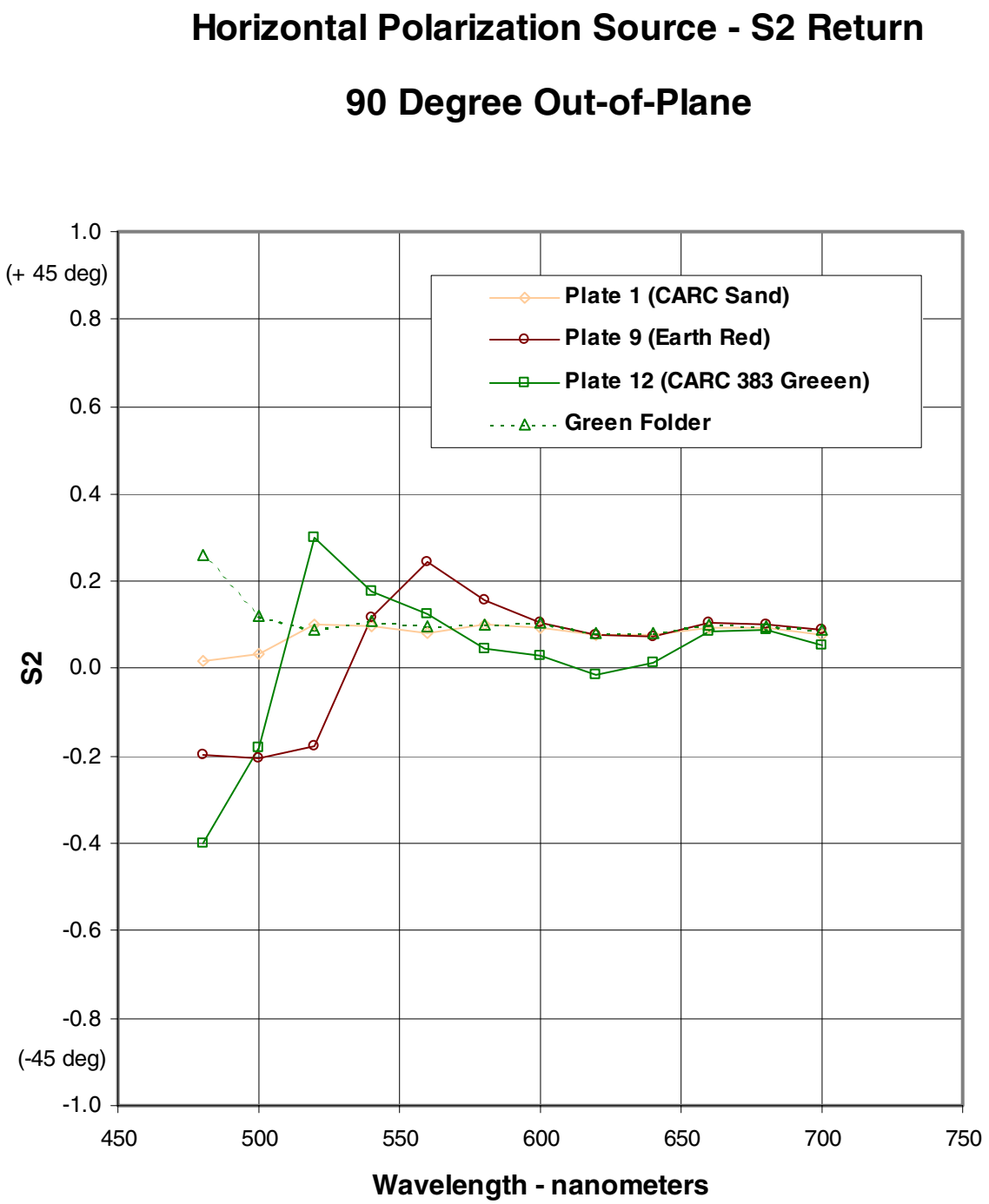

Figure 37. Out-of-plane S2 spectral response of colored surfaces - horizontal source

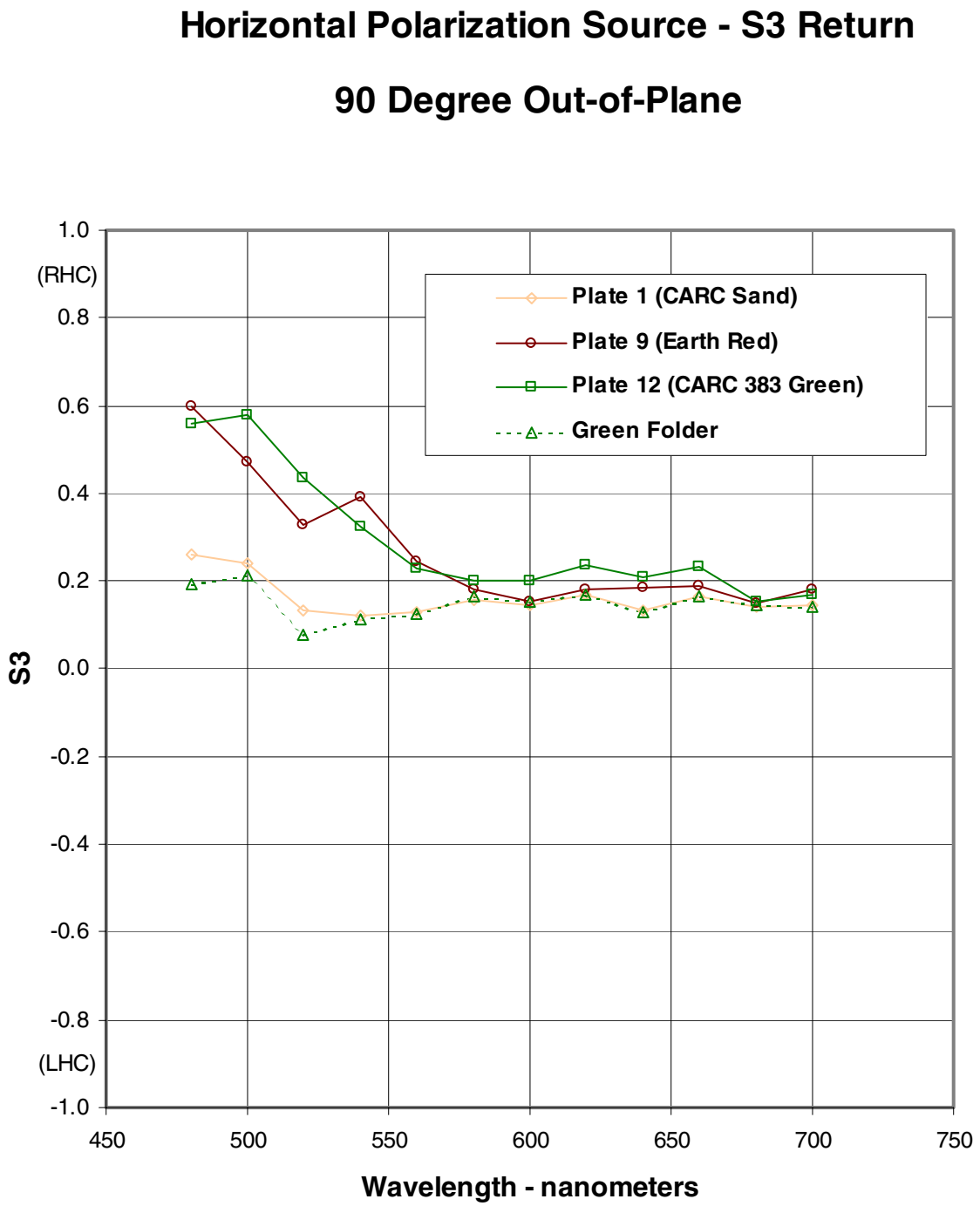

Figure 38. Out-of-plane S3 spectral response of colored surfaces - horizontal source

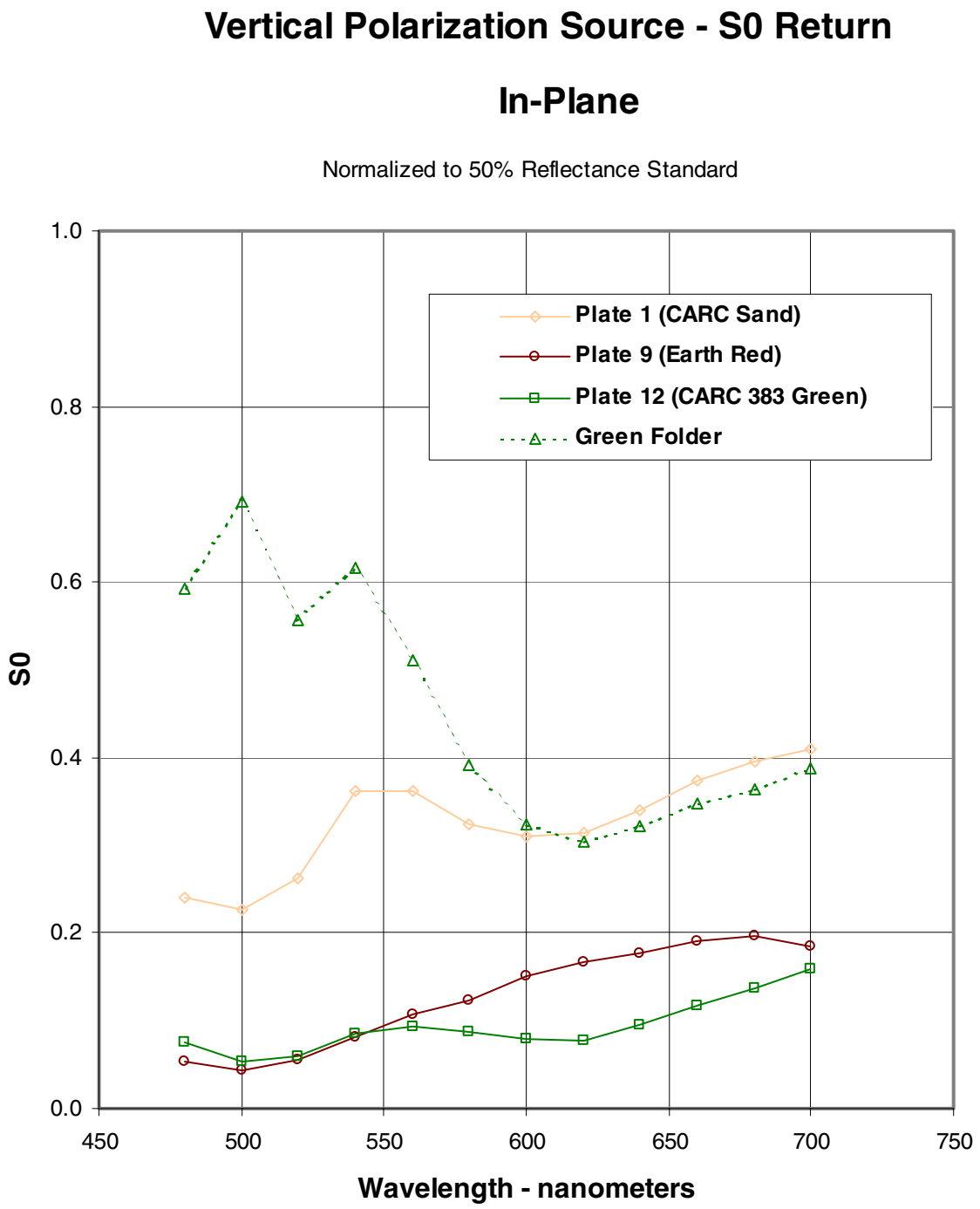

Figure 39. In-plane S0 spectral response of colored surfaces - vertical source

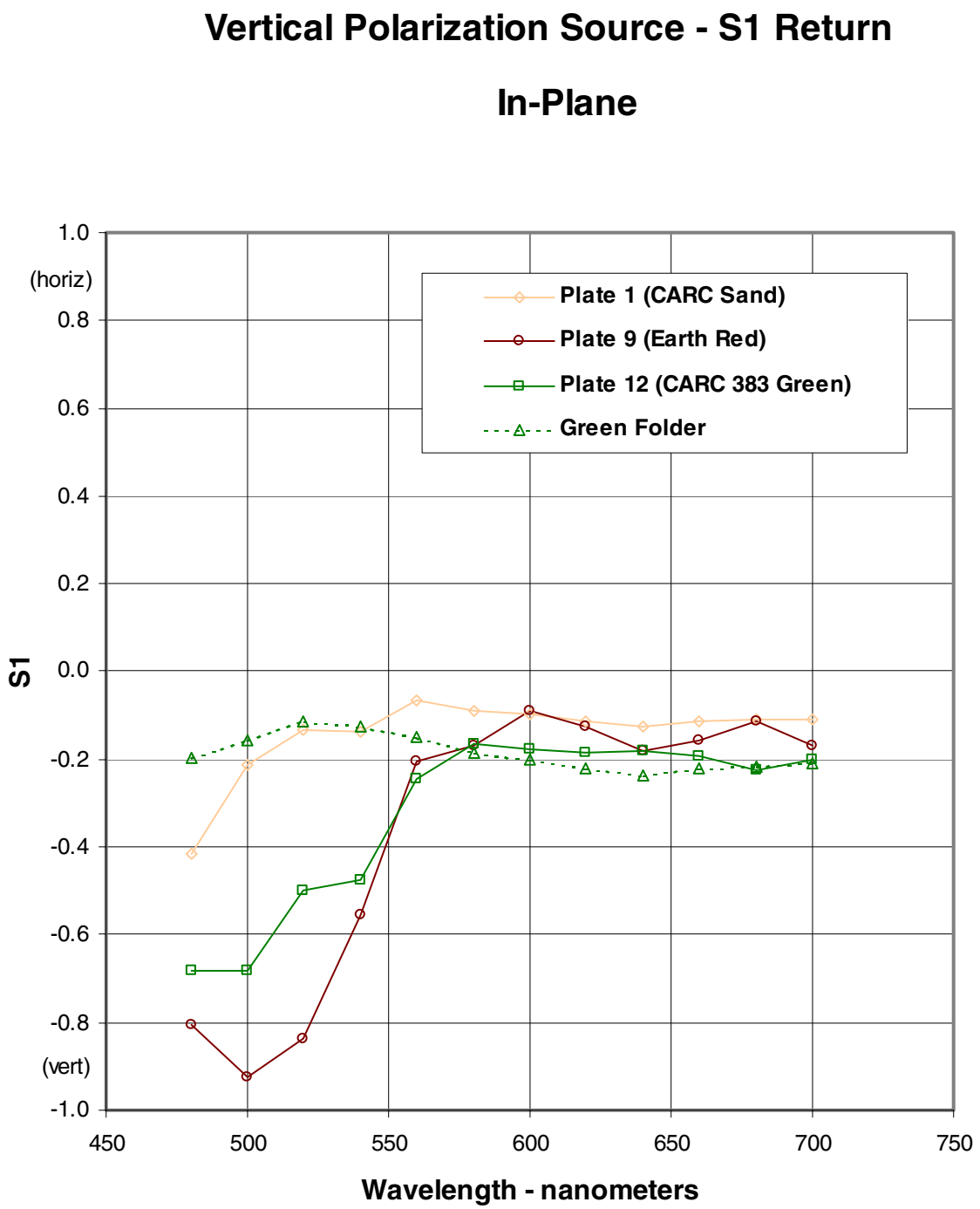

Figure 40. In-plane S1 spectral response of colored surfaces - vertical source

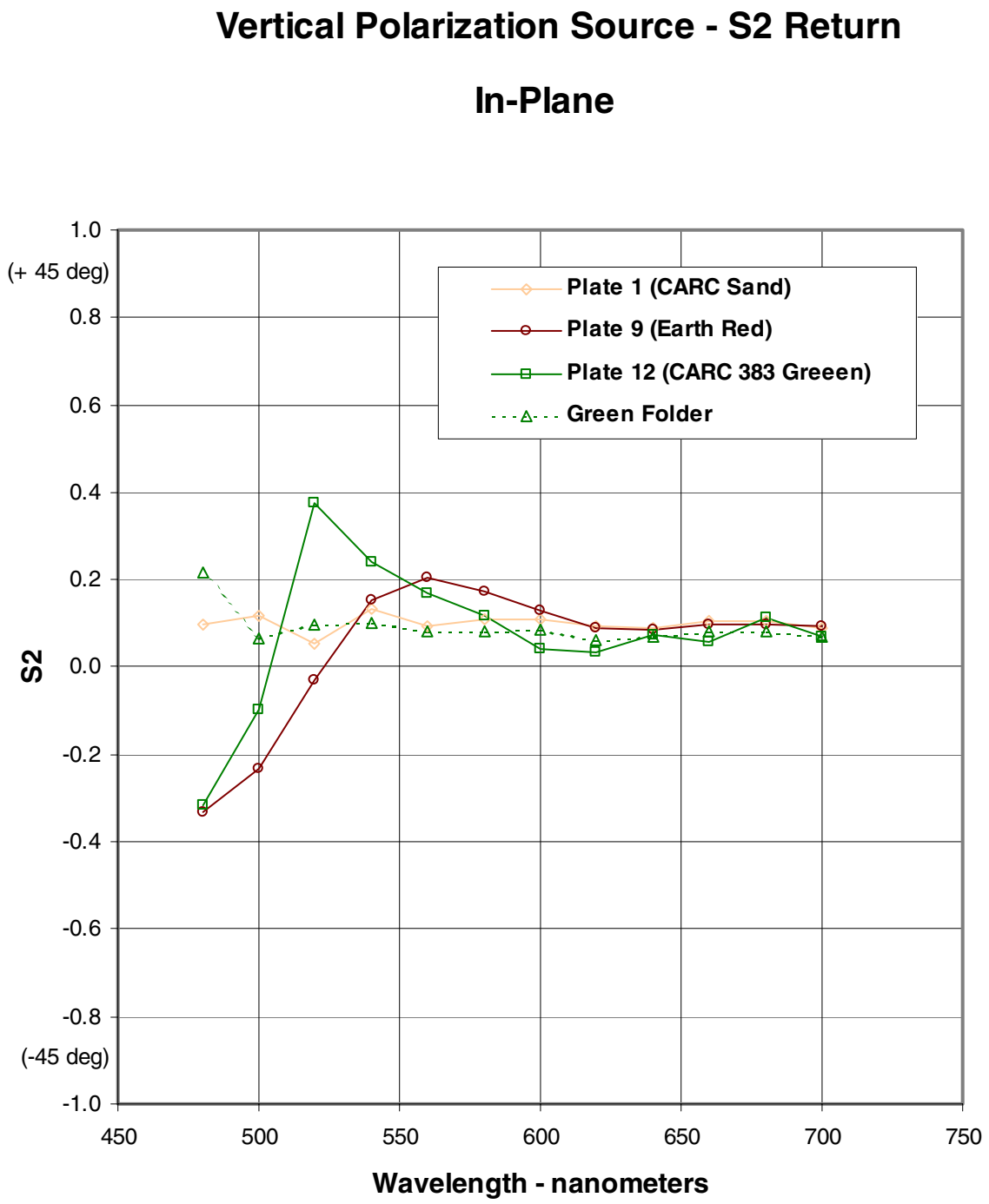

Figure 41. In-plane S2 spectral response of colored surfaces - vertical source

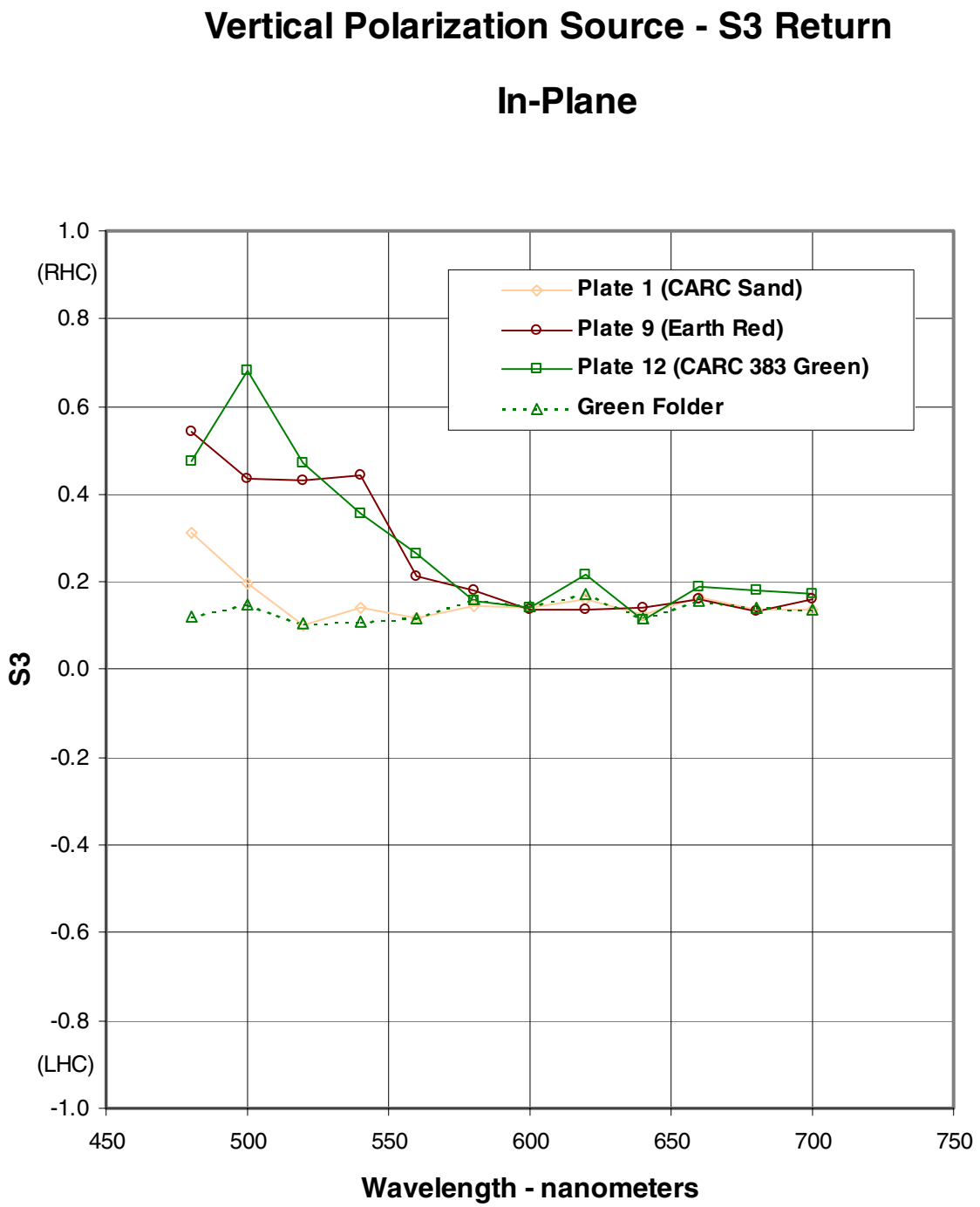

Figure 42. In-plane S3 spectral response of colored surfaces - vertical source

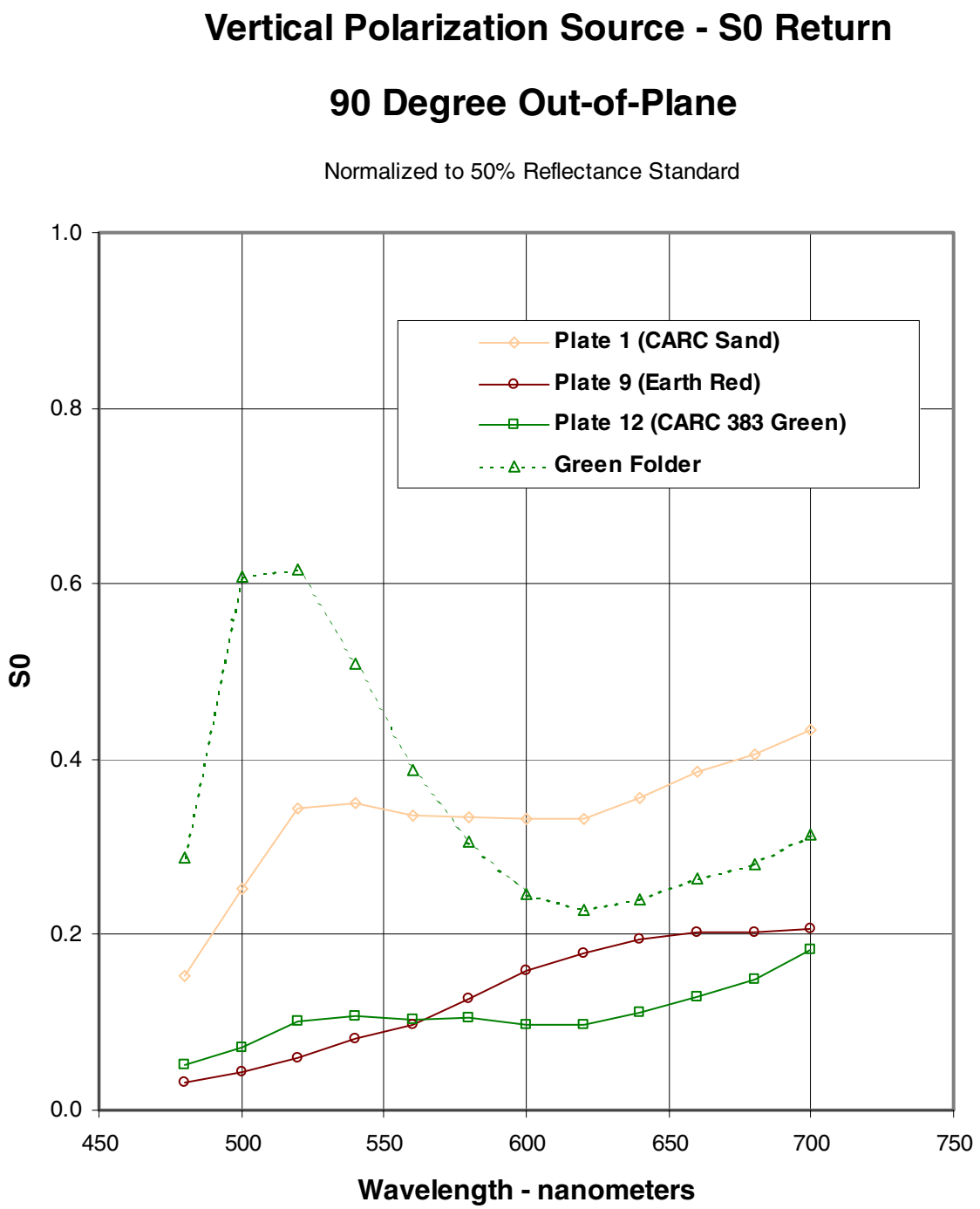

Figure 43. Out-of-plane S0 spectral response of colored surfaces - vertical source

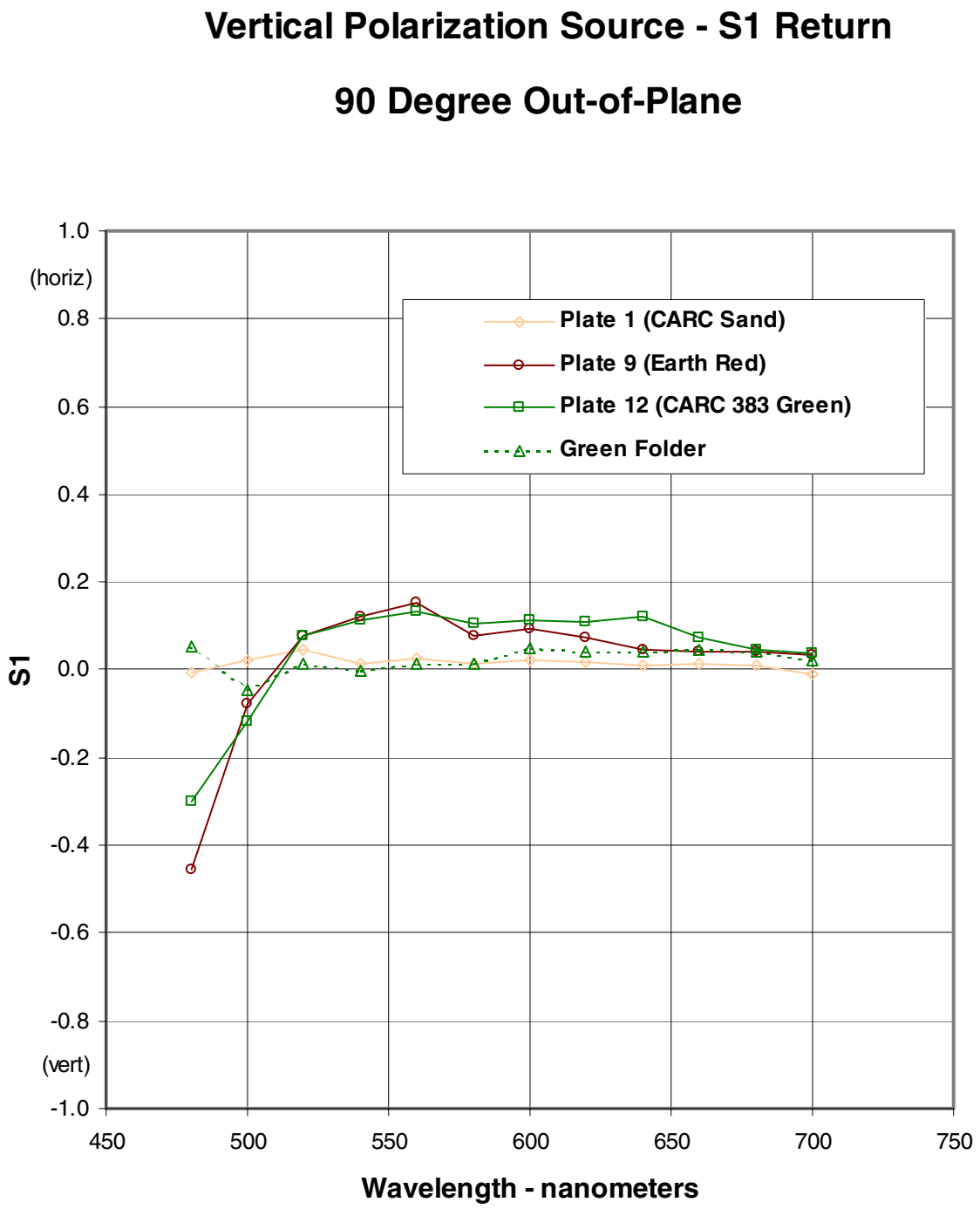

Figure 44. Out-of-plane S1 spectral response of colored surfaces - vertical source

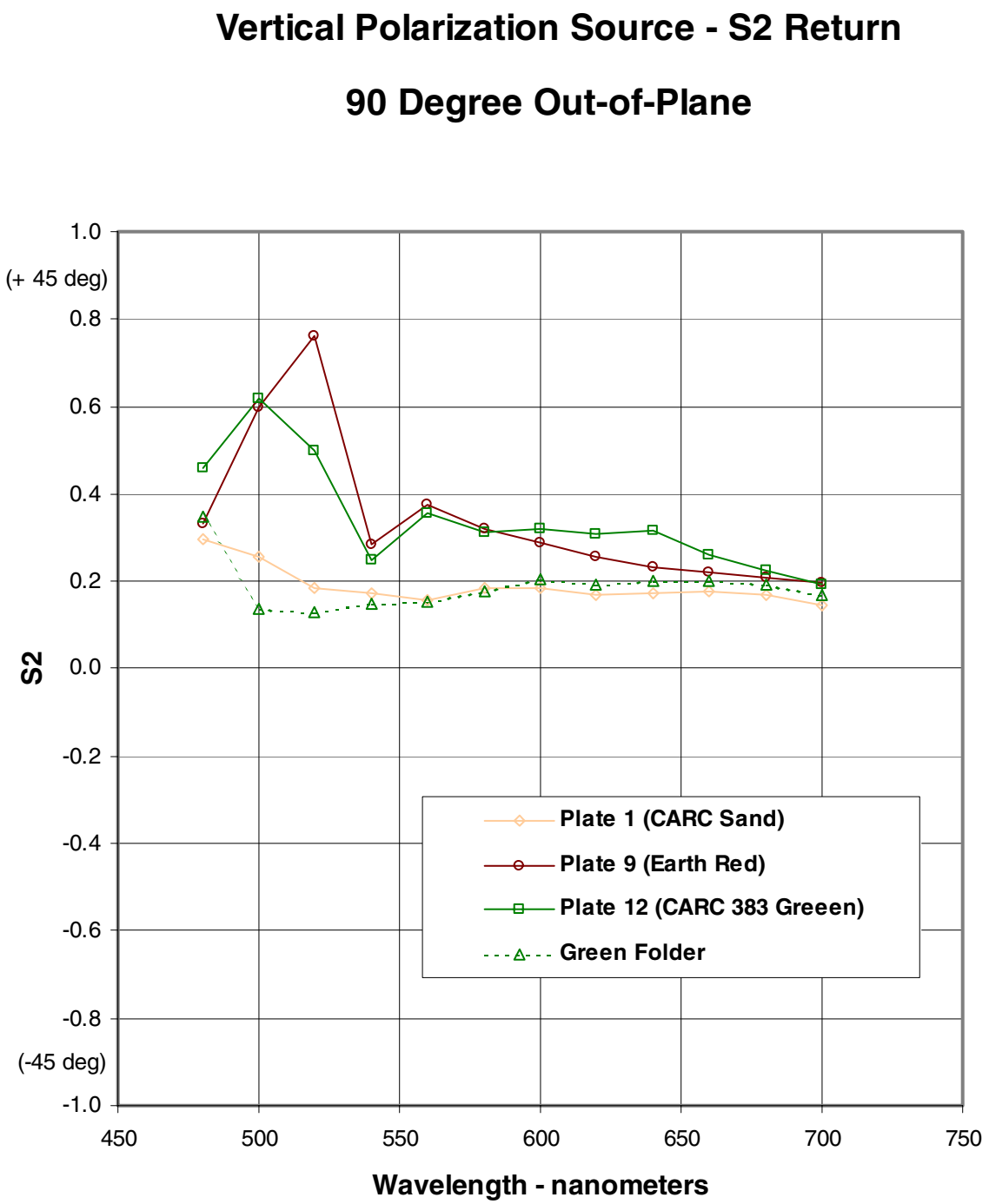

Figure 45. Out-of-plane S2 spectral response of colored surfaces - vertical source

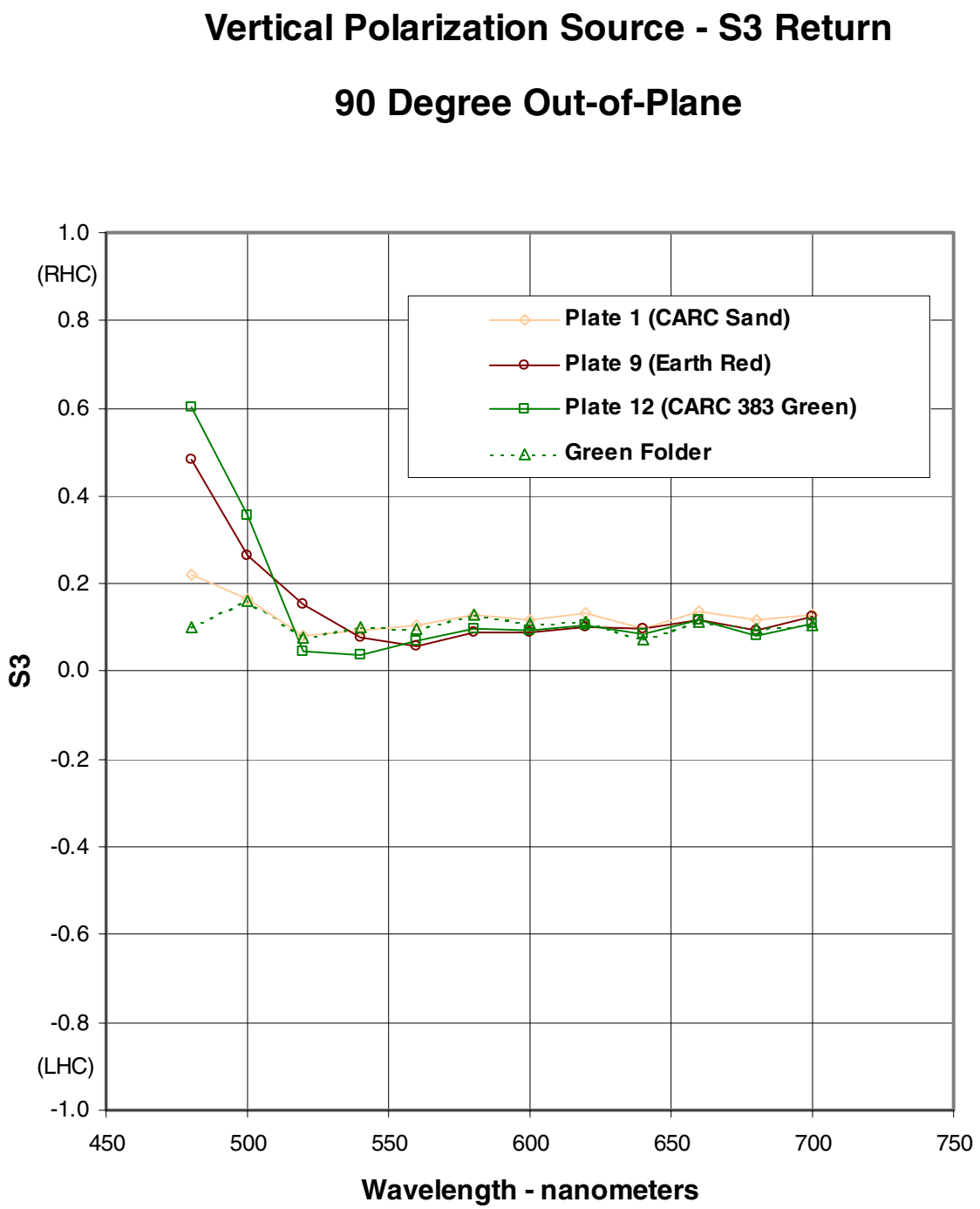

Figure 46. Out-of-plane S3 spectral response of colored surfaces - vertical source

CTISP Polarization Data for Nonstandard Surfaces

As a start on looking at nonstandard surfaces (again, with hind sight, the colored surfaces were anything but standard from a polarization perspective), a series of Stokes parameter measurements were made on artificially illuminated targets such as the reddish-orange bomblet shown in Figure 12 as well as a patch of healthy green sod and a container of sand. Table 2 contains the summary of charts on the following pages produced from these measurements.

Table 2
Stokes Parameter Spectra Charts for Nonstandard Surface Measurements

Light Source Polarization	In-Plane Measurements	Out-of-Plane Measurements
Random	Figure 49 - Figure 52	Figure 53 - Figure 56
Horizontal	Figure 57 - Figure 60	Figure 61 - Figure 64
Vertical	Figure 65 - Figure 68	Figure 69 - Figure 72

The bomblet was placed on a black cloth background and, when viewed in-plane from the perspective of CTISP, was positioned horizontally with the tail to the left. In the out-of-plane view, the axis of the bomblet was oriented vertically with the nose closest to CTISP. Figure 47 and Figure 48 show the grass and sand samples, respectively.

Two curves are shown on each of the following charts for the bomblet Stokes parameters. One is labeled ‘glare’ and the other is labeled ‘slope’. Because the bomblet surface was relatively smooth and curved, there was always a specular reflection spot on the painted surface that shone more than the rest of that surface. The shiny spot was chosen for processing as the ‘glare’ surface, and another non-shiny patch of the surface was chosen as the ‘slope’ surface.

While many of the same observations can be made for these nonstandard surfaces as were made for the colored surfaces, two additional observations are worth noting. One is that there is a significant difference in magnitude of certain Stokes parameters for the man-made surface vs. the natural materials (e.g., Figure 50, Figure 58, Figure 63, Figure 66, and Figure 67). One would expect a certain amount of depolarization of light by the natural materials made up of nearly randomly-oriented facets. The other observation is that there appears to be significant circularly polarized components generated by reflection from the bomblet. This may be the result of geometrical effects associated with its curved surface.

Figure 47. Grass sod used for nonstandard surface measurements

Figure 48. Sand used for nonstandard surface measurements

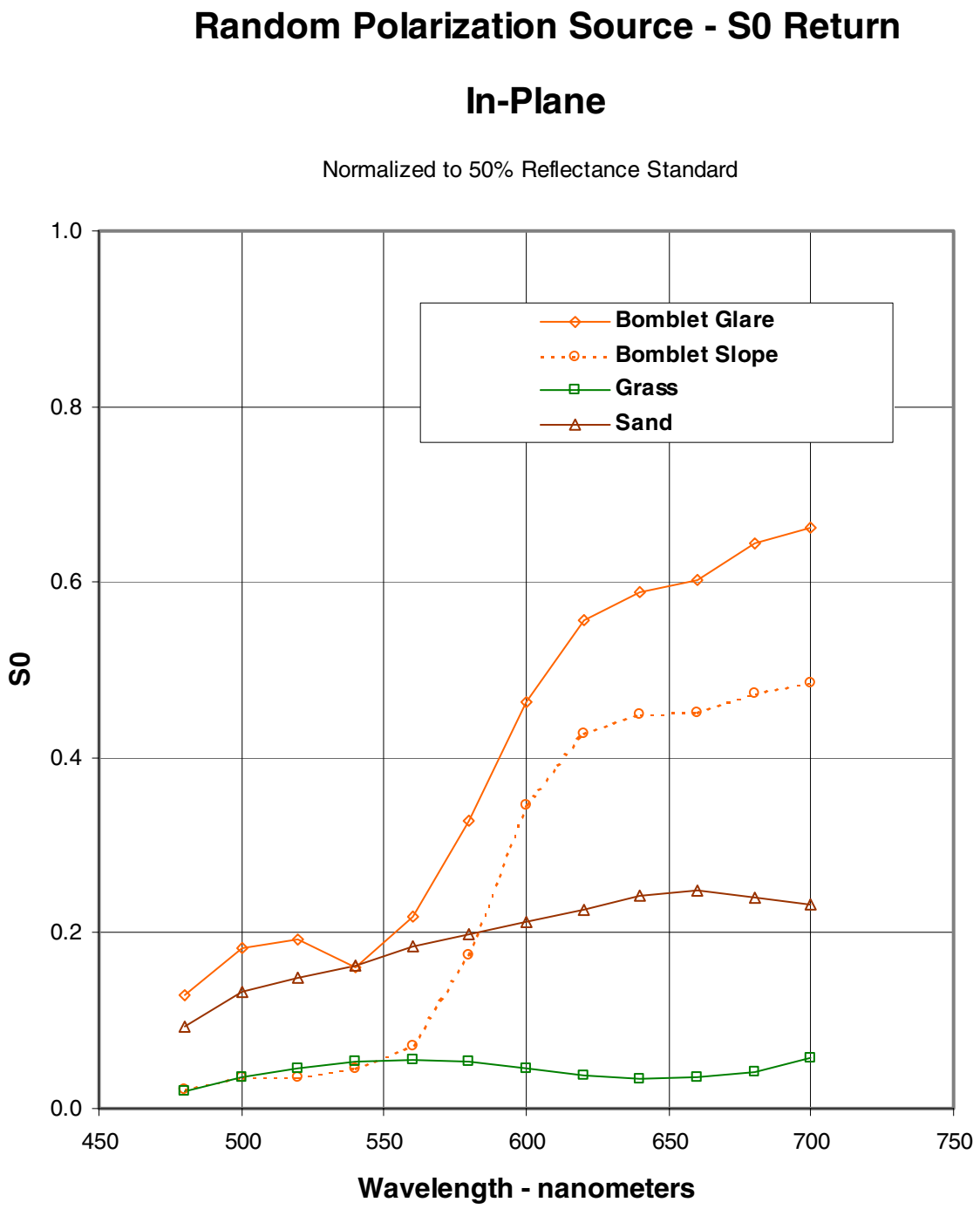

Figure 49. In-plane S0 spectral response of nonstandard surfaces - random source

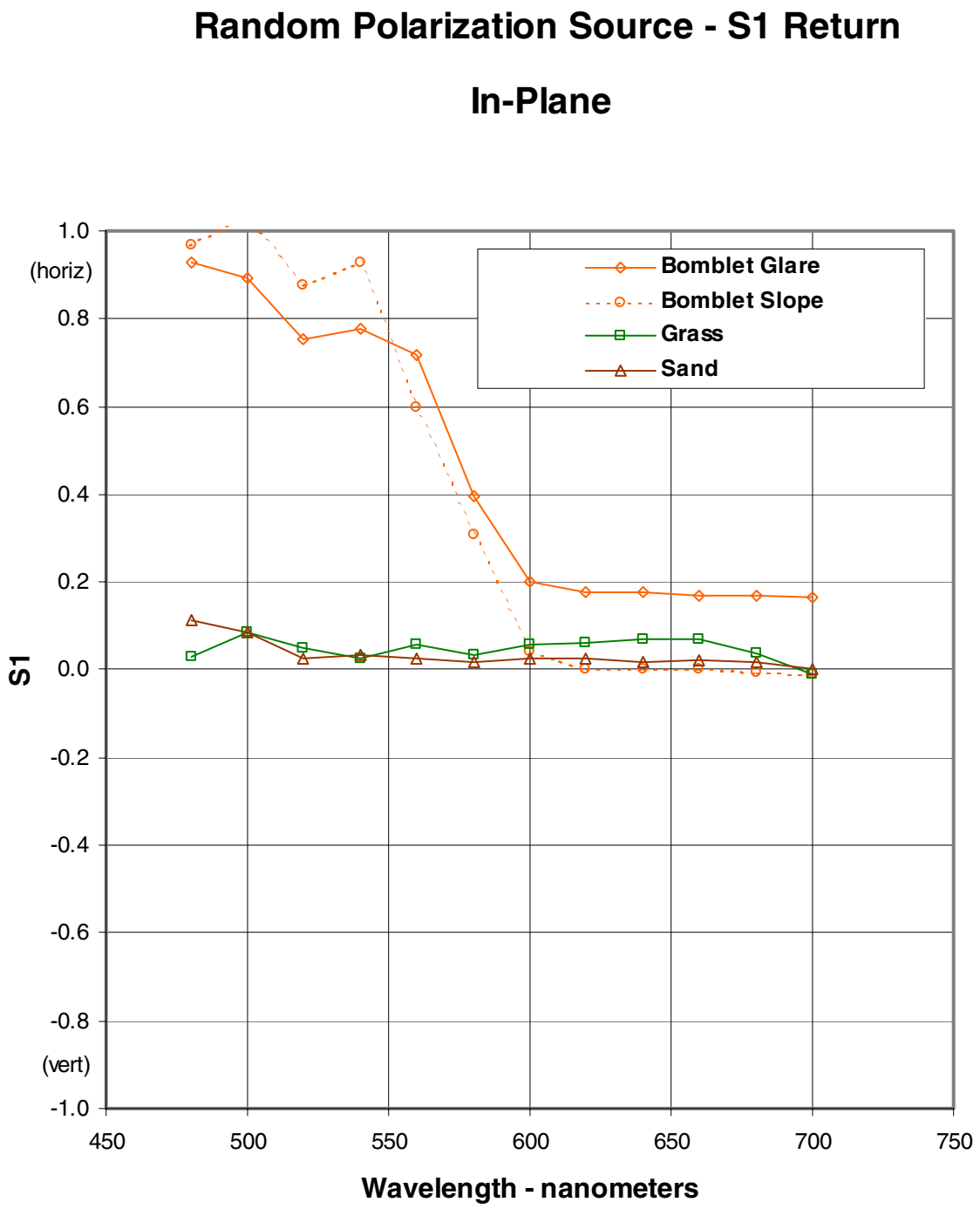

Figure 50. In-plane S1 spectral response of nonstandard surfaces - random source

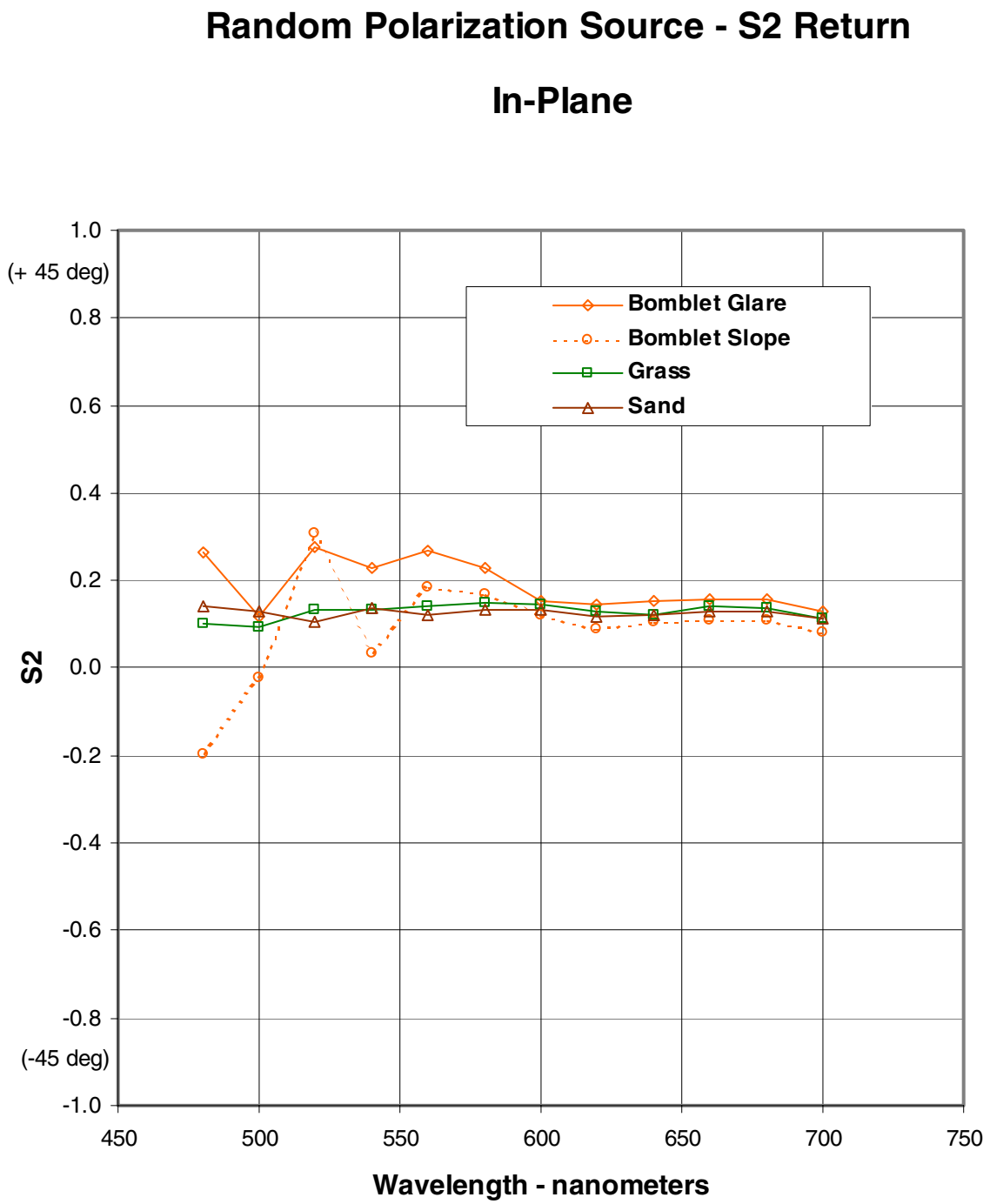

Figure 51. In-plane S2 spectral response of nonstandard surfaces - random source

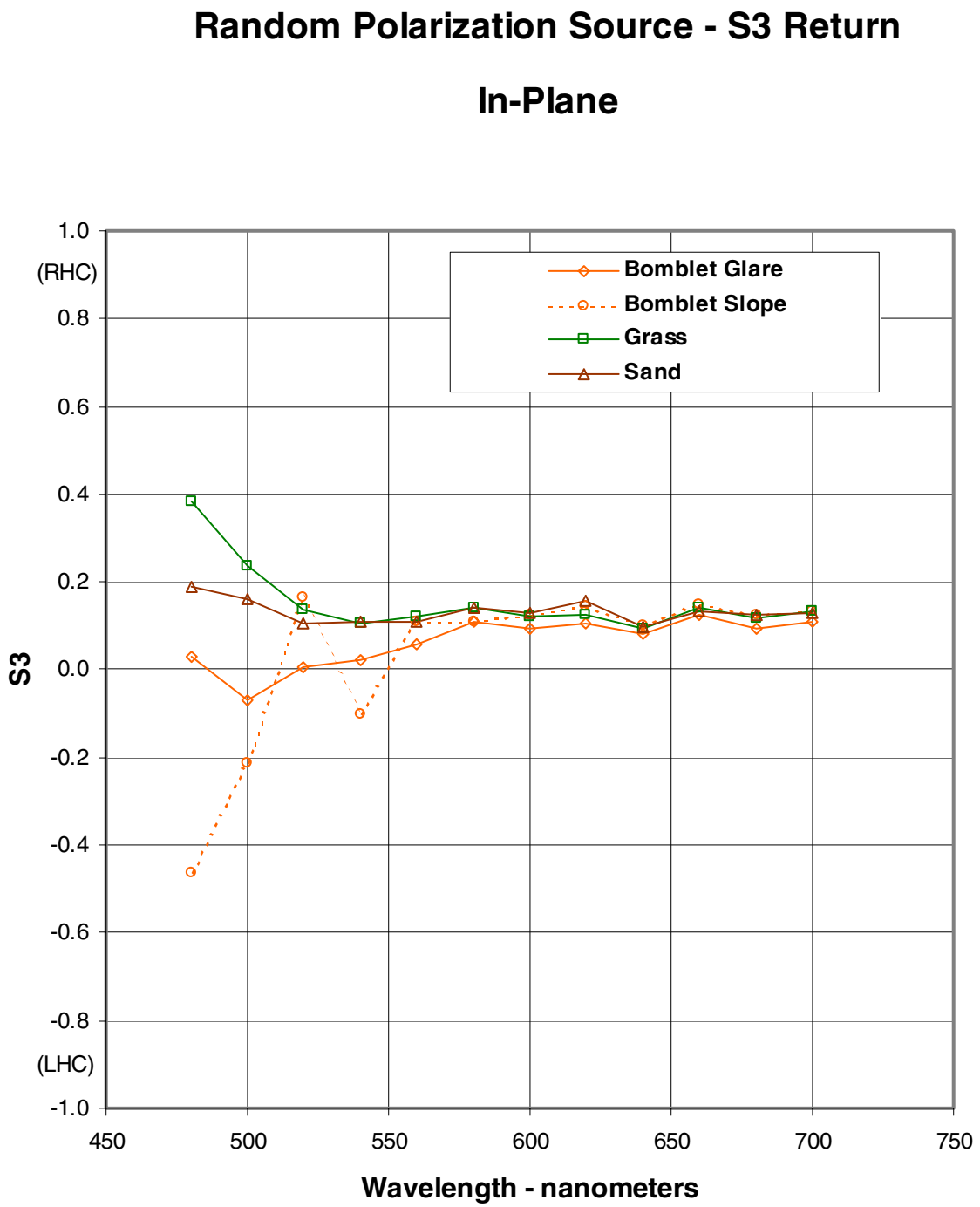

Figure 52. In-plane S3 spectral response of nonstandard surfaces - random source

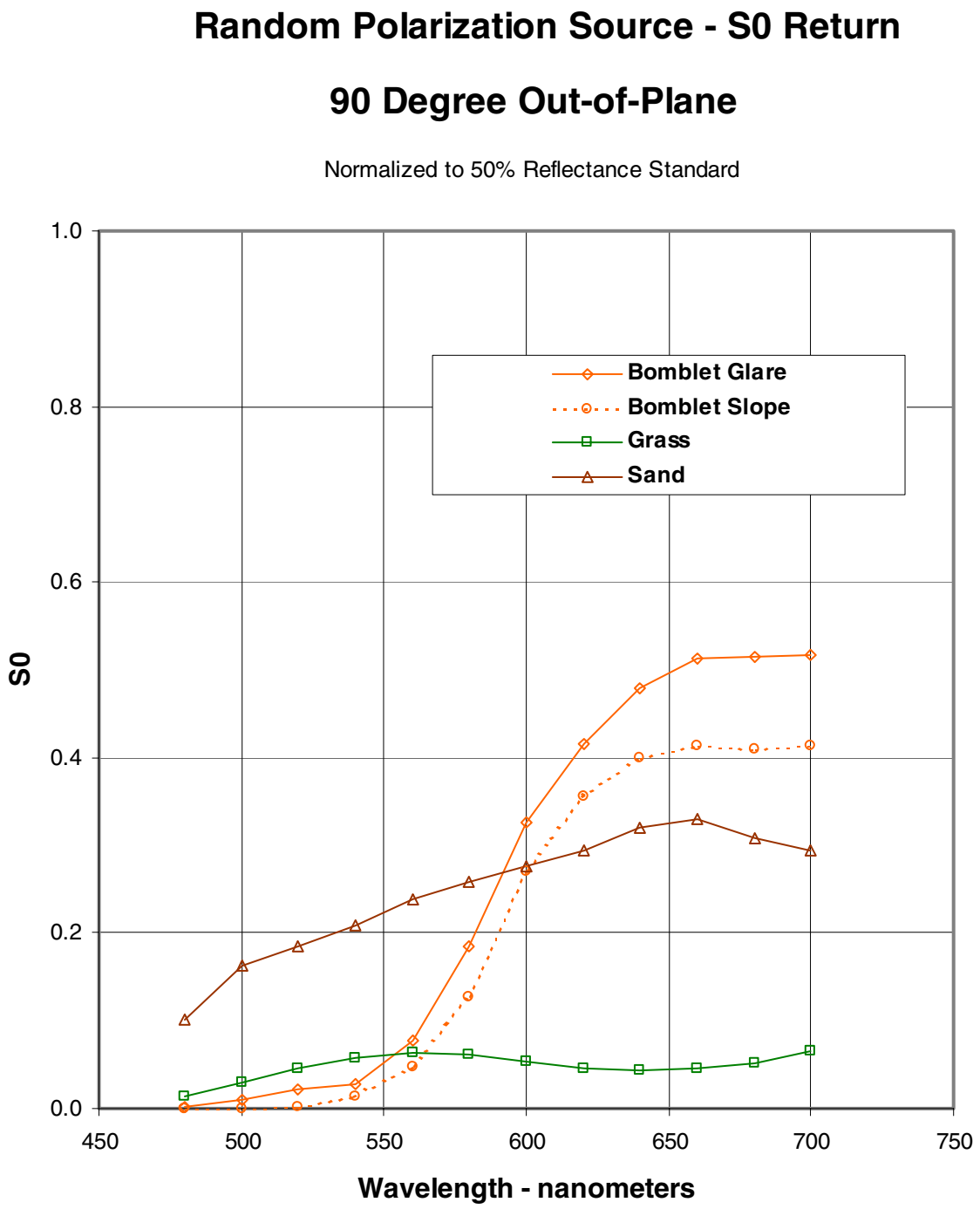

Figure 53. Out-of-plane S0 spectral response of nonstandard surfaces - random source

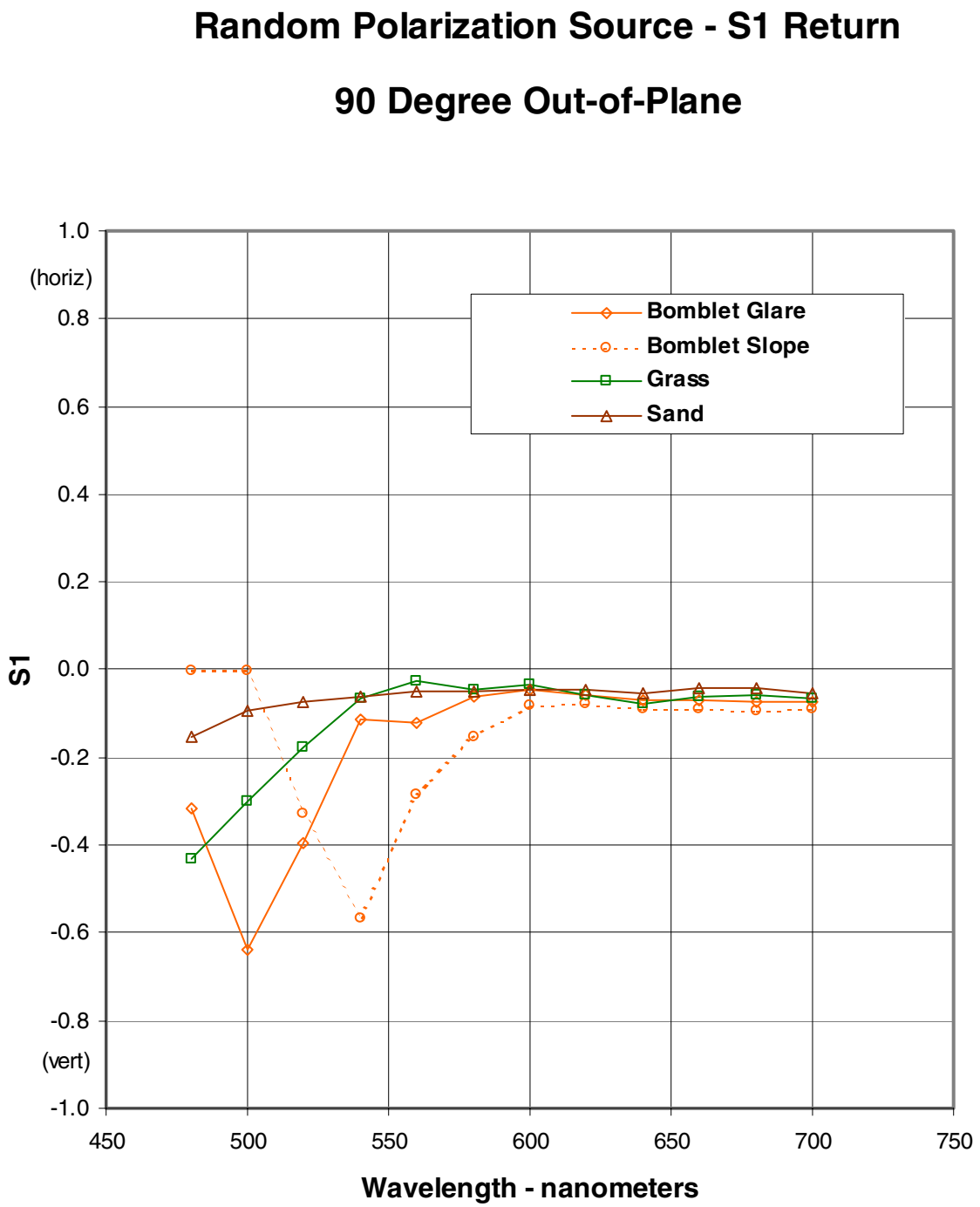

Figure 54. Out-of-plane S1 spectral response of nonstandard surfaces - random source

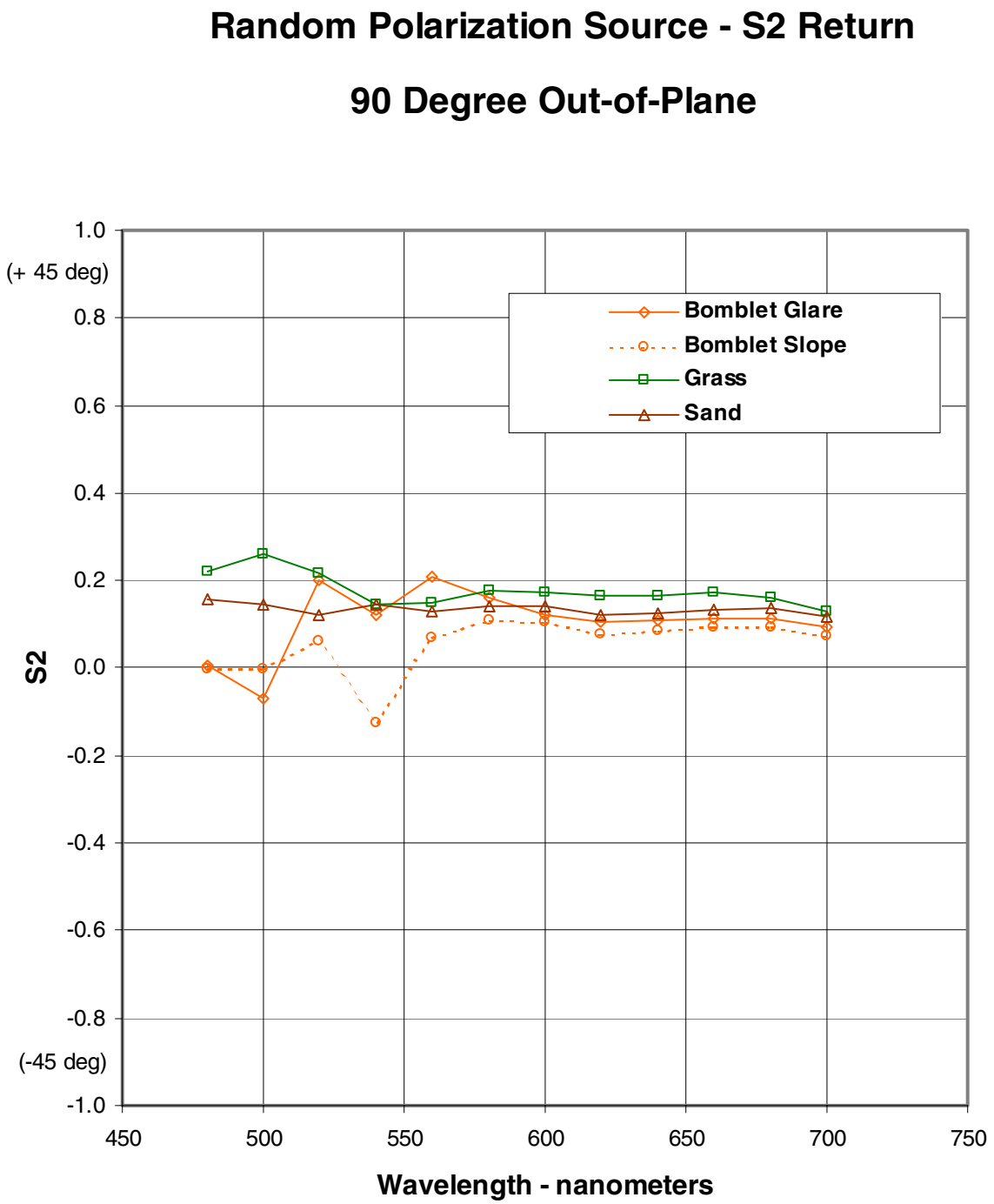

Figure 55. Out-of-plane S2 spectral response of nonstandard surfaces - random source

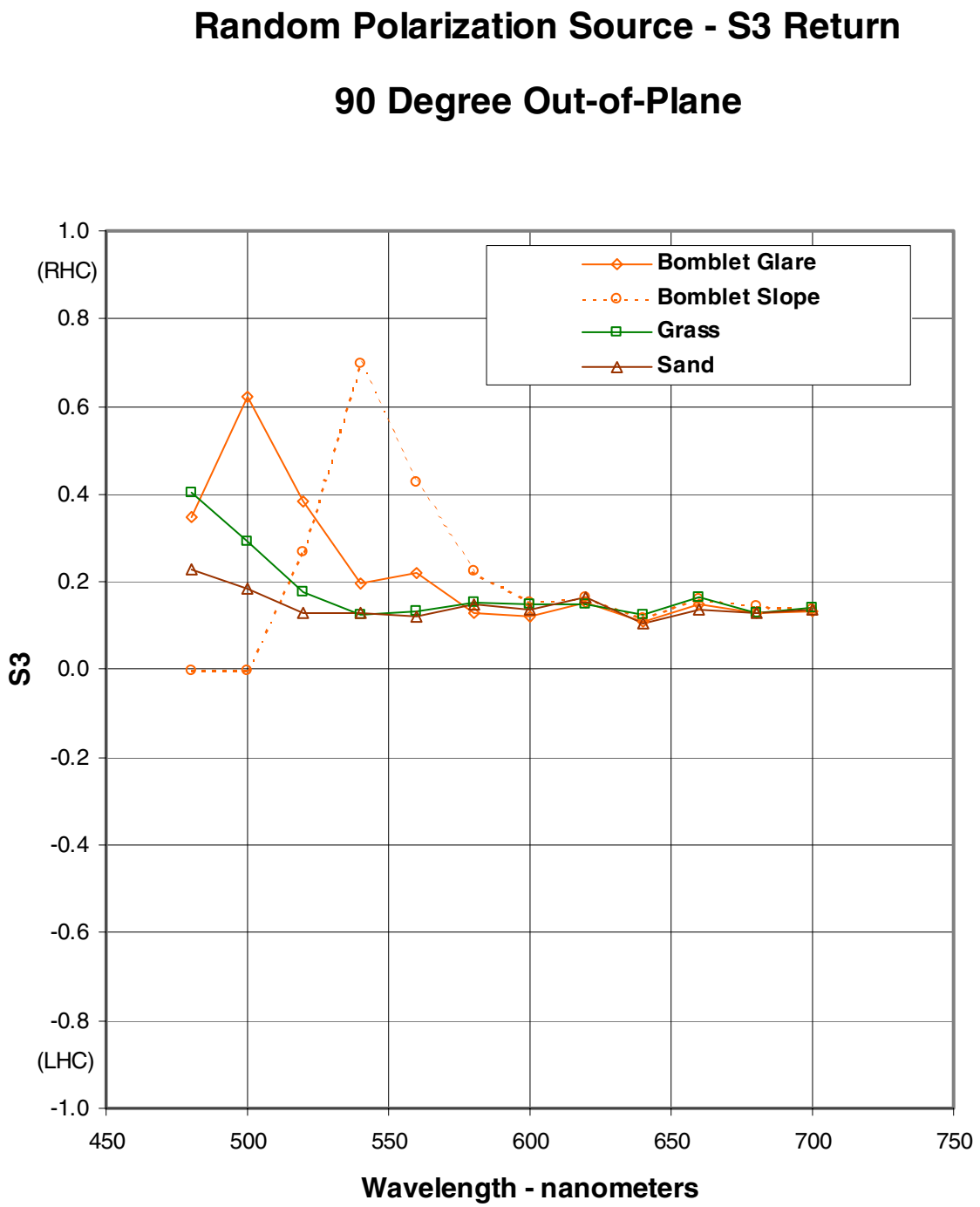

Figure 56. Out-of-plane S3 spectral response of nonstandard surfaces - random source

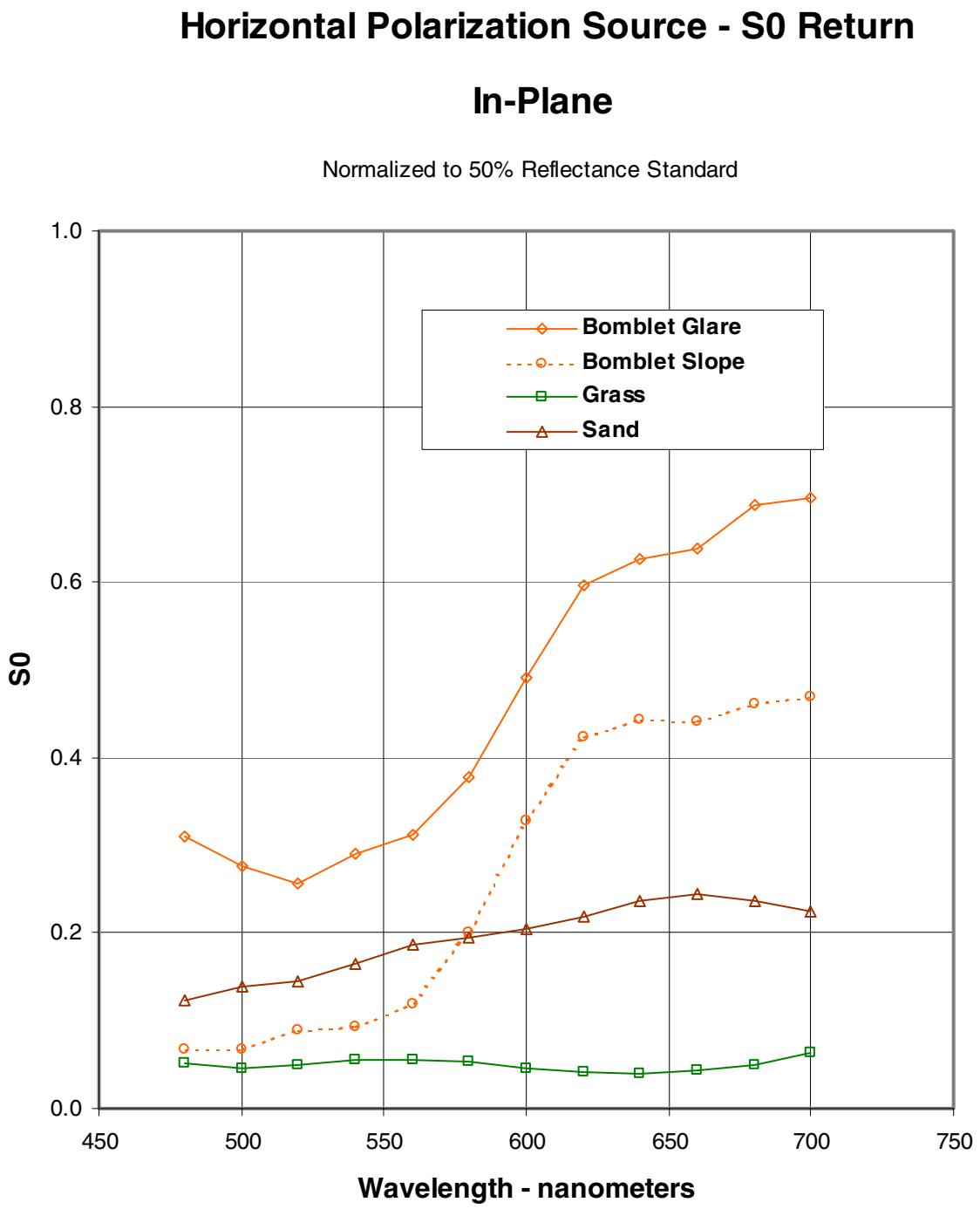

Figure 57. In-plane S0 spectral response of nonstandard surfaces - horizontal source

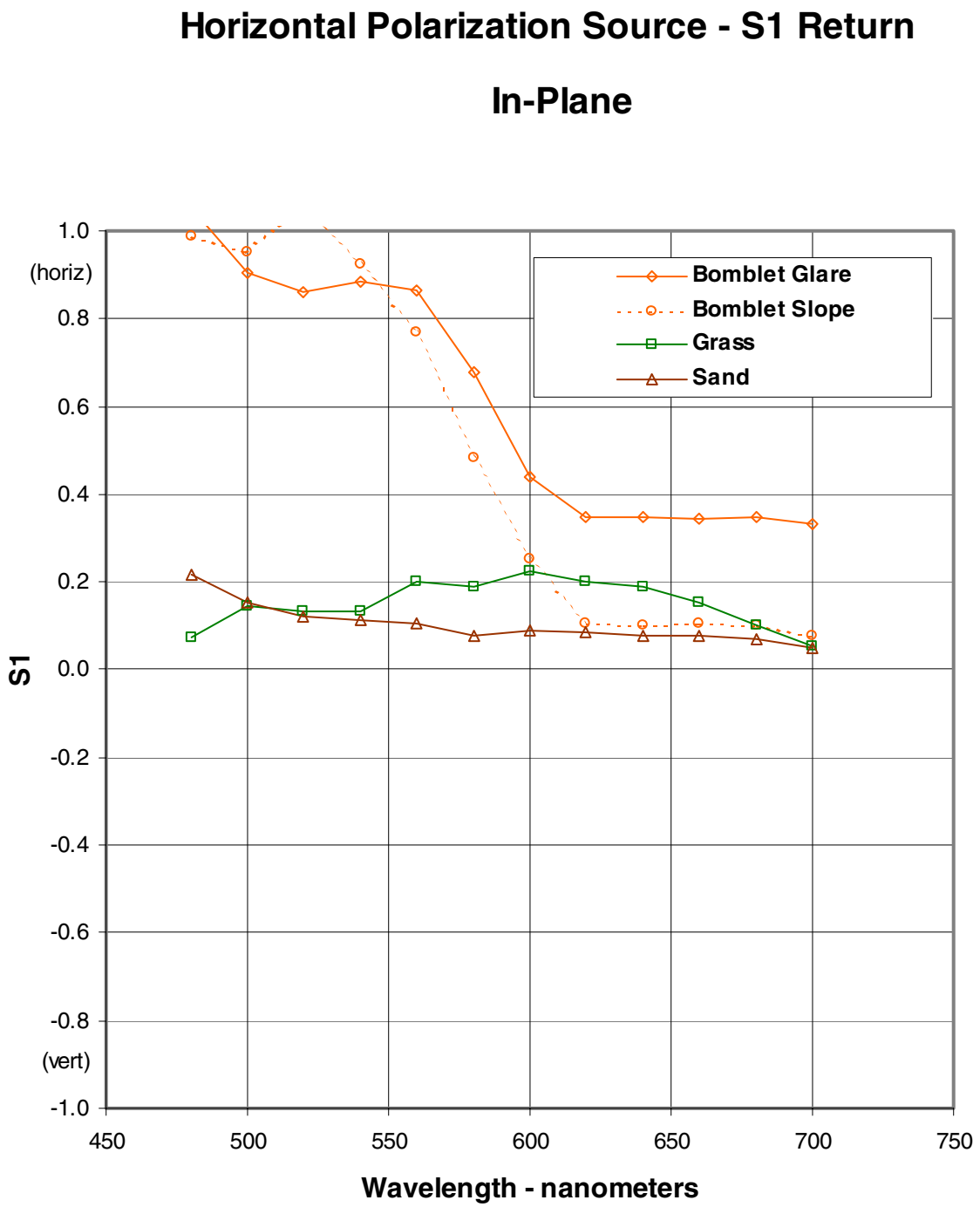

Figure 58. In-plane S1 spectral response of nonstandard surfaces - horizontal source

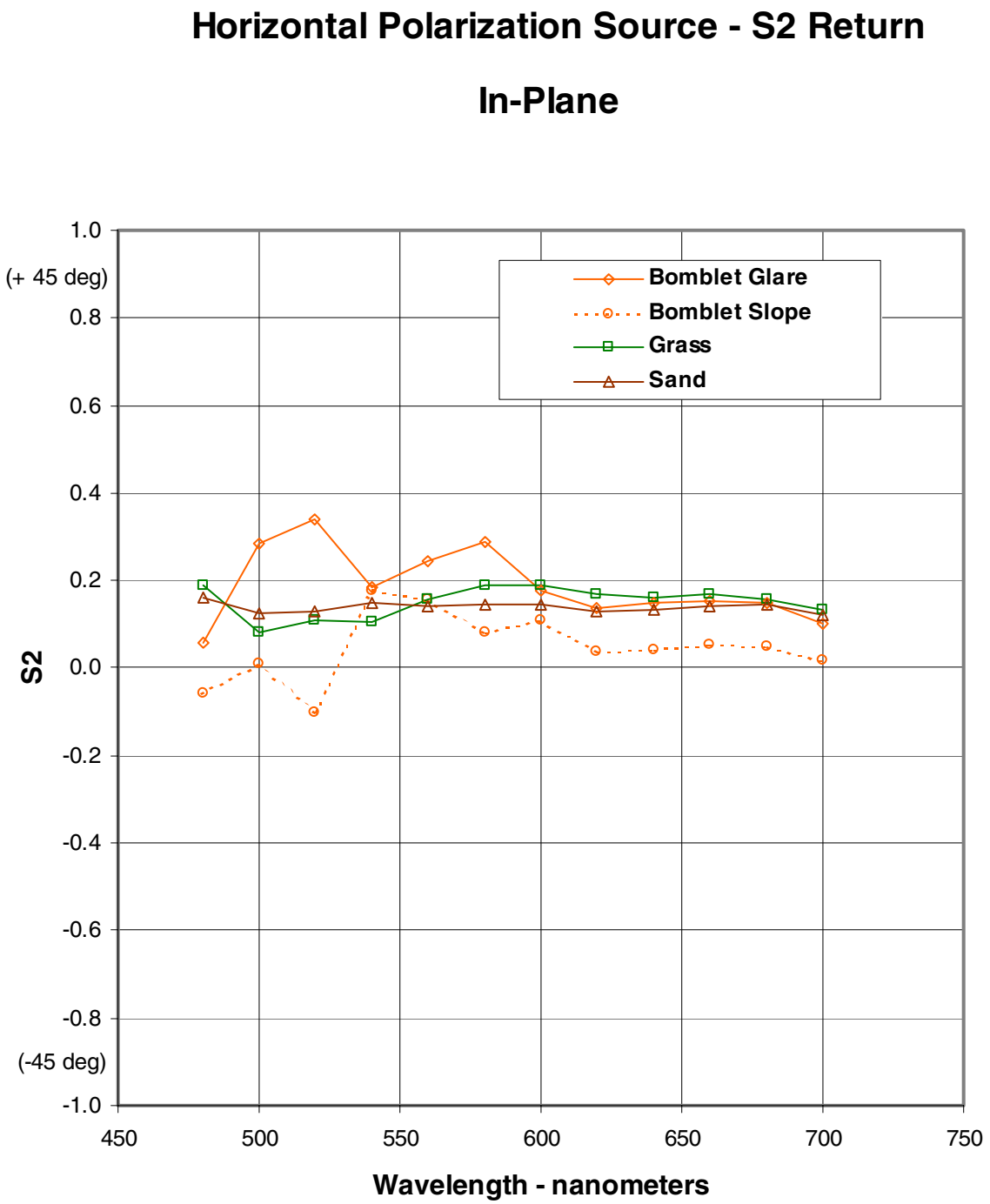

Figure 59. In-plane S2 spectral response of nonstandard surfaces - horizontal source

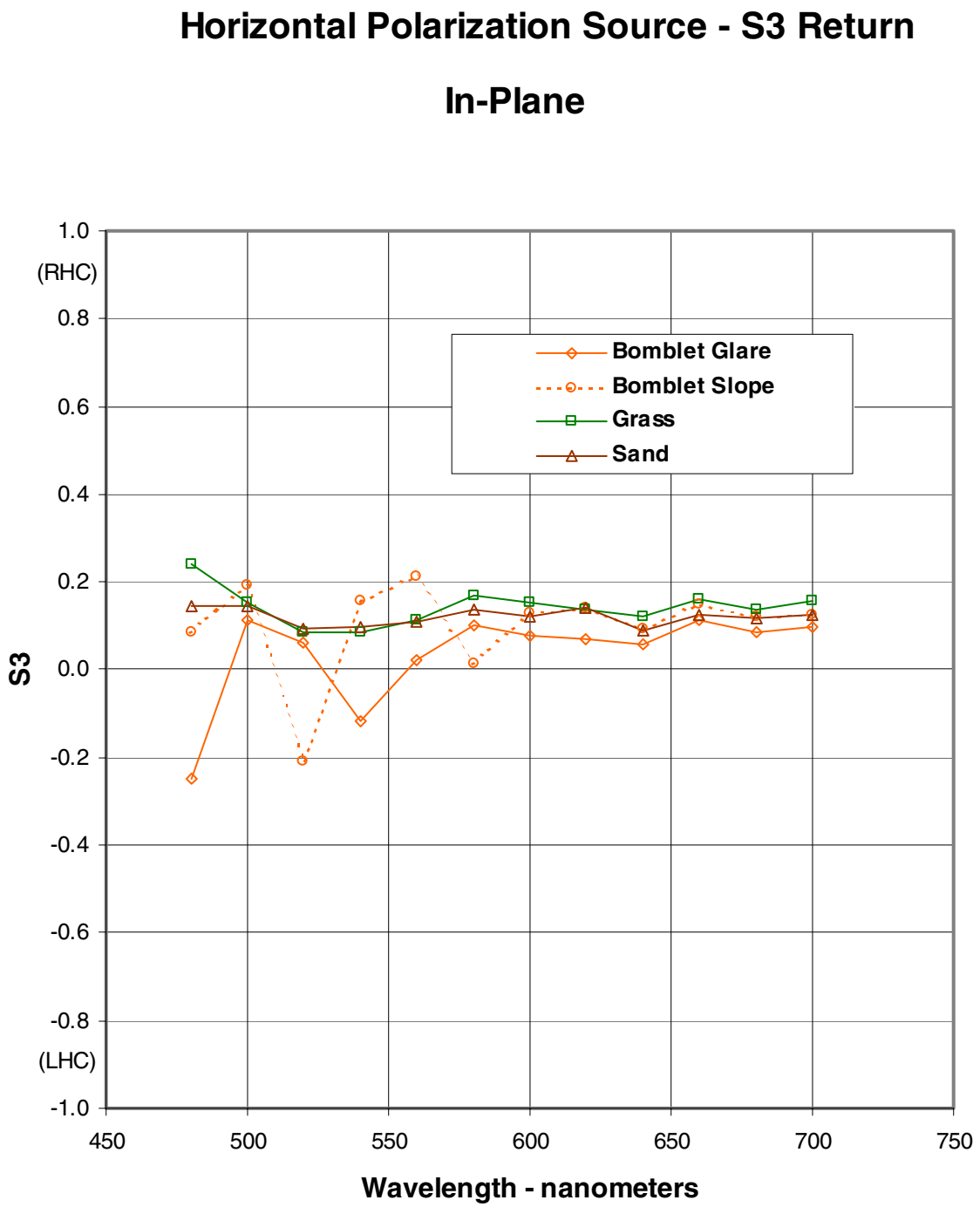

Figure 60. In-plane S3 spectral response of nonstandard surfaces - horizontal source

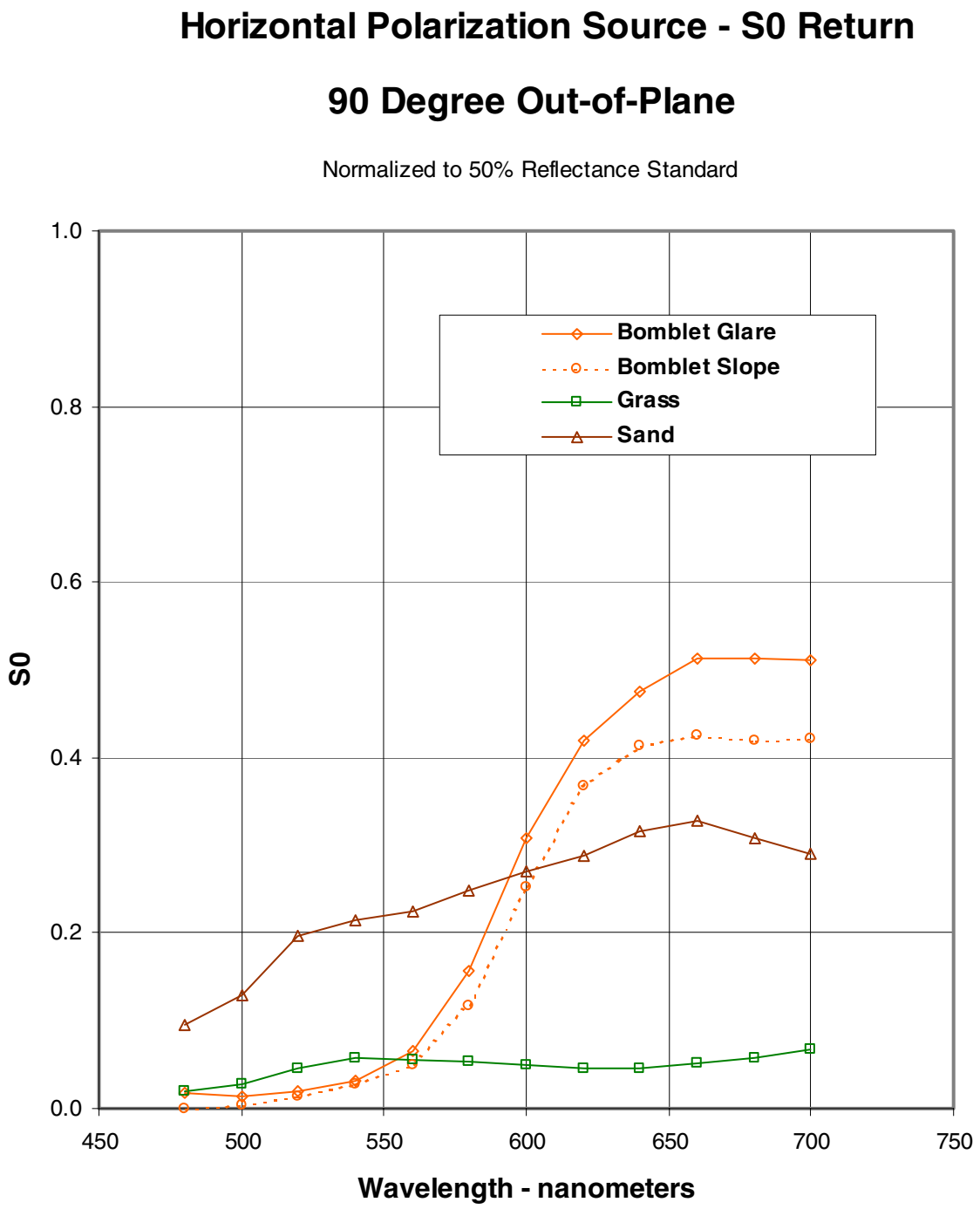

Figure 61. Out-of-plane S0 spectral response of nonstandard surfaces - horizontal source

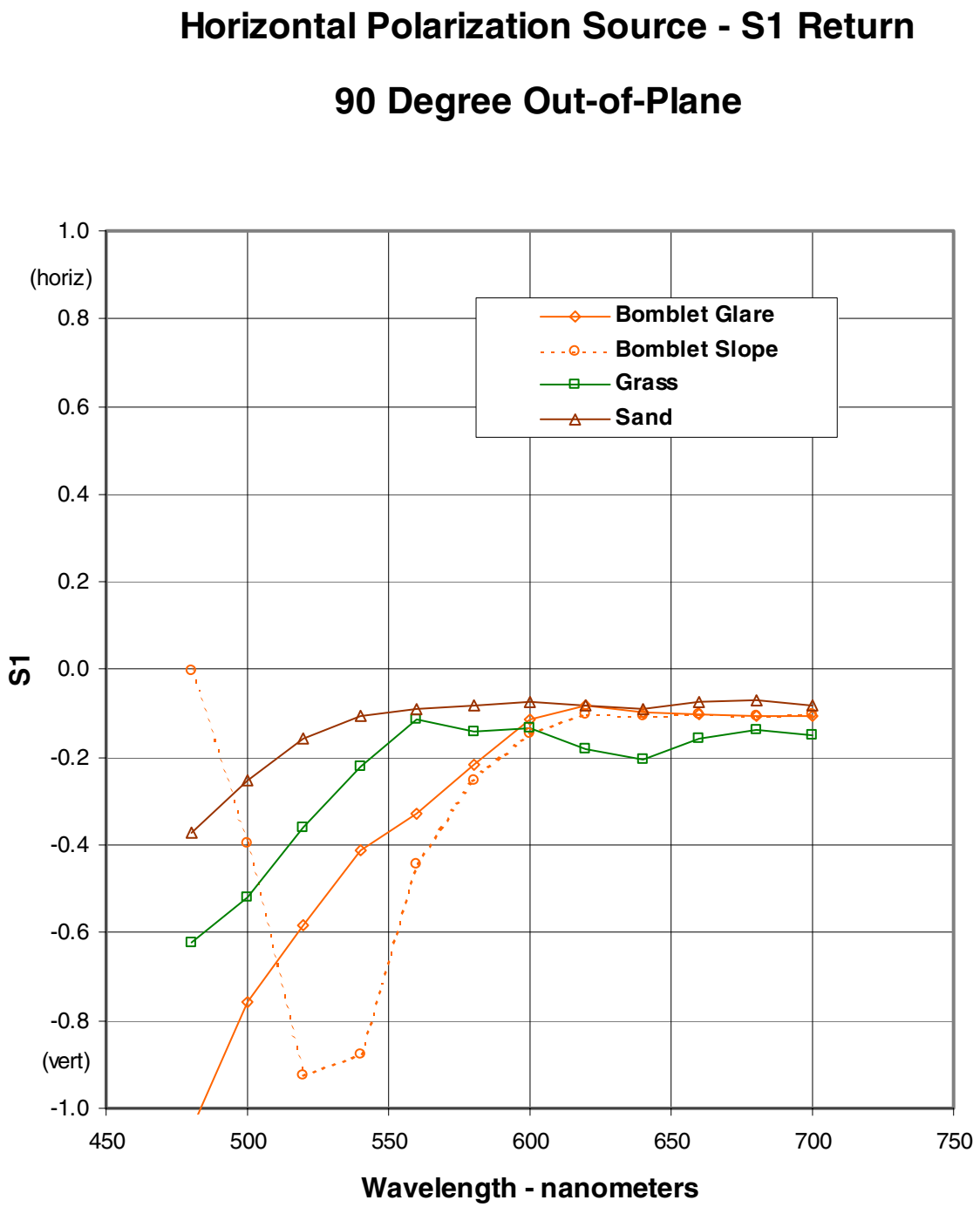

Figure 62. Out-of-plane S1 spectral response of nonstandard surfaces - horizontal source

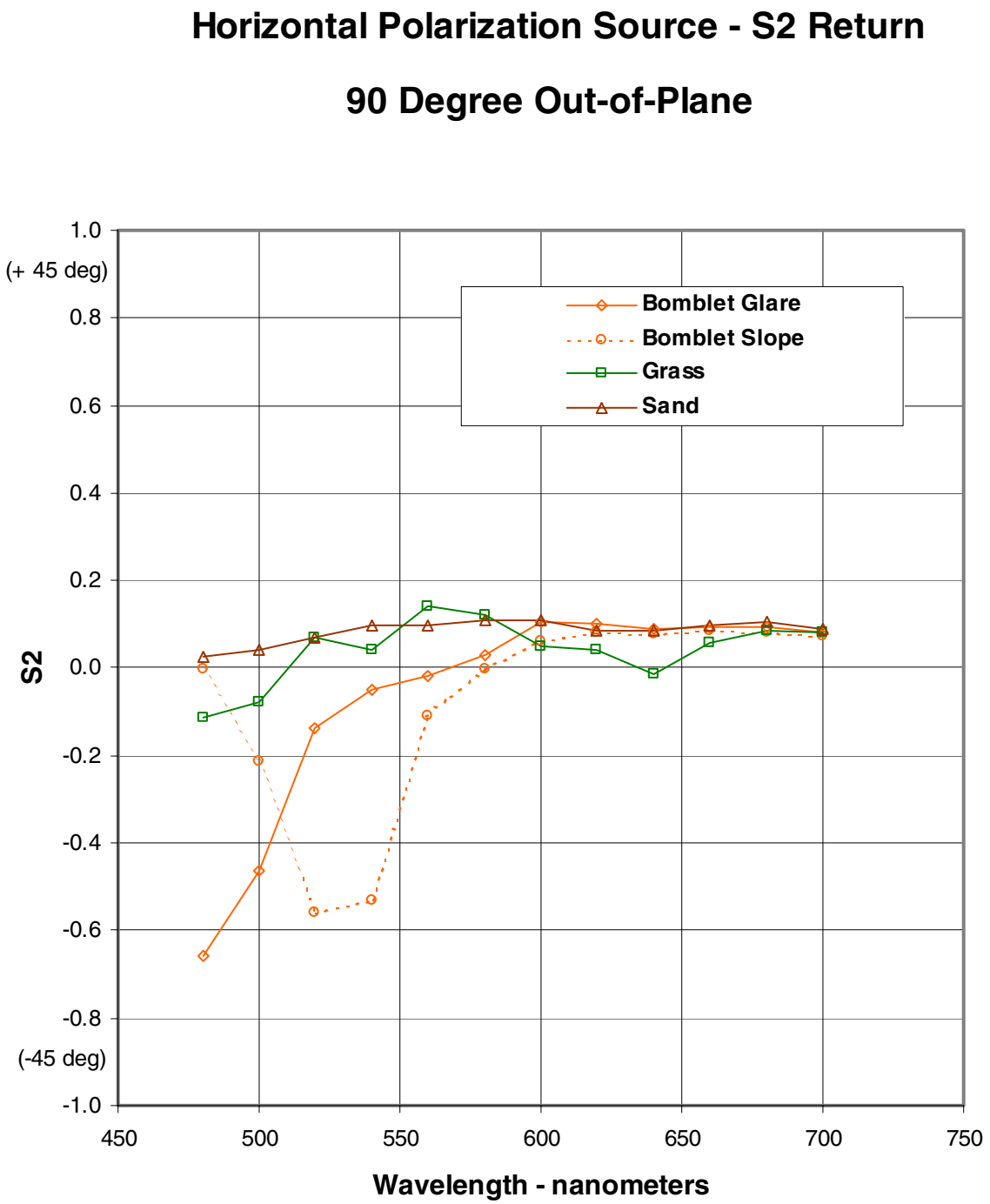

Figure 63. Out-of-plane S2 spectral response of nonstandard surfaces - horizontal source

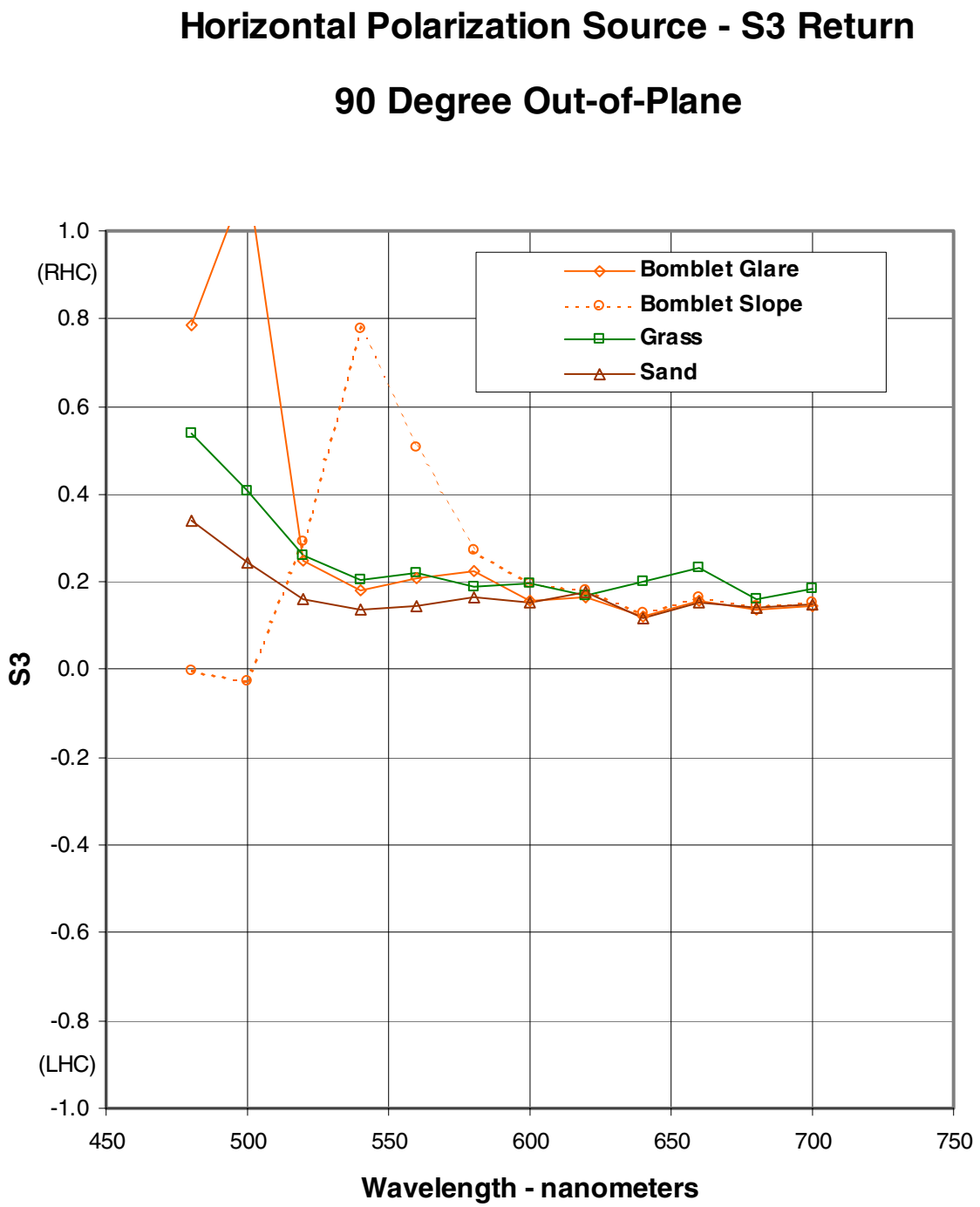

Figure 64. Out-of-plane S3 spectral response of nonstandard surfaces - horizontal source

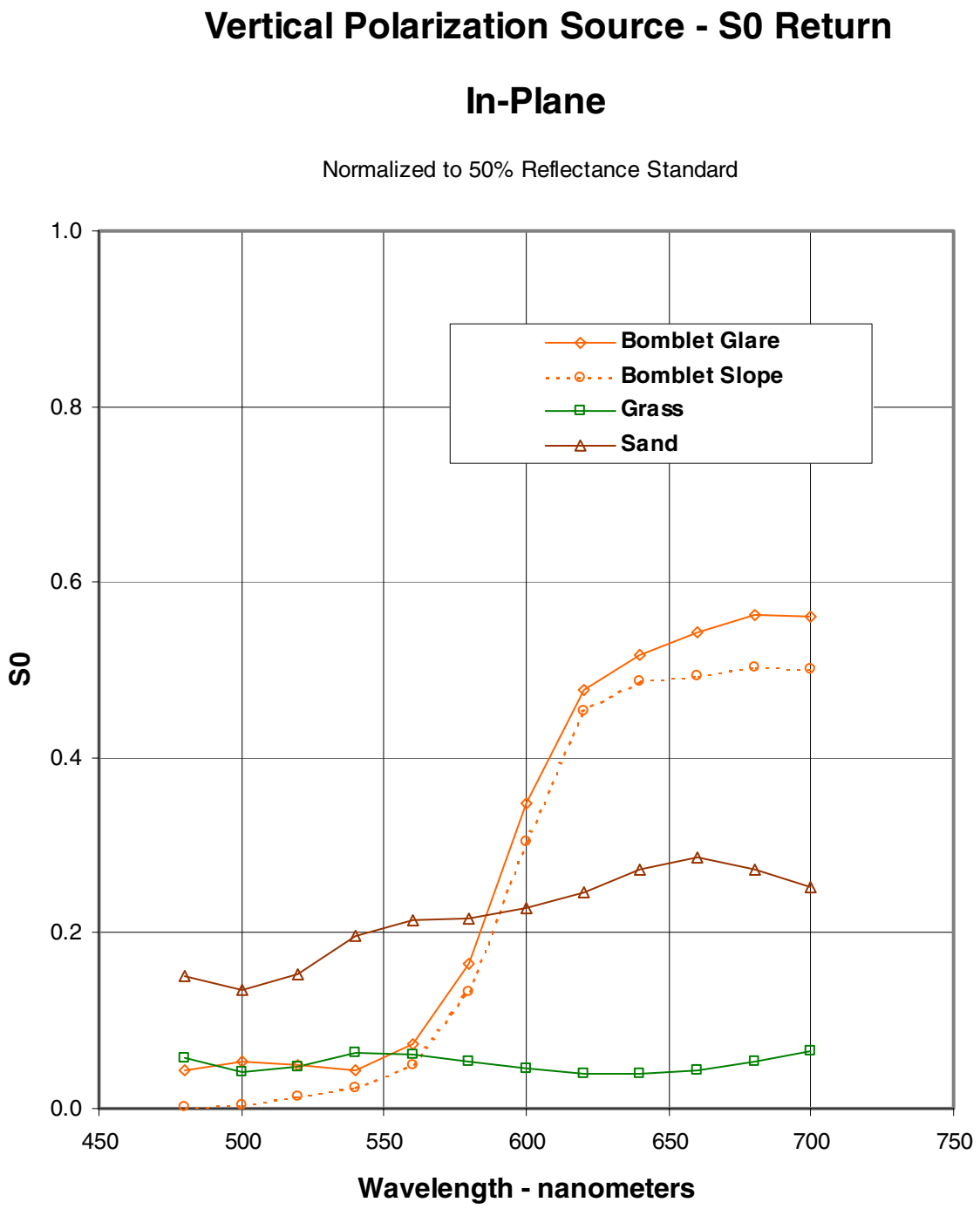

Figure 65. In-plane S0 spectral response of nonstandard surfaces - vertical source

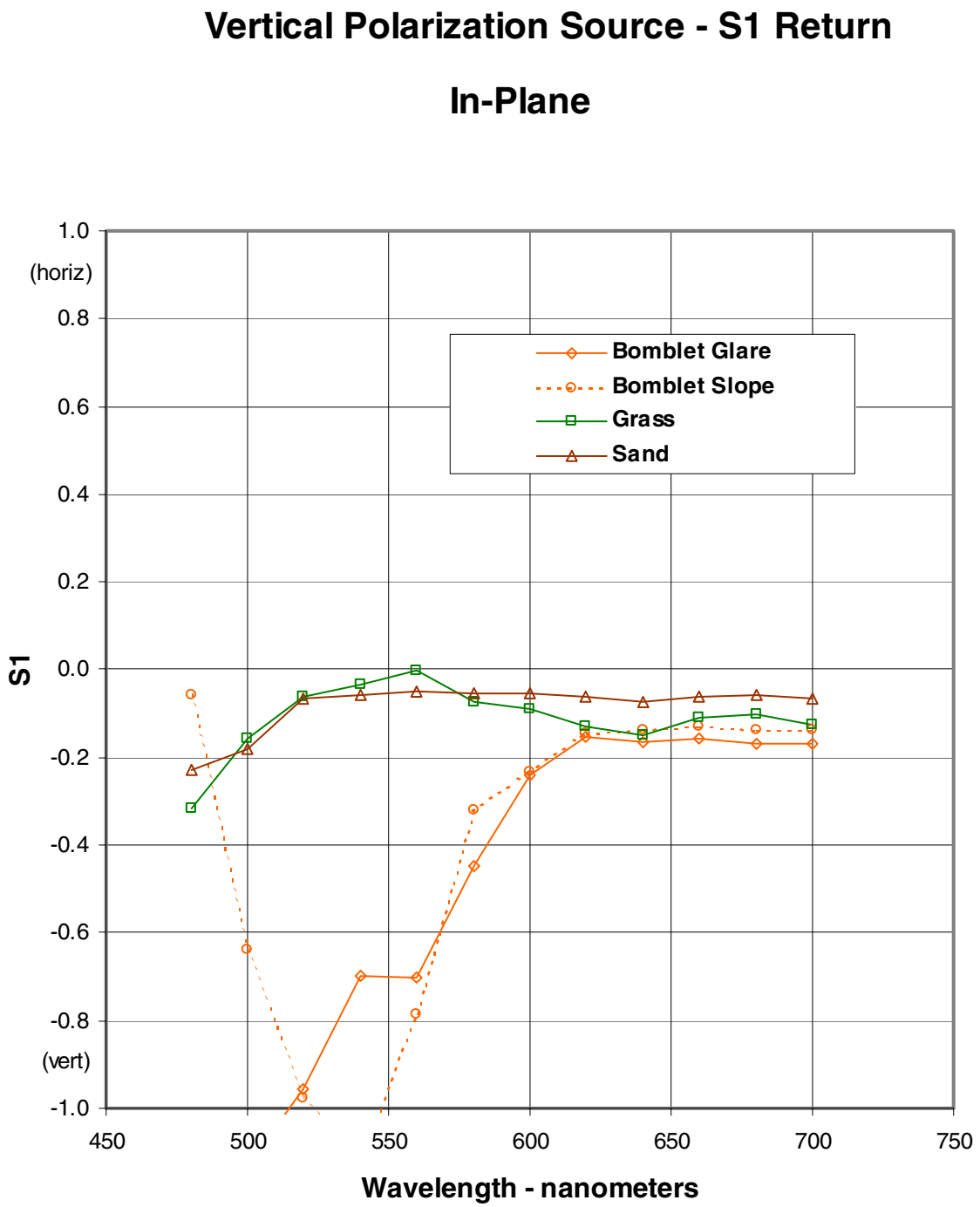

Figure 66. In-plane S1 spectral response of nonstandard surfaces - vertical source

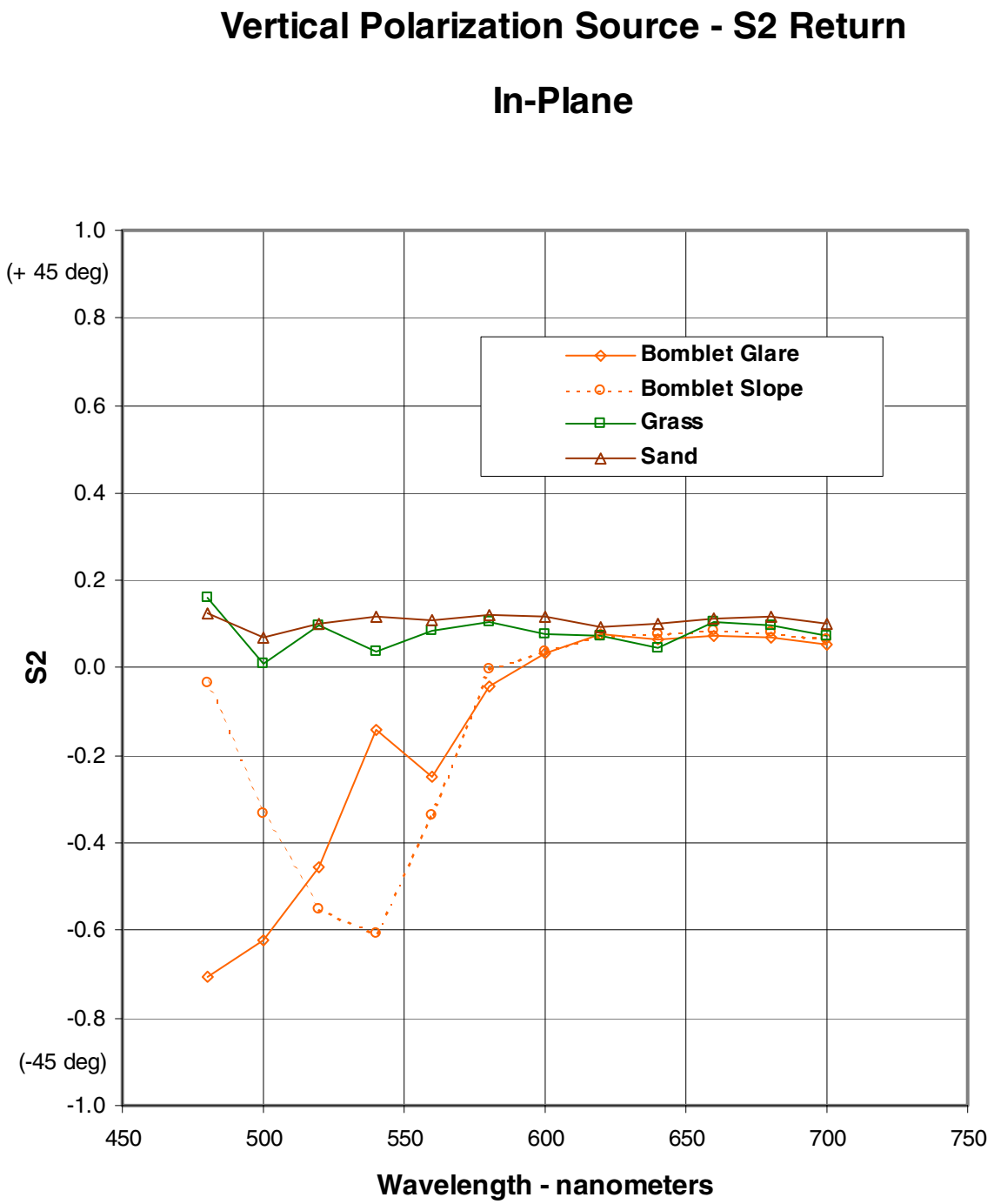

Figure 67. In-plane S2 spectral response of nonstandard surfaces - vertical source

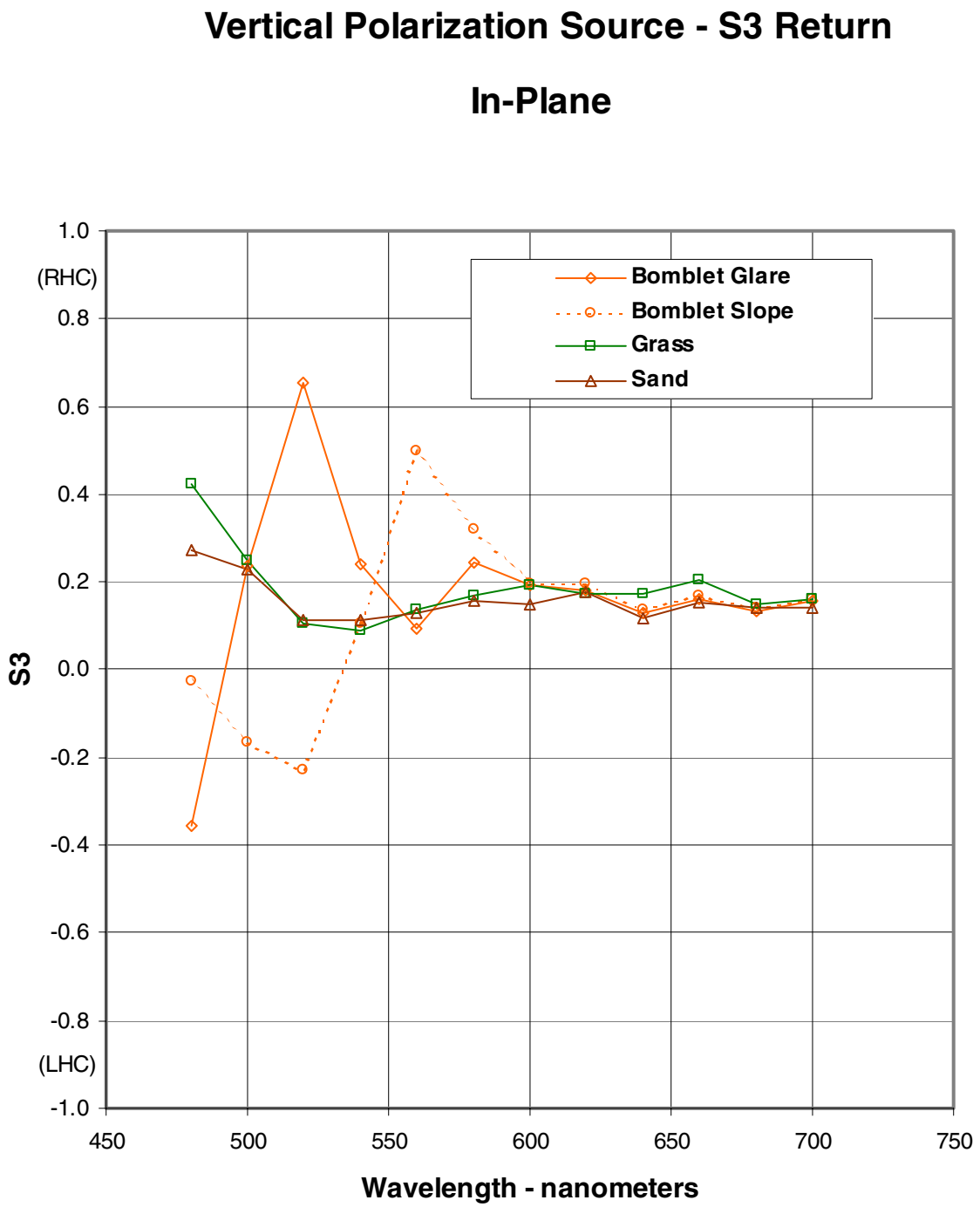

Figure 68. In-plane S3 spectral response of nonstandard surfaces - vertical source

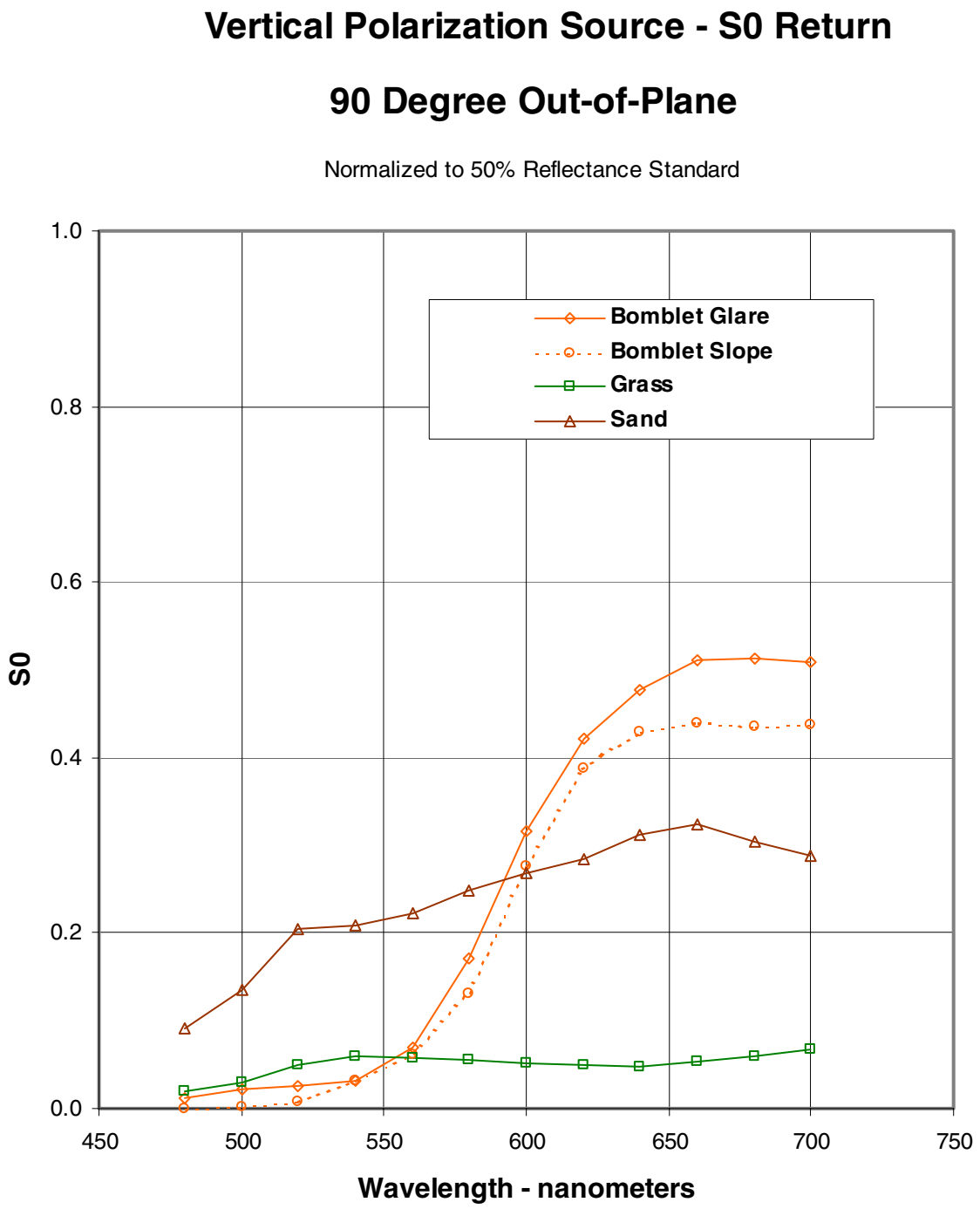

Figure 69. Out-of-plane S0 spectral response of nonstandard surfaces - vertical source

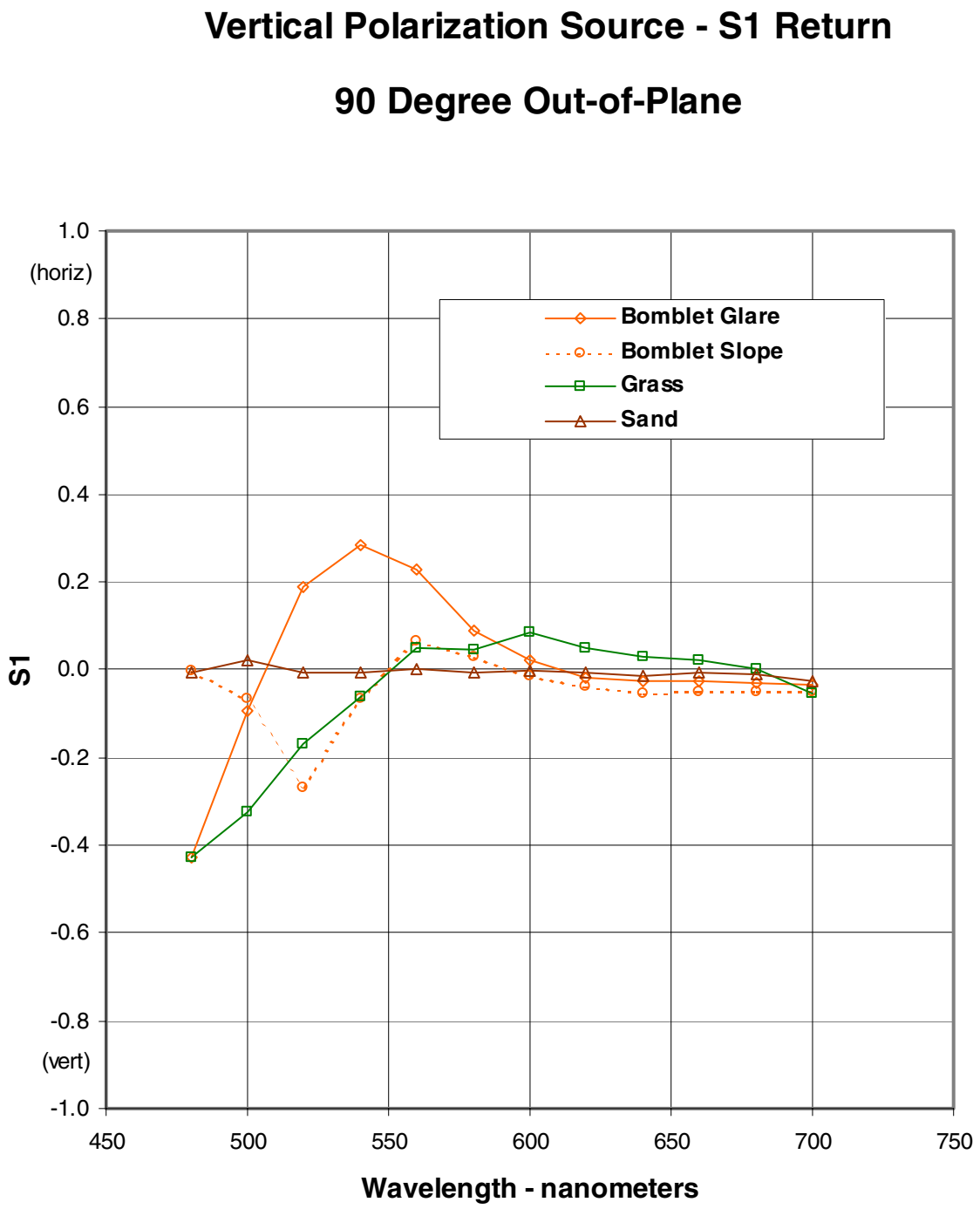

Figure 70. Out-of-plane S1 spectral response of nonstandard surfaces - vertical source

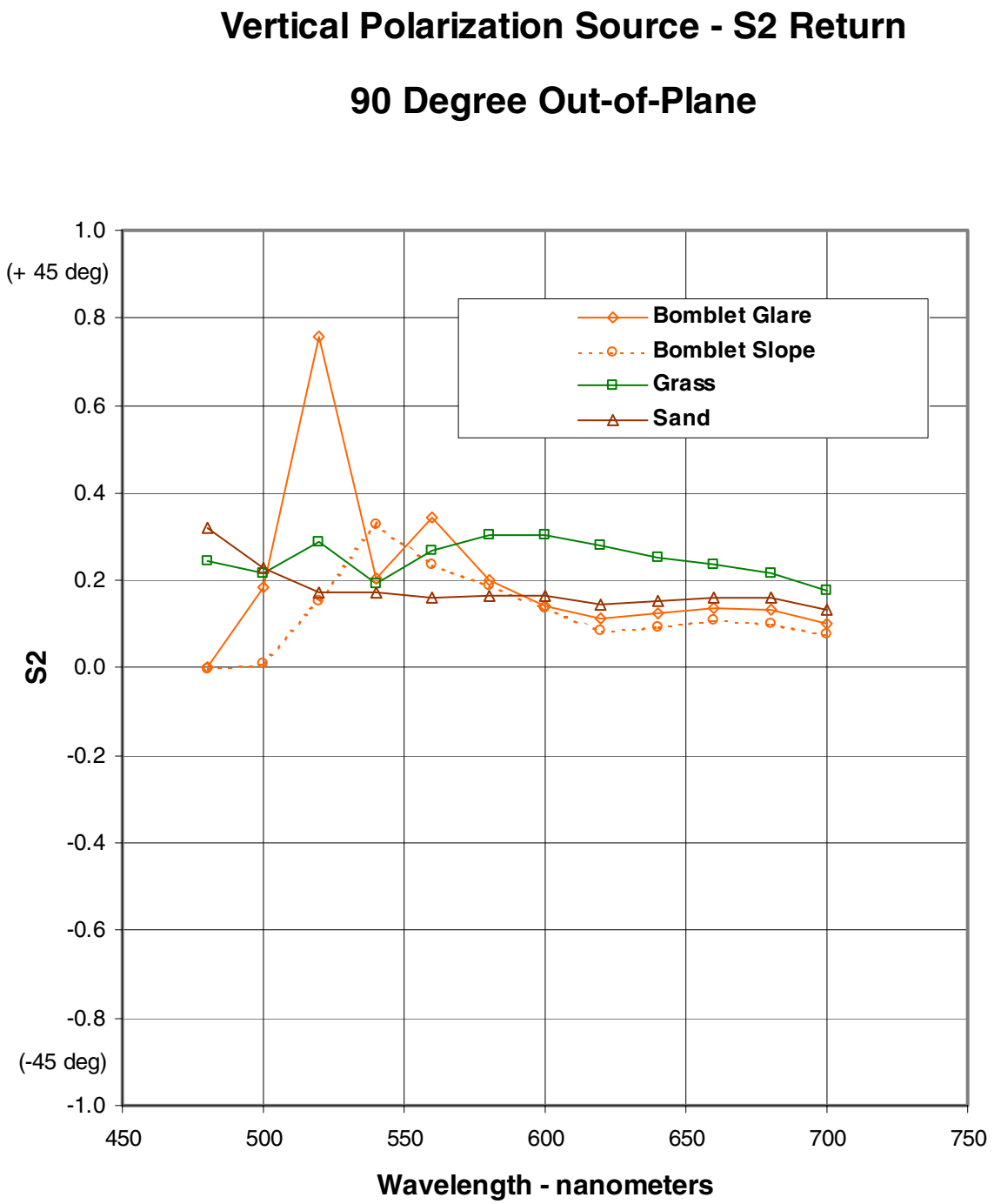

Figure 71. Out-of-plane S2 spectral response of nonstandard surfaces - vertical source

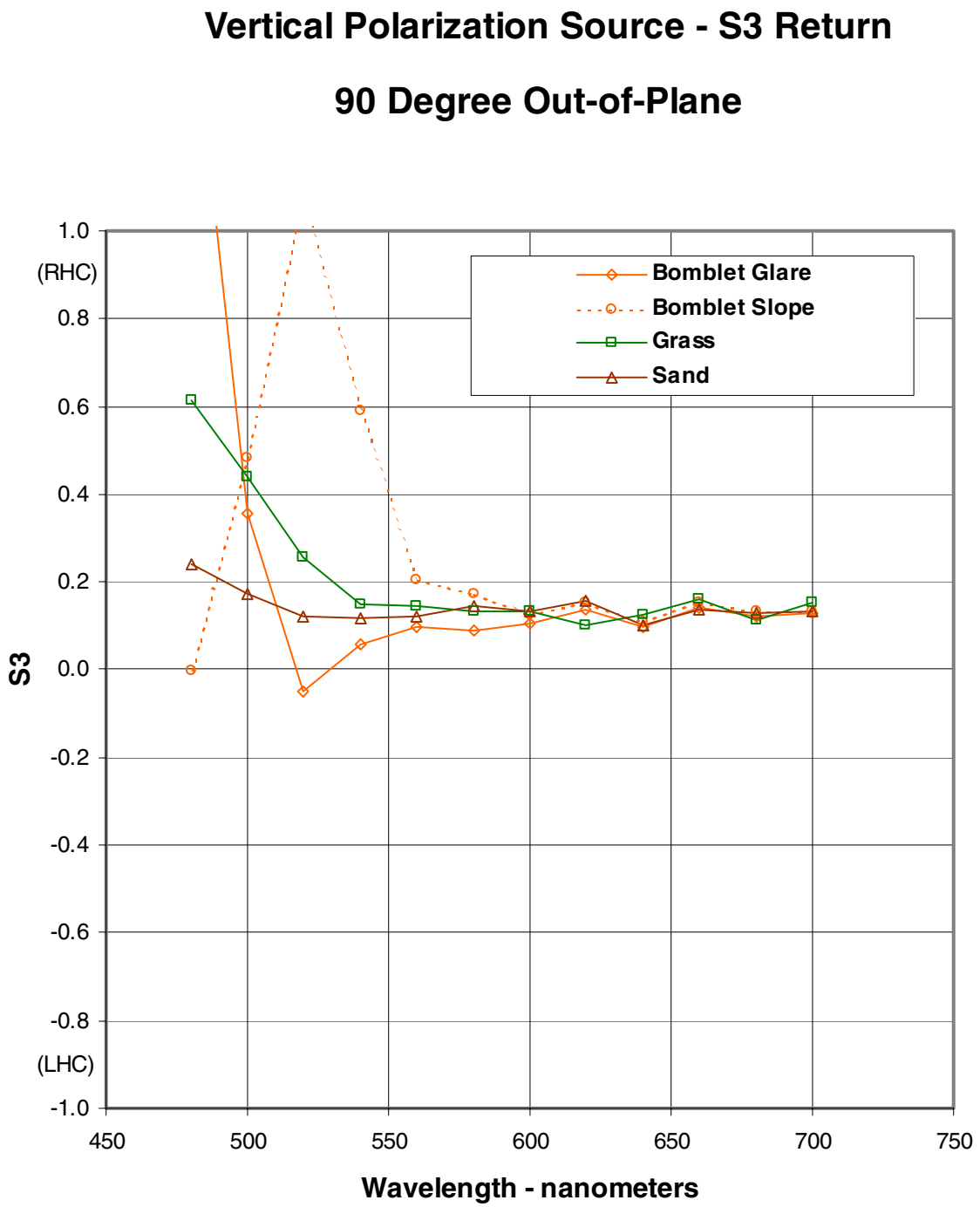

Figure 72. Out-of-plane S3 spectral response of nonstandard surfaces - vertical source

4 Summary and Recommendations

A unique optical imaging system called the Computed-Tomography Imaging SpectroPolarimeter, or CTISP, has been presented as a passive sensor with potential for both military and civilian applications. The system measures both spectral signatures and the polarization characteristics of reflected light. Spatial and spectral content of what is seen within the sensor FOV is reconstructed from diffraction images generated by passing the light through a phase-only computer-generated holographic disperser. Polarization properties are measured through the use of four optical filters.

Data are presented for both flat colored surfaces illuminated by artificial light as well as a bomblet, grass sod, and course sand. Many predictable responses in terms of wavelength dependence and polarization characteristics were observed. However, many issues still remain unresolved and further research is warranted.

For example, it is clear that a polarization standard, or a set of standards, must be developed to absolutely validate the polarization response of CTISP. Inseparable from the polarization question is one of filter geometry on the CTISP hardware. While calibration of the system is performed on an optical bench, there is no assurance that all of the optical filters on the measurement device are oriented exactly as they need to be for proper data collection and analysis when the device is mounted on tripod in a laboratory or in natural sunlight.

Another recommendation for future studies is to move the apparatus to an outdoor test site. Combining solar radiation measurements with CTISP measurements of sunlight-illuminated targets over the course of a day would lead to empirical models for different surface types. While a good deal of empirical data exists for sun-angle-dependent exitances from natural and man-made surfaces, little, if any, data exist for the polarization/depolarization response of those surfaces.

Modifying CTISP to operate in a backscatter mode would provide an opportunity to conduct nighttime measurements from a helicopter, or remotely piloted platform. In terms of military applications, such as surface mine detection, such measurements would be the optical analog of today's radar sensors.

One more recommendation is to strive for near real-time processing of data through hardware and software modifications. For example, as CTISP is currently configured, four filters must be positioned in the optical path of the hardware one at a time. One simple, but expensive option would be to have four sensors operating simultaneously, each with a single filter. Another, more sensible, approach would be to split the energy from a single FOV into four optical paths and use four detector arrays to image the diffraction patterns simultaneously. One more option, would be to display the four diffraction patterns onto a larger CCD array while maintaining the current level of spatial resolution.

A final consideration for future studies is to focus only on improving spatial resolution of the current system by using a larger CCD array. At its present level of resolution, CTISP cannot be positioned very far from small targets such as surface mines. Proven mine detection technologies rely, in part, on images having several pixels on the target.

References

Chipman, R. A. (1993). “Introduction to polarization and polarimetry,” Short course notes, Huntsville, AL.

Curran, P. J. (1982). “Polarized visible light as an aid to vegetation classification,” *Remote Sensing of Environment* 12, 491-499.

Descour, M. R., Volin, C. E., Dereniak, E. L., Gleeson, T. M., Hopkins, M. F., Wilson, D. W., and Maker, P. D. (1997). “Demonstration of a computed-tomography imaging spectrometer using a computer-generated hologram disperser,” *Applied Optics* 36(16), 3694-3698.

Hecht, E. (1987). *Optics*. 2nd ed., Addison-Wesley, Reading, MA.

Miles, B. (1999). “Computed-tomography imaging spectropolarimeter (CTISP),” Ph.D. diss., University of Arizona.

Miles, B. H., Goodson, R. A., Dereniak, E. L., and Descour, M. R. (1999a). “Computed-tomography imaging spectropolarimeter (CTISP): Instrument concept, calibration and results.” *Polarization: measurement, analysis, and remote sensing II*, *Proceedings of SPIE.* Vol. 3754, Denver, Colorado, 19-21July 1999. D. H. Goldstein, D.B. Chenault, ed., SPIE, Bellingham, Washington, 235-245.

Miles, B. H., Goodson, R. A., Dereniak, E. L., and Descour, M. R. (1999b). “Computed-tomography imaging spectropolarimeter (CTISP): Instrument design, operation and results.” *Imaging spectrometry V*, *Proceedings of SPIE*. Vol. 3753, Denver, Colorado, 19-21 July 1999. M. R. Descour and S. S. Shen, ed., SPIE, Bellingham, Washington, 169-179.

Bibliography

Barrios, M. C. D., Ustin, S. L., Pinzon, J. E., Perry, G. L., Vanderbilt, V. C., Livingstone, G. P., Morrissey, L. A., Breon, F. M., and Leroy, M. M. (1998). "Discrimination of inundated and non-inundated community types with multi-spectral multi-angle POLDER data," http://vache.ucdavis.edu/papers/html/diazbarriosetal1998b/paperfr.html (26 April 2001).

Breon, F. M., and Deschamps, P. Y. (1993). "Optical and physical parameter retrieval from POLDER measurements over the ocean using an analytical model," *Remote Sensing of Environment* 43, 193-207.

Deschamps, P. Y., Breon, F. M., Leroy, M., Podaire, A., Bricaud, A., Buriez, J. C., and Seze, G. (1994). "The POLDER mission: Instrument characteristics and scientific objectives," *IEEE Transactions on Geoscience and Remote Sensing* 32(3), 598-615.

Descour, M., and Dereniak, E. (1995). "Computed-tomography imaging spectrometer: Experimental calibration and reconstruction results," *Applied Optics* 34(22), 4817-4826.

Gibbs, D. P., Betty, C. L., Fung, A. K., Blanchard, A. J., Irons, J. R., and Balsam, W. L. (1993). "Automated measurement of polarized bi-directional reflectance," *Remote Sensing of Environment* 43, 97-114.

Kimes, D. S. (1983). "Dynamics of directional reflectance factor distributions for vegetation canopies," *Applied Optics* 22(9), 1364-1372.

Kimes, D. S., Newcomb, W. W., Tucker, C. J., Zonneveld, I. S., Van Wijngaarden, W., De Leeuw, J., and Epema, G. F. (1985). "Directional reflectance factor distributions for cover types of northern Africa," *Remote Sensing of Environment* 18, 1-19.

Lacaze, R., and Roujean, J. L. (2001). "G-function and HOt SpoT (GHOST) reflectance model application to multi-scale airborne POLDER measurements," *Remote Sensing of Environment* 76, 67-80.

Pinty, B., Verstraete, M. M., and Dickinson, R. E. (1989). "A physical model for predicting bi-directional reflectances over bare soil," *Remote Sensing of Environment* 27, 273-288.

Pinty, B., Verstraete, M. M., and Dickinson, R. E. (1990). "A physical model of the bi-directional reflectance of vegetation canopies 2. inversion and validation," *Journal of Geophysical Research* 95(D8), 11767-11775.

Roujean, J. L., Leroy, M., and Deschamps, P. Y. (1992). "A bi-directional reflectance model of the earth's surface for the correction of remote sensing data," *Journal of Geophysical Research* 97(D18), 20455-20468.

Verstraete, M. M., Pinty, B., and Dickinson, R. E. (1990). "A physical model of the bi-directional reflectance of vegetation canopies 1. Theory," *Journal of Geophysical Research* 95(D8), 11755-11765.

Appendix A
Controller Hardware and Software Configuration

Hardware Modifications for Portable Operation of Computed-Tomography Imaging SpectroPolarimeter (CTISP)

A Dell Laptop Latitude model is used for data collection and as the equipment controller for the CTISP system. This laptop is chosen because the C/Dock II Expansion Station, for the laptop, supports the PCI interface card. This card type is used to communicate with the camera system in CTISP.

The following modifications and updates were made to the Laptop for the support of CTISP:

The Laptop's BIOS was updated from A04 to A07 to work with the C/Dock expansion station and to handle save-2-disk (s2d) for hard drives larger than 8 GBytes. The file Lcpi-a07.exe is used to make the A07 upgrade floppy disk. It is located in the C:\dell\downloads\bios directory.

The Toshiba XM-1802B 24X CD-ROM firmware was upgraded from ver. 1915 to ver. 1919. This is needed to allow for the CD-ROM to operate properly from the C/Dock expansion station. File tosh1919.exe is used to make the 1919 upgrade floppy disk. It is located in the C:\dell\downloads\patches directory.

Drivers and documents were installed for the 3Com 3CCM156 Global Modem. This allows for uploading of data from remote sites. File 3ccm1561.exe is used to make the driver installation floppy disk. The file 3ccm1562.exe is used to make the documentation installation floppy disk. The files are located in the C:\dell\downloads\miscdr directory.

The display adapter driver was updated from Q6.13.03 to Q6.17.01 to prevent Laptop system from hanging during operation. The file 96699A05.exe is used to

create the installation files on the hard drive in directory C:\dell\Util\Video\617Q. File 96699A05.exe is located in the C:\dell\downloads\video directory.

The touch pad driver was updated from 4.1.28 (Win98 Driver) to 5.0.42 (Dell's latest driver). This added extra options for the configuration of the touch pad. These additional configuration options allow for improved control from the touch pad. The file TP9EA06z.exe is used to create the installation files on the hard drive in directory C:\dell\Drivers\Tpa06. File TP9EA06z.exe is located in the C:\dell\downloads\inputdev directory.

Updated S2D utility files from A03 to A05. Version A05 must be used on hard drives larger than 8 GBytes so the S2D partition is in the first 8 GBytes of the hard drive. File S2D-HA05.exe is used to make the A05 utility files on the hard drive in directory C:\dell\Util\s2d. File S2D-HA05.exe is located in the C:\dell\downloads\sysutil directory.

Drivers were installed for Latitude C/Dock II Expansion Station (Dell Version A07). The Dock Quick version A07 installation file contains the following updated drivers for the hardware in the expansion station: 3COM version 5.04 (A03), CMD 2.1.0 (A02), Adaptec 3.01 (A00). File DQA07.exe is used to make the Dock Quick installation files on the hard drive in directory C:\dell\Drivers\DQA07. File DAA07.exe is located in the C:\dell\downloads\sysutil directory.

Software Modifications for Portable Operation of CTISP

The Pixview.keep archive directory, which contains all Pixview related software, was used to install the PixelView Ver. 3.02 Beta 1 software.

Installation is done as follows:

a. Copy all files in the C:\Pixview.keep\PixelView 3.02 Beta 1\ directory to the C:\Program Files\PixelView 3.02 Beta 1\ directory.

b. Copy all files in the C:\Pixview.keep\WindowsPV3.02\Inf\ directory to the C:\Windows\Inf\ directory.

c. Copy all files in the C:\Pixview.keep\WindowsPV3.02\Start Menu\ directory to the C:\Windows\Start Menu\ directory.

d. Copy most of the files in the C:\Pixview.keep\WindowsPV3.02\System\ directory to the C:\Windows\System\ directory. Note: The Mfc42.dll and the Msvcrt.dll were not copied.

Also note: The Inetwh32.dll is needed by the Pixview.hlp file.

Also note: When help is used for the first time, the user needs to find the help file in the C:\Program Files\PixelView 3.02 Beta 1\Help\ directory.

e. Shutdown system and install the PixelView PCI card.

f. Make sure camera is powered off. Connect camera to PCI card and serial communication (COM) port.

g. Turn on system. The Windows98 system should automatically install the drivers for the PixelView PCI card.

Note: All configuration information is maintained in the registry and is not copied over to the laptop. The user must reconfigure the camera parameters (COM port, frame size, operation temperature, etc.) before using.

h. Place PVAPI.DLL into directory C:\Windows\system from directory C:\Pixview.keep\PixelView 3.02 Beta 1.

i. Copy PVAPI.REG to PVAPIMOD.REG in directory C:\Pixview.keep\Original SDK Disk.

Change "Port"=dword:00000002 to "Port"=dword:00000001 in the [HKEY_LOCAL_MACHINE\SOFTWARE\PixelVision\PixelView\3.0\Board 0\CCD Default Setup] section of the PVAPIMOD.REG file and save the file. Double click on PVAPIMOD.REG file to load it into the registry.

NOTE: Parameters in PixelView software will need to be readjusted.

Mainly, set the gain to high and the pixels to 1024 × 1024.

Finally, the acquire image program must be updated to use system calls for serial I/O. This allows the USB COMM Ports to work with CTISP. The updated acquire image program is labeled as version 1.1.

Appendix B
Code Listings

Please refer to Volume 2 of this report for the code listings of the project. Volume 2 is available electronically in pdf file format at http://www.wes.army.mil/el/elpubs/pdf/trel01-32-2.pdf .

Volume 1 is also available electronically in pdf file format at http://www.wes.army.mil/el/elpubs/pdf/trel01-32-1.pdf .

REPORT DOCUMENTATION PAGE

Form Approved
OMB No. 0704-0188

Public reporting burden for this collection of information is estimated to average 1 hour per response, including the time for reviewing instructions, searching existing data sources, gathering and maintaining the data needed, and completing and reviewing this collection of information. Send comments regarding this burden estimate or any other aspect of this collection of information, including suggestions for reducing this burden to Department of Defense, Washington Headquarters Services, Directorate for Information Operations and Reports (0704-0188), 1215 Jefferson Davis Highway, Suite 1204, Arlington, VA 22202-4302. Respondents should be aware that notwithstanding any other provision of law, no person shall be subject to any penalty for failing to comply with a collection of information if it does not display a currently valid OMB control number. **PLEASE DO NOT RETURN YOUR FORM TO THE ABOVE ADDRESS.**

1. REPORT DATE ***(DD-MM-YYYY)***
September 2001

2. REPORT TYPE
Final report

3. DATES COVERED *(From – To)*

4. TITLE AND SUBTITLE
Computed-Tomography Imaging SpectroPolarimeter (CTISP) - A Passive Optical Sensor
Volume 1, Main Text and Appendix A; Volume 2, Appendix B

5a. CONTRACT NUMBER

5b. GRANT NUMBER

5c. PROGRAM ELEMENT NUMBER

6. AUTHOR(S)
Hollis H. (Jay) Bennett, Jr., Ricky A. Goodson, John O. Curtis

5d. PROJECT NUMBER

5e. TASK NUMBER

5f. WORK UNIT NUMBER

7. PERFORMING ORGANIZATION NAME(S) AND ADDRESS(ES)
U.S. Army Engineer Research and Development Center
Environmental Laboratory, In-House Laboratory Independent Research Program
3909 Halls Ferry Road
Vicksburg, MS 39180-6199

8. PERFORMING ORGANIZATION REPORT NUMBER
ERDC/EL TR-01-32

9. SPONSORING/MONITORING AGENCY NAME(S) AND ADDRESS(ES)
Assistant Secretary of the Army
Washington, DC 20315

10. SPONSOR/MONITOR'S ACRONYM(S)

11. SPONSOR/MONITOR'S REPORT NUMBER(S)

12. DISTRIBUTION/AVAILABILITY STATEMENT
Approved for public release; distribution is unlimited.

13. SUPPLEMENTARY NOTES

14. ABSTRACT

An optical imaging system is described that simultaneously measures the wavelength dependence and polarization state dependence of light reflected from any surface. Potential applications of this technology include identifying man-made objects from natural backgrounds, land cover classification, and a myriad of agricultural problems such as ground moisture measurements, estimation of crop health, etc. Polarization effects are quantified through the use of Stokes parameters. Both spatial and wavelength-dependent data are collected simultaneously through the use of a phase-only computer-generated hologram as a diffraction grating. Image reconstruction is achieved through an inversion procedure called computed tomography.

15. SUBJECT TERMS
Classification system
Computed-tomography
Optical imaging system
Polarization
Spectropolarimeter

16. SECURITY CLASSIFICATION OF:			**17. LIMITATION OF ABSTRACT**	**18. NUMBER OF PAGES**	**19a. NAME OF RESPONSIBLE PERSON**
a. REPORT	**b. ABSTRACT**	**c. THIS PAGE**		Vol 1 - 108 Vol 2 - 211	**19b. TELEPHONE NUMBER** *(include area code)*
UNCLASSIFIED	UNCLASSIFIED	UNCLASSIFIED			

Destroy this report when no longer needed. Do not return it to the originator.